SEPARATION OF TANTALUM AND NIOBIUM FROM NIGERIAN TANTALITE USING AQUEOUS BIPHASE SYSTEM

BY

NEHEMIAH SAMUEL MAINA

DEPARTMENT OF CHEMICAL ENGINEERING
FACULTY OF ENGINEERING
AHMADU BELLO UNIVERSITY, ZARIA - NIGERIA

AUGUST, 2014

SEPARATION OF TANTALUM AND NIOBIUM FROM NIGERIAN TANTALITE USING AQUEOUS BIPHASE SYSTEM

By

Nehemiah Samuel MAINA, M. Sc. (Moscow) 1993
PhD/Eng/9051/2009-2010

A DISSERTATION SUBMITTED TO THE SCHOOL OF POSTGRADUATE STUDIES, AHMADU BELLO UNIVERSITY, ZARIA

IN PARTIAL FULFILLMENT OF THE REQUIREMENTS FOR THE AWARD OF A
DOCTOR OF PHILOSOPHY (PH.D) IN CHEMICAL ENGINEERING

DEPARTMENT OF CHEMICAL ENGINEERING
FACULTY OF ENGINEERING
AHMADU BELLO UNIVERSITY, ZARIA
NIGERIA

MAY, 2014

DECLARATION

I declare that the work in this dissertation entitled Separation of tantalum and niobium from Nigerian tantalite using aqueous biphase system has been carried out by me in the Department of Chemical Engineering. The information derived from the literature has been duly acknowledged in the text and a list of references provided. No part of this dissertation was previously presented for another degree or diploma at this or any other Institution.

Nehemiah Samuel MAINA	_____	_____
Name of Student	Signature	Date

CERTIFICATION

This dissertation entitled SEPARATION OF TANTALUM AND NIOBIUM FROM NIGERIAN TANTALITE USING AQUEOUS BIPHASE SYSTEM, by Nehemiah Samuel MAINA, meets the regulations governing the award of the degree of Doctor of Philosophy (Ph.D) in Chemical Engineering of Ahmadu Bello University, Zaria, Nigeria; and is approved for its contribution to knowledge and literary presentation.

Professor A.S. Ahmed	_____	_____
Chairman, Supervisory committee	Signature	Date
Professor M.T. Ityokumbul	_____	_____
Member, Supervisory committee	Signature	Date
Dr. P.C. Okwonkwo	_____	_____
Member, Supervisory committee	Signature	Date
Dr. I.A. Mohammed-Dabo	_____	_____
Member, Supervisory committee	Signature	Date
Dr. I.A. Mohammed-Dabo	_____	_____
Head of Department	Signature	Date
Professor A.A. Joshua	_____	_____
Dean, Postgraduate School	Signature	Date

DEDICATION

This dissertation is dedicated to The Almighty God who, out of LOVE gave his only begotten Son JESUS CHRIST to die for my sins so that I can be saved; and to the memory of my late mother, Mrs. Victoria Nayen Samuel Maina who went to be with the LORD on 15th May, 2006, after a brief illness. May her Soul continue to rest in peace with the LORD, Amen!

ACKNOWLEDGEMENTS

I am very grateful to God Almighty for His grace upon me. His perpetual grace has given me the strength, determination, patience, resilience and good health during this research.

I am deeply indebted to Prof. J.O. Bello, who provided the necessary advice and guidance for this work, from the beginning before he left Zaria to Covenant University, Ota – Nigeria. I am also indebted to my supervisors, Prof. A.S. Ahmed, Dr. P.C. Okonkwo, Dr. I.A. Mohammed-Dabo of Ahmadu Bello University, Zaria – Nigeria and Prof. M.T. Ityokumbul of Penn State University, U.S.A. Their professional knowledge and constructive criticisms have been extremely useful in the successful execution of the research. I'd like to emphasize that Prof. Ityokumbul made the most contribution in this work which we really appreciate as a family. We pray that God will continue to bless him for his support to the department.

I am particularly grateful and appreciative of the Department of Chemical Engineering, Ahmadu Bello University, Zaria, for its affirmative action and support through procurement of some materials and reagents for me as a staff-in-training. My appreciation also goes to all the staff of Chemical Engineering Department, Ahmadu Bello University, Zaria for their support and criticisms, especially during the seminar presentations in the course of this research work.

I also wish to express my sincere appreciation and love to my lovely wife, Vanessa Esther and children - Michelle Nanret, Isabel Plangnan and Felix Biplang for their support and care. The affection and care of my parents, brothers and sisters were the driving forces behind the work. For this, I say a very big thank you to you all. I really want to

acknowledge and appreciate the McArthur Foundation of Ahmadu Bello University, Zaria, the Federal Government of Nigeria and the IOT – STEP-B Projects of the World Bank through The Federal Ministry of Science and Technology for funding parts of this project. Thanks a lot!

Finally, I want to thank God Almighty for making this come through, especially for His revelation knowledge, inspiration, unlimited blessing and guidance that made it possible for me to scale through and over the obstacles. May God bless the PhD award, Amen!

Table of Contents

Title **Page**

Title page ……i

Declaration ……...iv

Certification ……...v

Dedication …….....vi

Acknowledgements ……vii

Table of Contents …….....ix

List of Tables ……..……xii

List of Figures ……..……xv

List of Plates ……..……...xvii

List of Appendices ……...xviii

List of Symbols ……..xix

List of Abbreviations …….....xx

Abstract …….....xxiii

1.0 INTRODUCTION ……..…….....1

1.1 Background ..…….……...1

1.2 Problem Statement …..…….3

1.3 Justification ..…….……...3

1.4 Aim and Objectives ...…….4

1.5 Scope …….5

2.0 LITERATURE REVIEW ……6

2.1 Introduction……...6

2.2 History of Tantalum and Niobium ……...……..10

2.2.1 Tantalum and niobium properties ……...11

2.2.2 Markets for metals and uses of tantalum ……12

2.2.3 Source of ore ……15

2.2.4 Mining ……..15

2.2.5 Demand and supply …….....16

2.2.6 Tantalum price ……20

2.3 Solvent Extraction …..……24

2.3.1 Extractants in solvent extraction …….....25

2.3.2 Theory of extraction …….....27

2.3.3 The organic phase ……29

2.3.4 The aqueous phase ……...31

2.3.5 Engineering aspects of extraction ……32

2.3.6 Applications of solvent extraction ……36

2.4 Polyethylene Glycol and Separations of Polyethylene Glycol ……36

2.4.1 Introduction ……..36

2.4.2 Aqueous PEG solution properties …….....37

2.4.3 Liquid PEG as reaction solvent ……43

2.4.4 PEG as phase-transfer catalyst (PTC) …….....44

2.4.5 Aqueous biphasic reactive extraction (ABRE) ……....44

2.5 Aqueous Biphasic Systems ……..……...47

2.5.1 Phase diagrams, systems and properties……...53

2.6 Methods of Separating Tantalum and Niobium …..…….....55

3.0 MATERIALS AND METHODS …..……61

3.1 Materials and Reagents …..……...61

3.2 Methodology ……...62

3.2.1 General outline of methodology ……..……..62

3.2.2 Preparation and analysis of feed material……63

3.2.3 Protocol for digesting samples…….……63

3.2.4 Preparation of aqueous biphase systems……...66

3.2.5 Separation of tantalum and niobium in aqueous biphase systems ……...67

4.0 RESULTS ……..……...69

4.1 Introduction……69

4.2 Preparation and Analysis of Feed Material ……..……....69

4.2.1 Characterization of the feed materials……...69

4.3 Protocol for Digesting Samples ……..…....70

4.3.1 Mineral acid leaching of the tantalite ore sample …….....70

4.3.2 Alkali fusion of the tantalite ore sample ……..….....91

4.4 Preparation of Aqueous Biphase System Solutions ……...….92

4.5 Separation of Tantalum and Niobium in the Aqueous Biphase ……97

5.0 DISCUSSION ……...104

5.1 Introduction……..104

5.2 Preparation and Analysis of Feed Material ……..104

5.2.1 Crushing, grinding, ball-milling and analysis of feed material…...……...104

5.2.2 Effect of ball milling time …….105

5.3 Protocol for Digesting Samples ……105

5.3.1 Mineral acid leaching of the tantalite ore sample ……..……..…….....105

5.3.2. Alkali fusion of the tantalite ore sample …..…….111

5.4 Preparation of Aqueous Biphase Systems Solutions ……111

5.5 Separation of Tantalum and Niobium in Aqueous Biphase systems ……...114

6.0 CONCLUSIONS AND RECOMMENDATIONS ….……122

6.1 Conclusions ……...……....122

6.2 Recommendations..……..……..123

REFERENCES ……....124

APPENDICES……...130

APPENDIX A ……...130

APPENDIX B ……132

APPENDIX C ……...133

APPENDIX D ……...137

APPENDIX E ……147

LIST OF TABLES

Table 4.1 EDXRF Analysis Showing Chemical Composition of the three Tantalite Ore Samples Procured ……..69

Table 4.2 XRF Analysis of Tantalite Ore from Plateau before Leaching and Residue After Leaching for 0.2M HF and 15M HF respectively in 10.8M H_2SO_4 ...70

Table 4.3 XRF Analysis of Tantalite Ore from Plateau before Leaching and Residue After Leaching for 20M HF, 15M HF and 2M HF respectively in 10.8M H_2SO_4 ……...71

Table 4.4 XRF Analysis of Tantalite Ore from Plateau before Leaching and Residue After Leaching for 2M HF in 10.8M H_2SO_4 ……....72

Table 4.5 XRF Analysis for 2M HF and 0.2M HF Residues after Leaching in 10.8M H_2SO_4 ……..73

Table 4.6 XRF Analysis for Tantalite Ore Sample from Plateau before Leaching.....74

Table 4.7 XRF Analysis for 15M HF Residues after Leaching in 10.8M H_2SO_4……75

Table 4.8 XRF Analysis for Tantalite Ore from Plateau before Leaching ……..76

Table 4.9 XRF Analysis for 2M HF and 15M HF Residues after Leaching of the Tantalite Ore in 10.8M H_2SO_4 ……77

Table 4.10 XRF Analysis of Leached Liquors for 2M HF and 15M HF in 10.8M H_2SO_4 ……..78

Table 4.11 XRF Analysis of Tantalite Ore from Plateau and Residues after Fusion with KOH and NaOH ……..…91

Table 4.12 Summary of the ABS sets of Experiments Carried Out……...…92

Table 4.12.1 Two-phase Formed from ABS and Liquor from Fusion with NaOH……..92

Table 4.12.2 Two-phase Formed from ABS and Liquor from Fusion with KOH…..…..92

Table 4.12.3 Two-phase Formed from ABS and Fresh Tantalum/Niobium Liquor …....93

Table 4.13 ICP-AES Analysis of the PEG –rich Phase and Salt-rich Phase (I)…..…...97

Table 4.14 Distribution Coefficients for Niobium, Tantalum and Molybdenum from Sample BA (Leached Liquor from Fusion with NaOH) ……....98

Table 4.15 Distribution Coefficients for Niobium and Tantalum from Sample DE (Leached Liquor from Fusion with KOH) ……..99

Table 4.16 Total Mass from Sample BA (Leached Liquor from Fusion with NaOH) ……100

Table 4.17 Total Mass from sample DE (Leached Liquor from Fusion with KOH) …….100

Table 4.18 Separation Factor of Tantalum and Niobium from Sample DE……..101

Table 4.19 ICP-AES Analysis of the PEG –rich Phase and Salt-rich Phase (II)…....101

Table 4.20 Distribution Coefficients for Niobium and Tantalum from Table 4.19…..102

Table 4.21 Separation Factor of Tantalum and Niobium from Table 4.20……..103

Table 4.22 Total Mass of Tantalum and Niobium in the Upper and Lower Phases….103

LIST OF FIGURES

Figure 2.1 Separation Processes Play a Critical Role in the CPI …….6

Figure 2.2 Operations Involved in Solvent Extraction ……...….8

Figure 2.3 Tantalum Consumption by Sector …….....14

Figure 2.4 Tantalum Supply/Demand Balance, 1991 – 2000 …….....18

Figure 2.5 World Tantalum Supply 2005 to 2011……..20

Figure 2.6 Estimated World Consumption of Tantalum 2005 to 2011……..20

Figure 2.7 Tantalum Prices, March 1988-December, 2001 ……...22

Figure 2.8 Historical Tantalite Ore Prices, November 2005-2013…….23

Figure 2.9 Three-phase ABRE ……..46

Figure 2.10 Typical Enzyme Hydrolysis Reaction in ABS …….....46

Figure 2.11 Binodal Curve……...55

Figure 3.1 The Flow Diagram of the Experimental Procedure …….62

Figure 4.1 XRD Analysis of the Tantalite Ore from Plateau before Leaching …….79

Figure 4.2 XRD Analysis of the Leached Tantalite Ore Residues …….....80

Figure 4.3 SEM Images of the Tantalite Ore from Plateau before Leaching at 10 µm and Mag at 1.00 K X …….81

Figure 4.4 SEM Images of the Tantalite Ore from Plateau before Leaching at 20 µm and Mag at 200 X ……..82

Figure 4.5 SEM Images of the Tantalite Ore from Plateau before Leaching at 2 µm and Mag at 2.03 K X …….....83

Figure 4.6 SEM Images of the Tantalite Ore from Plateau before Leaching at 30 µm and Mag at 500 X ……..84

Figure 4.7 SEM Images of the Tantalite Ore from Plateau before Leaching at 20 µm and Mag at 500 X ……..85

Figure 4.8 SEM Images of the Tantalite Ore from Plateau before Leaching at 2 µm and Mag at 5.00 K X …….....86

Figure 4.9 SEM Images of the Residues after Leaching at 10 µm and Mag at 1.01K X ……87

Figure 4.10 SEM Images of the Residues after Leaching at 2 µm and Mag at 2.00 K X …….....88

Figure 4.11 SEM Images of the Residues after Leaching at 20 µm and Mag at 200 X ……89

Figure 4.12 SEM Images of the Residues after Leaching at 2 µm and Mag at 5.00 K X …….....90

Figure 4.13 Fused Mass after Alkali Fusion a) with KOH and b) with NaOH ….....92

Figure 4.14 Binodal Curves and the tie lines for PEG of varying Molecular Weight + Sodium Sulphate + Water…….....94

Figure 4.15 Binodal Curves and the tie lines for PEG of varying Molecular Weight + Potassium Carbonate + Water……...95

Figure 4.16 Binodal Curves and the tie lines for PEG of varying Molecular Weight + Ammonium Sulphate + Water……...96

LIST OF PLATES

Plate D1 Lump of Tantalite Ore Sample……..…..……137

Plate D2 Ball-milled and Sieved Tantalite Ore Sample……. ...……138

Plate D3 PEG being Dissolved in Deionized Water……..139

Plate D4 Dissolved PEG in Deionized Water……140

Plate D5 Picture Showing PEG Sample Packaging……...141

Plate D6 Picture Showing Sample Packaging Specifications……142

Plate D7 Picture Showing PEG Molecular Weight……143

Plate D8 Picture Showing Separation in Aqueous Biphase System Formed…..…...144

Plate D9 Picture Showing More Separation in Aqueous Biphase System Formed...145

Plate D10 Picture Showing More Aqueous Biphase System Formed…….146

LIST OF APPENDICES

APPENDIX A	Procedure for Analysis of Sample using EDXRF ….	130
APPENDIX B	Procedure for Analysis of Sample using XRF ...	132
APPENDIX C	Procedure for Analysis of Sample using ICP–AES ……..	133
APPENDIX D	Selected Laboratory Pictures …...	137
APPENDIX E	Samples of Detailed Analytical Data ……	147

LIST OF SYMBOLS

Ta	Tantalum
Nb	Niobium
Fe	Iron
Mn	Manganese
Ta_2O_5	Tantalum pentoxide
lb	Pound
CCl_4	Carbon tetrachloride
HF	Hydrofluoric acid
H_2SO_4	Sulphuric acid
C	Carbon
CO	Carbon monoxide
Ti	Titanium
Si	Silicon
$(Fe,Mn)(Ta,Nb)_2O_6$	Tantalite/Niobite
K_2TaF_7	Potassium heptafluorotantalate
gm/cc	Gram per centimeter cube
MPa	Mega Pascals
g	Gram
n	Integer
ml	Millilitre
µm	Micrometer
pH	Measure of hydrogen ion concentration

LIST OF ABBREVIATIONS

Å	Angstrom
AAS	Atomic Absorption Spectroscopy
ABEC	Aqueous biphasic extraction chromatographic resins
ABES	Aqueous biphasic extraction system
ABRE	Aqueous biphasic reactive extraction
ABS	Aqueous biphase (biphasic) system
ABU	Ahmadu Bello University
ATPS	Aqueous Two-phase system
CERT	Center for Energy Research and Training
CPI	Chemical process industries
CS	Collapsed structure
D	Distribution coefficient
DG_{hyd}	Gibbs free energy of hydration
DICON	Defense Industry Corporation of Nigeria
EDTA	Ethylene diaminetetraacetic acid
EDXRF	Energy dispersive x-ray fluorescence
EDXS	Energy dispersive x-ray spectrometry
ES	Expanded structure
$ET_{Scale\ of\ polarity}$	Molar electronic transition energy
g/L	gram per liter

gov	Government
ICP-AES	Inductively Coupled Plasma Atomic Emission Spectrometry
K_{part}	Partition coefficient
L	Lower (phase)
LCST	Lower critical solution temperature
M	Molar
MIBK	Methyl isobutyl ketone
m*lb*	Million pounds
MSDS	Material safety data sheet
MW	Molecular weight
NA	Not available
ND	Not detected
NGSRL	National Geoscience Research Laboratory
NMDC	Nigerian Metallurgical Development Centre
PC	Personal computer
PDAs	Personal digital assistants
PEG	Poly(ethylene glycol)
pH	Hydrogen ion concentration
PPG	Poly(propylene glycol)
ppm	Parts per million
PTC	Phase transfer catalyst
RMRDC	Raw Materials Research and Development Council

RPM	Revolutions per minute
SEM	Scanning Electron Microscopy
TBA	Tribenzylamine
TBP	Tributyl phosphate
TIC	Tantalum Niobium International Study Center
TLL	Tie-line length
U	Upper (phase)
UCST	Upper critical solution temperature
UK	United Kingdom
US FDA	United States Food and Drug Agency
Va	Volume of aqueous phase
Vo	Volume of organic phase
VOCs	Volatile organic compounds
w	Weight
www	world wide web
XRF	X-ray fluorescence
β	Separation factor

ABSTRACT

The study was carried out to determine the separation of tantalum (Ta), niobium (Nb) and other metal ions using aqueous biphase system (ABS). The metal ions were produced from alkali fusion and dissolution of local tantalite ores procured from Plateau, Nasarawa and Niger states. The tantalite ore samples were crushed, ground and ball-milled for six hours in a laboratory ball mill and sieved through a 200 sieve mesh (74 μm). The elemental/oxide composition was determined using energy dispersive X-ray florescence (EDXRF) and X-ray florescence (XRF). From the elemental analysis results, the Ta content was highest, about 29 %, for the ore from Plateau state; as such all experiments were done using this ore. X-ray diffraction (XRD) and scanning electron microscopy (SEM) were also carried out on the tantalite ore and its residues after leaching with mineral acids. A number of leaching processes were carried out using mineral acids (H_2SO_4 and HF) varying the molar concentration of the HF used. Fifty grams of the -74 μm ball-milled sample was leached with 150 g (≈ 81.6 ml) of 10.8M H_2SO_4 acid at an acid/ore wt. ratio of 3:1 and also with 81.6 ml a mixture of 15M HF and 2M HF acid (1:1 ratio) in order to improve on the dissolution of Ta and Nb. The residues and leached liquors were analyzed by XRF. Results showed that the mineral acid leaching was not effective and therefore alkali fusion method was employed. Two g of the ground tantalite ore was weighed and mixed with 10 g of potassium hydroxide (KOH), which was earlier crushed in a ceramic hand mortar and pestle. Another 2 g of tantalite ore was weighed and mixed with 10 g of crushed sodium hydroxide. The fusion experiments were performed in an electric furnace using ceramic crucibles at 400^{o}C for one hour. After the reaction, the fused mass was cooled and subsequently leached with de-ionized water at room temperature. The resulting leached solution known as the leached liquor and the residues were analyzed for Ta and Nb by XRF

and inductively coupled plasma – atomic emission spectroscopy (ICP – AES). The leached liquor was the stock solution used in the aqueous biphase separation experiments. Polyethylene glycol (PEG) of various molecular weights (PEG3350, PEG4000, PEG6000, PEG8000, PEG7000-9000, PEG10,000, PEG12,000 and PEG20,000) and three salts- Na_2SO_4, $(NH_4)_2SO_4$ and K_2CO_3 were used to form the aqueous biphase systems (ABS) at PEG to salt ratio of 2:1. The ABS formed was subsequently mixed with 1ml each of the leached liquor and shaken vigorously to facilitate partitioning between the two phases formed. Results showed that Ta and Nb were extracted and separated using ABS, the calculated distribution coefficients (D) were from 0.1 to 1.0 for Ta and 0.1 to 1.1 for Nb. The separation factors for Ta and Nb being 1.83, 3.01, 2.41, 1.27, 1.94 and 0.93 for the various PEG molecular weights used. For a second set of extractions, results further showed that Ta and Nb were extracted in ABS with D from 0.1 to 0.5 for Ta and 1.0 to 1.2 for Nb with separation factors of 3.43, 4.15, 8.0, 10.7, 3.55, 2.62 and 2.87 for the PEGs used. Tantalum and niobium were effectively separated using ABS. The separation factor was highest, 10.7 for PEG of average molecular weight 7000-9000.

Chapter one focuses on the general background of the study, it also examines the research problem statement, research aim and objectives, justification and the significance of the study. The scope of the study was also highlighted. Chapter two looks at separation processes and their roles. It further looks at the history of tantalum and niobium, their properties, markets for the metals and their uses; sources of ore and mining methods. The demand and supply trends and tantalum prices were examined. The chapter also looks at solvent extraction and separations of polyethylene glycols; aqueous biphase systems were examined and methods of separating tantalum and niobium were examined.

Chapter three focuses on the materials and methods, showing general outline of the procedure with reference to preparation of feed materials and protocol for digesting samples, preparation of aqueous biphase systems and actual separation of tantalum and niobium in aqueous biphase systems. Chapter four presents the results of the analyses of the feed materials, the leaching process and alkali fusion; the ABS formation and actual separation of tantalum and niobium in ABS. chapter five is concerned with the general discussion of the various results obtained in the study.

Chapter six concludes the investigation by bringing out numbered statements of facts proven in the work and also made some recommendations on ways to further improve the work.

CHAPTER ONE

INTRODUCTION

1.1 Background

Separation processes are the main cog in the manufacturing wheel of the chemical process industries (CPI) (Humphrey, 1995). They are used for such essential chores as removal of contaminants from raw materials, recovery and purification of primary products, and elimination of contaminants from effluent water and air streams. The heart of the separation process is the mass-separating agent (Humphrey, 1995). In distillation, it is heat; in extraction, the solvent; in adsorption, the adsorbent; and in membrane separation processes, the membrane material.

Tantalum is a shiny grey, but ductile metal that resembles platinium. It was discovered in 1802 by Anders Gustaf Ekeberg, a professor at Uppsala University in Sweden. The metal oxide was obtained from minerals taken from pegmatite (an igneous rock of coarse grain size) at Ytterby, Sweden, and Kimoto, Finland (Bureau of Mines, 1975 and Forest, 2002). Niobium is a rare, soft, malleable, ductile, gray-white metal. It has a body-centered cubic crystalline structure and in its physical and chemical properties it resembles tantalum. Niobium, named after Niobe, the daughter of Tantalus was discovered in 1801 by Hatchett in an ore sent to England. The metal was first prepared in 1864 by Blomstrand, who reduced the chloride by heating it in a hydrogen atmosphere.

Tantalum ores are found in Australia, Brazil, Mozambique, Thailand, Portugal, Nigeria, DR Congo, and Canada. It is also obtained as a by product in the extraction of tin from mineral

deposits in Malaysia and Nigeria (British Columbia, 2005). Separation of tantalum from niobium requires several complicated steps.

Tantalite and niobite are the only commercially important minerals of tantalum, with formula $(Fe,Mn)(Ta,Nb)_2O_6$ (Soisson *et al*, 1961). When the mineral contains more tantalum pentoxide, it is called tantalite. The price of tantalite varies according to the tantalum pentoxide content. Typically a tantalite ore contains less than 1kg of tantalum in every tonne ore (Burt, 2003); beneficiation of the ore is therefore an essential step in the production of tantalum. Increasing public demand for the miniaturization of electronic products with increased performance, and hence more complex circuitry, has led to an increasing reliance being placed on the high volumetric efficiency offered by tantalum capacitors.

Poly(ethylene glycol) – based aqueous biphasic systems (PEG – ABS) can be utilized to separate and recover metal ions in environmental and hydrometallurgical applications. Aqueous biphasic systems (ABS) is formed when a water soluble polymer, [e.g., poly (ethylene glycol), PEG] is mixed with certain water–structuring salts [e.g., $(NH_4)_2SO_4$, K_2CO_3, K_3PO_4] (Rogers *et al*, 1996; Kamalika *et al*, 2006; Graber *et al*, 2000 and Liu *et al*, 2006). Solute partitioning depends only on the composition of the phase-forming components, PEG and salt (Willauer *et al*, 2002).

Nigeria is richly endowed with a variety of solid minerals of various categories, including tantalite, much of which are yet to be exploited (Nigeria Business Info, 2003). Statistically, the level of exploitation of the minerals is low compared to the extent of deposit found in the country (Phillips Consulting, 2003 and Nigeria Business Info, 2003). Nothing much has

been done in mining Nigeria's mineral wealth. Tremendous opportunities exist in this sector. Moreso, the Federal Government is trying to diversify the revenue base of the country, thereby reducing over dependence on petroleum resources. Tantalite in Nigeria is found in Takwashera, Bize, Kusaki in the F.C.T. and the following states: Nasarawa, Plateau, Ekiti, Katsina, Kaduna, Kogi, Kwara, Oyo, Kebbi and Sokoto (RMRDC, 2007 and Nasarawa State, 2007).

1.2 Problem Statement

The existing methods employed in the extraction of tantalum and niobium from tantalite ores involves the use of corrosive mineral acids, flammable and toxic volatile organic compounds (VOCs) as solvents. Environment concerns, health and safety at work places are issues of importance globally. The goal of 'Technology Vision 2020' is to enable the chemical industry to continue to lead in technology development, manufacturing and profitability, while optimizing health and safety, and ensuring environmental stewardship. Hence, the need for the development of new separation processes or methods for tantalum and niobium, that eliminate the use of VOCs. So far, to the best of my knowledge and literature available to me, no research efforts have been undertaken to study the use of ABS in the separation of tantalum and niobium. ABS has been used to separate various solutes such as biomolecules, particulates and metal ions in environmental applications.

1.3 Justification

Nigeria is abundantly blessed with the mineral ore – tantalite. Tantalum is not being produced or processed in Nigeria; only the ore is being exported or smuggled out of the country. Process Technology in Nigeria is not available (RMRDC, 2007). The Federal

Government of Nigeria is trying to diversify the revenue base of the country, thereby reducing over dependence on petroleum resources. The added local production would help bridge the gap between the current demand and supply of the product worldwide, thereby increasing job opportunities and foreign exchange earnings.

The use of ABS for the extraction of tantalum and other metals will be an original contribution to knowledge. The use of ABS will eliminate the need for VOCs in liquid/liquid extraction technology.

1.4 Aim and Objectives

The aim of this research is to use aqueous biphase system (ABS) in separating tantalum and the other constituent metals in the tantalite ore.

The specific objectives include:

- To investigate the extraction of tantalum, niobium and molybdenum in an aqueous biphase system.
- To investigate the dissolution of tantalum and niobium in mineral acids.
- To investigate the effect of PEG molecular weight on the formation of aqueous biphase system.
- To investigate the effect of type of salt (e.g. Na_2SO_4) in the formation of aqueous biphase system.
- To investigate the leaching of tantalum and niobium by fusion with KOH and NaOH; and subsequent dissolution in de-ionized water.
- To investigate the effect of PEG molecular weight on the distribution coefficient of tantalum and niobium.

1.5 Scope

The scope of work will entail the dissolution of tantalite and the laboratory extraction study using ABS. The process variables to be covered include extraction time, concentration of PEG/salt and effect of molecular weight of PEG. For each set of parameters, the concentration of aqueous leached solution and ABS phases and reaction time will be varied. Recovery of tantalum and niobium will be determined.

CHAPTER TWO

LITERATURE REVIEW

2.1 Introduction

Separation processes are the main cog in the manufacturing wheel of the chemical process industries (CPI). They are used for such essential chores as removal of contaminants from raw materials, recovery and purification of primary products, and elimination of contaminants from effluent water and air streams (Humphrey, 1995). Figure 2.1 shows some of the separation processes involved in the CPI.

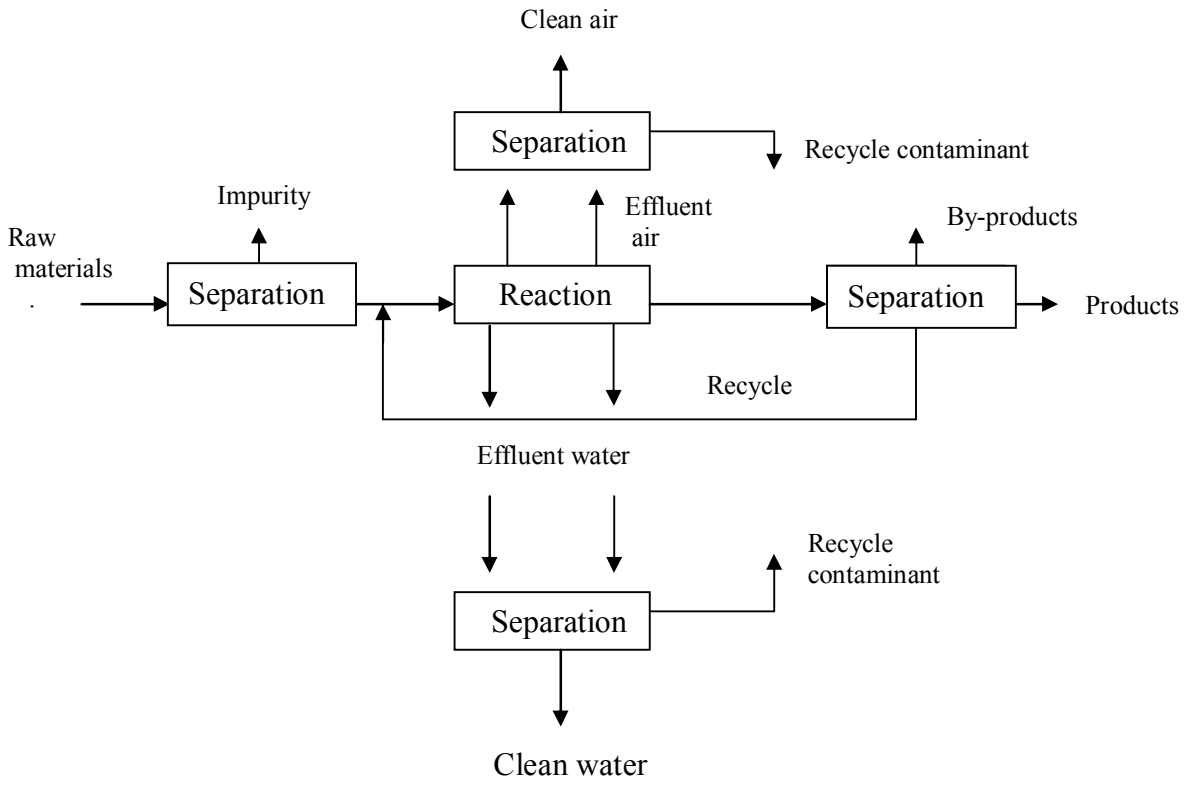


Figure 2.1 Separation processes play a critical role in the CPI (Humphrey, 1995)

The heart of the separation process is the mass-separating agent (Humphrey, 1995). In distillation, it is heat; in extraction, the solvent; in adsorption, the adsorbent; and in membrane separation processes, the membrane material. The two-key design and operating

parameters for any process are efficiency, which indicates how well it separates components, and capacity, which relates to the hydraulics and the rate at which materials can be processed without a loss in efficiency. Solvent extraction may be carried out in various ways. In the simplest, case the solvent is added to a liquid mixture, causing a second liquid phase to form. Sometimes, it is desirable to add two liquids, insoluble in each other, permitting the components of the solution being treated to distribute between the two liquid phases. It may be desirable to add salt to an aqueous phase to enhance the activity of a component, causing it to transfer into a non-aqueous phase in which the salt is insoluble. The processes taking place are primarily physical, since the solutes being transferred are ordinarily recovered without chemical change. On the other hand, the physical equilibrium relationships on which such operations are based depends mainly on the chemical characteristics of the solutes and solvents. Thus, use of a solvent that chemically resembles one component of a mixture more than the other components will lead to concentration of that component in the solvent phase, with the exclusion from that phase of the dissimilar components.

Solvent extraction involves two operations (Habashi, 1970):

1.) Extraction The metal values in the aqueous phase are extracted by agitation with an organic solvent immiscible in that phase. The two phases are then allowed to separate; the aqueous phase is discarded or recycled and the loaded organic phase saved.

2.) Stripping Recovery of the metal values from the loaded organic phase by agitation with a small volume of suitable solution. The stripped solvent is then recycled. In this way, a concentrated solution containing the metal values in a relatively pure form is obtained. Figure 2.2 shows some of the operations involved in solvent extraction.

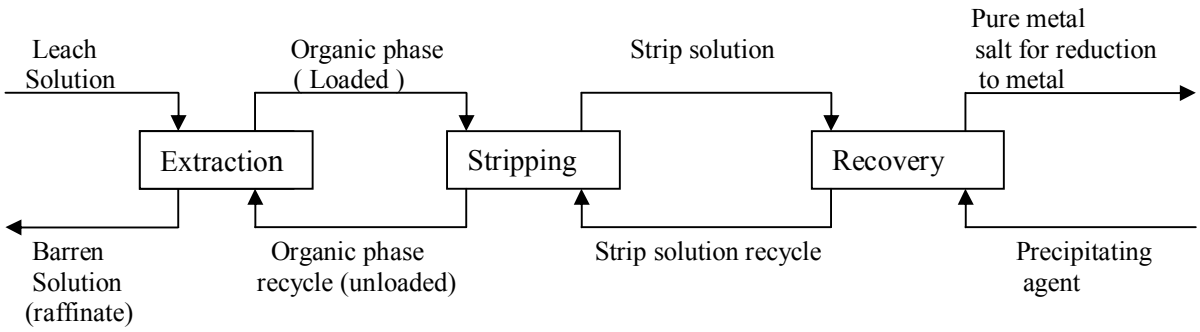


Figure 2.2 Operations involved in solvent extraction

Poly(ethylene glycol) – based aqueous biphasic systems (PEG – ABS) can be utilized to separate and recover metal ions in environmental and hydrometallurgical applications. Aqueous biphasic systems (ABS) is formed when a water soluble polymer, [e.g., poly (ethylene glycol), PEG] is mixed with certain water–structuring salts [e.g., $(NH_4)_2SO_4$, K_2CO_3, K_3PO_4] (Rogers *et al*, 1996; Kamalika *et al*, 2006; Graber *et al*, 2000 and Liu *et al*, 2006). The related aqueous biphasic extraction chromatographic resins (ABEC) are comprised of poly(ethylene glycol) covalently bonded to an inert support, and may represent relatively benign systems for extractive processes for the separation of metal ions and organic molecules in industrial separations as well as environmental applications (Rogers and Griffin, 1998). Solute partitioning depends only on the composition of the phase-forming components, PEG and salt (Willauer *et al*, 2002).

Tantalum is a shiny grey, but ductile metal that resembles platinium. It was discovered in 1802 by Anders Gustaf Ekeberg, a professor at Uppsala University in Sweden. The metal oxide was obtained from minerals taken from pegmatite (an igneous rock of coarse grain size) at Ytterby, Sweden, and Kimoto, Finland (Bureau of Mines, 1975 and Forest, 2002). Over the following decades, several scientists discovered other facets of the new oxide, but

it was not until 1844 that Heinrich Rose, who had studied under Berzelius, who in turn had studied under Ekeberg, was able to determine that the oxide contained two elements, tantalum and a second element that he named niobium, Niobe being the daughter of Tantalus (Dave, 2002 and British Columbia, 2005). However, many chemists thought niobium and tantalum were identical elements; and Marignac, in 1866, showed that niobic and tantalic acids were two different acids. Tantalum, atomic number 73, is a member of Group V in the Periodic Table. It does not occur in nature in the free state, found in a number of minerals, usually associated with niobium (Glinka, 1981 and Dave, 2002). Niobium is also a member of Group V, having atomic number 41. Both metals-with their high melting points and good corrosion resistance, are excellent refractory metals (Soisson *et al*, 1961). The content of niobium in the earth's crust is 0.002, and of tantalum .0002% by mass (Glinka, 1981). The two elements have much in common with vanadium.

Tantalum ores are found in Australia, Brazil, Mozambique, Thailand, Portugal, Nigeria, DR Congo, and Canada. It is also obtained as a by product in the extraction of tin from mineral deposits in Malaysia and Nigeria (British Columbia, 2005). Separation of tantalum from niobium requires several complicated steps.

Tantalite and niobite are the only commercially important minerals of tantalum, with formula $(Fe,Mn)(Ta,Nb)_2O_6$ (Soisson *et al*, 1961). When the mineral contains more tantalum pentoxide, it is called tantalite. The price of tantalite varies according to the tantalum pentoxide content. Typically a tantalite ore contains less than 1kg of tantalum in every tonne ore (Burt, 2003); beneficiation of the ore is therefore an essential step in the production of tantalum. Increasing public demand for the miniaturization of electronic products with increased performance, and hence more complex circuitry, has led to an

increasing reliance being placed on the high volumetric efficiency offered by tantalum capacitors.

2.2 History of Tantalum and Niobium Production

The content of niobium in the earth's crust is 0.002% (mass), and of tantalum 0.0002% (mass) (Glinka, 1981). The two elements have much in common with vanadium. Both metals derive their names from ancient Greek mythology. Tantalus was the son of Zeus, and had a daughter named Niobe. He was sentenced to the eternal punishment of being tantalized with food and water just out of his reach. Similarly, early chemists were "tantalized" with these strange elements which they could name easily enough but could not isolate.

Tantalum in nature is closely related to niobium and tin. Tantalite and tantalum containing tin slags provide the raw material basis (Burt, 2003). Structural changes in the industry affected very seriously the production of tin slags, so that tantalite became by far the most important resource. The tantalum industry is of relative modest size. The total world consumption in 1994 was 997,920 kg Ta. Over 60% of Ta was used in electronics in the form of powder, wire and furnace hardware for the production of solid electrolyte capacitors. Typically, a tantalum ore contains less than 1kg of tantalum in every tonne of ore (Burt, 2003); beneficiation of the ore is therefore, an essential step in the production of tantalum. Tantalum metal was first produced in Germany on a commercial scale in the early 1900's by the reduction of potassium heptafluorotantalate (K_2TaF_7) with sodium. The first commercial producer of tantalum in the United States was Fansteel Metallurgical Corp., North Chicago, Ill. In 1922, the Director of Research at Fansteel, succeeded in making ductile tantalum bars. And until 1956, Fansteel had much of the tantalum field to

itself. At that time, Kawecki Chemical entered the picture and became the other principal producer of tantalum. Also making the metal were Kennametal, Union Carbide Metals, and Wah Chang (Soisson *et al*, 1961). Today, virtually all the tantalum produced in the world is obtained by variations of a stirred reactor version of this process. The modern industrial production of tantalum compounds, like potassium heptaflourotantalate (K_2TaF_7), is not restricted to the wet chemical processing of tantalum bearing ores, but includes the pyrometallurgical upgrading of tantalum containing slags and residues as well as the chlorination of ferroalloys and ores.

2.2.1 Tantalum and Niobium Properties

Tantalum has a myriad of useful properties. It melts at 2996°C (3269K) and has a density of 16.654 $g/cm^{3.}$ Thus it ranks behind only tungsten and rhenium among the refractory metals (Forest, 2002 and Sputtering Targets, 2002). It almost completely resists chemical attack and is on a par with glass in its immunity to acids. Only two acids-hydrofluoric- and fuming sulphuric- or strong alkalis will attack the metal (Soisson *et al*, 1961). These properties make it suitable for chemical processing equipment and for use as surgical implants. It can be fabricated by bending, roll forming, and welding with relative ease. Its ductility and density have made it essential with the military for amour penetration. Its density and nuclear stability make it a valuable material for containers of radioactive elements (Soisson *et al*, 1961). Tantalum's thermal conductivity (0.130 W/mK at 20°C) is higher than that of glass and about the same as that of steel. Thus, it is ideal for heat transfer surfaces in acid or other corrosive surroundings. In ductility, it surpasses most other refractory metals. It can be drawn, stamped, or spun like steel. Annealed tantalum won't spring back when stamped or forged. In addition, the metal work-hardens slowly and

will not age-harden. Two rather unusual properties make tantalum attractive to the electronics industry. For one, the metal absorbs surrounding gas and vapour at high temperatures (Sputtering Targets, 2002). This helps it maintain high vacuum in electron tube applications. Secondly, the metal forms anodic films that are very stable thus can be used in electrolytic rectifiers, capacitors, and lightning arresters.

Niobium also boasts of a variety of useful properties that are of interest to not only the chemical industry, but also to the nuclear energy, electronics, and aircraft and missile industries as well. In many respects, niobium resists corrosion as tantalum. It also has a higher creep strength-to-weight ratio than titanium, zirconium, vanadium, and nickel. This is a very important property where weight is a factor, that is, the aircraft and missile field. Also of importance is niobium's density, only 8.57 g/cm^3, it is just about half that of tantalum. Thus, it is one of the lightest of refractory metals.

2.2.2 Markets for Metals and Uses of Tantalum

Tantalum is used as a raw material in several everyday applications. It forms the building blocks of passive capacitors, which are used to regulate voltage at high temperatures and also to store electric charge for many electronic applications (Soisson, *et al*, 1961; Bureau of mines, 1975 and Angus & Ross, 2003). The capacitors are used in electronic goods such as mobile phones, computers, car electronics, video cameras, pagers, the aerospace industry, sputtering, specialized tools, surgical and dental equipment. They are also used in the metal and specialty alloy industries, where tantalum is mixed with tungsten, titanium, cobalt and nickel for the aerospace and defense industry (Figure 2.3). Capacitors perform a vital function, storing electricity for a short period of time and ensuring that the current

supplied stays within narrowly defined parameters - particularly useful in low-voltage applications such as mobile phones and PDAs, in which these tolerances can be very tight. The advantage of tantalum in capacitors is its high volumetric efficiency, which enables miniaturization, high reliability and stability over a wide temperature range (-55°C to 125°C) (Metal Bulletin, 2006), attributes not matched by other types of capacitor material, such as ceramics (Forest, 2002). Such is the use of tantalum in capacitors that in 2001, 725,760 kg of a total of 1,542,240 kg or approximately 50% of the global consumption of tantalum went to capacitor production (Forest, 2002. The use of tantalum has been instrumental in reducing the size of mobile phones in recent years.

In addition to electronics, consumption has increased in metal alloying, chemicals, carbides and machined metal uses. Metal alloys containing tantalum (at levels between 2%-12%) are used in aircraft engines and in the static turbines used in power generation between 1993 and 2001 consumption in this sector increased four-fold to more than 136,534 kg. Overall tantalum consumption has risen from around 997,920 kg to more than 2,131,920 kg during the period 1993-2000, equivalent to an increase of 13% per annum, outstripping most other mined products, although in the period 2000-2001, the total fell as the cycle in customer goods declined (Metal Bulletin, 2006).

Tantalum's earliest uses were in battery charging rectifiers. Over the years, tantalum equipment has found widespread use in the chemical industries to handle highly corrosive processes. Tantalum is also used in heating elements in high vacuum furnaces, tantalum carbide cutting tools, and surgical implants (bone and nerve repair). Another use is as a container material, both for nuclear reactor applications and for preparing pure metals.

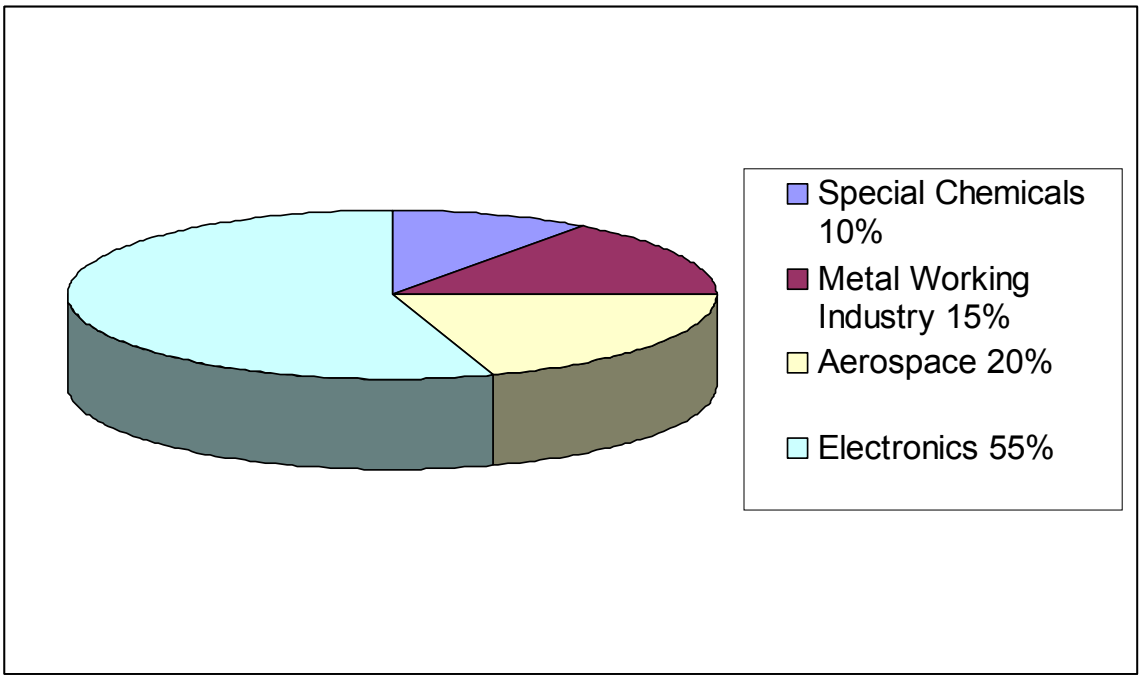


Figure 2.3 Tantalum Consumption by Sector (Source: Sons of Gwalia, 2008)

Other electronic applications included rectifiers, amplifiers, oscillators, controls, signal devices, alarm systems, and timing devices. Tantalum is also an important component metal in special-purpose vacuum tubes. The consumption of tantalum in these applications has increased because of its superior electrical properties, which include the highest dielectric constant of any known metal oxide, the ability to transmit alternating current in only one direction, and the high electrical resistance of some tantalum alloys. Tantalum acts as an absorber of residual gases and as a thermal emitter of electrons in electric tubes etc. Niobium's major market is ferroniobium. Ferroniobium is used in stainless steels to keep carbide from precipitating out at high temperatures. Pure niobium is still striving for wider industry acceptance. Many industries are eyeing it for heat exchangers, thermoelectric devices, and chemical processing equipment applications.

2.2.3 Source of Ore

Tantalite and niobite are the only commercially important minerals of tantalum. Formula for the mineral is (Fe, Mn) (Ta, $Nb)_2O_6$ (Soisson, *et al*, 1961 and Metal Bulletin, 2006). When the mineral contains more tantalum pentoxide, it is called tantalite. Price of tantalite varies according to the tantalum pentoxide content (Soisson, *et al*, 1961). Tantalum occurs in a number of oxide minerals associated with granite and other alkali igneous rocks. There is no shortage of tantalum in the world's geological inventory and although relatively rare, known reserves can more than meet foreseeable demand. However, many of the easiest to work resources, such as residues and high-grade deposits, have been depleted. Tantalum also occurs in the following mineral series: fergusonite, stibiotantalite, tapiolite-mossite, euxenite-polycrase, eschynite-priorite, betafite, samarskite, djalmaite, and yttrotantalite (Bureau of mines, 1975). In the 1980s, most tantalum originated as a by-product of tin smelting. Thailand and Malaysia accounted for nearly 40% of the world's production of 236,000 tonnes. The tin alluvials of Malaysia and Thailand were rich in tantalum and slags resulting from tin smelting contained between 10-15% tantalum. But by 1994, only 20% was derived from this source, and it has decreased further as other sources have been developed.

2.2.4 Mining

Mining developments generally are small, relatively high-cost intermittent operations that depend upon the recovery of byproduct or coproduct minerals for economic viability. Both alluvial and residual tantalum deposits are normally mined by hand, by hydraulic monitors, by dredges, or by mechanized open pit mining (Bureau of mines, 1975). The mining of pegmatite deposits is carried out by blasting, transporting, and crushing the rock to free the

tantalum and associated coproduct minerals, which are then concentrated by wet gravity methods (sluices, jigs, spirals, and tables) and finally separated from associated minerals by gravity and electrostatic and electromagnetic processes.

Tin slags are recovered for their tantalum content in Thailand, Malaysia, Nigeria, Brazil, and DR Congo. These slags are usually mined from dumps by power shovels and trucked or railed to the dock for shipment. In Thailand, slags from the tin smelter are cooled and shortly thereafter crushed and bagged prior to shipment. Tin slags from Thailand contain from 12-14% tantalum oxide. Brazilian tin slags normally contain about 9% tantalum oxide (Bureau of mines, 1975).

2.2.5 Demand and supply

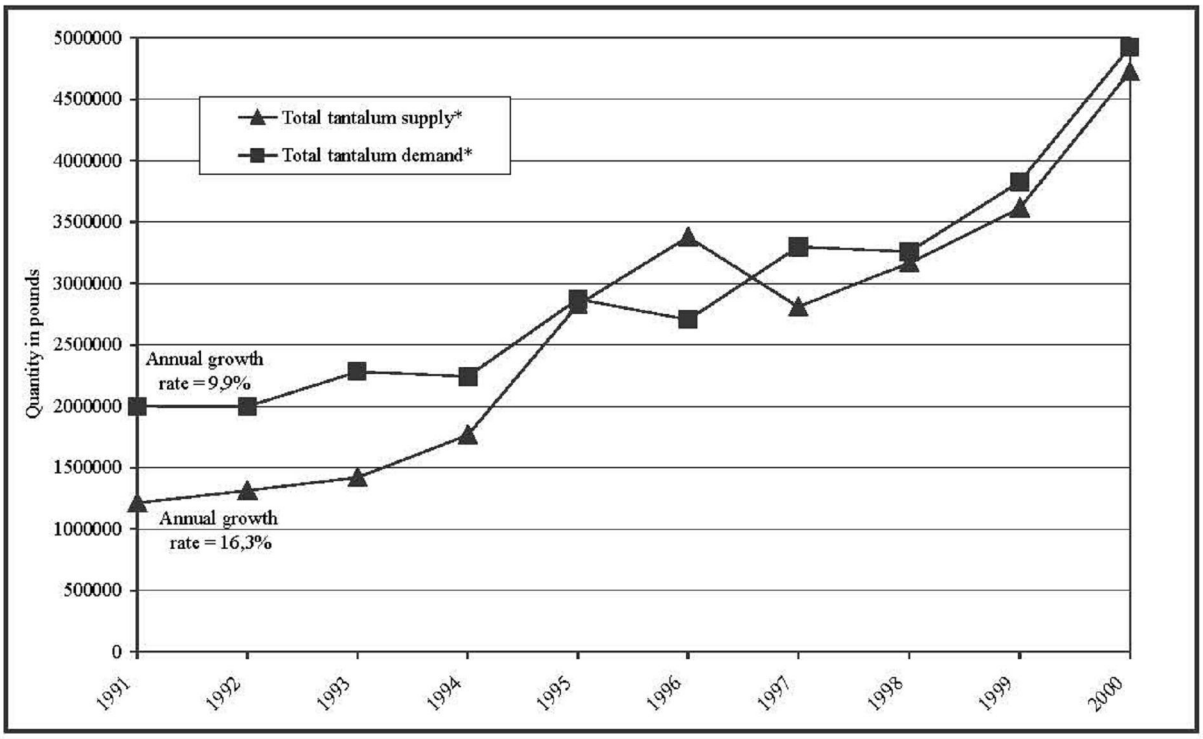
2.2.5.1 *Current demand and supply*

Increasing public demand for the miniaturization of electronic products with increased performance, and hence more complex circuitry, has led to an increasing reliance being placed on the high volumetric efficiency offered by tantalum capacitors. Global consumption surged dramatically in 2000 to approximately 2,268,000 kg, a 38% increase, principally driven by growth in the electronics sector. Supply of raw material could not keep pace during this period of rapid growth leading to an underlying supply deficit of at least 226,800 kg. This resulted in the price for tantalum raw material increasing to US$365 per 0.45 kg contained Ta_2O_5 by the end of year 2000. It is now evident that the pace of growth witnessed in 2000 is not being sustained as the global economy starts to slow. However, future growth expectations remain between 10-20% per annum and will require additional raw material production capacity to meet such demand.

Global tantalum demand increased to 2,268,000 in 2000 with the price of the metal escalating sharply. This growth was principally driven by the growth in the electronics industry. In 1999-2000 consumption of tantalum grew by 20 percent and would have grown further if there had been more metal to deliver. Figure 2.4 shows the supply/demand balance for 1991 – 2000 (Minerals Bureau, 2002). From 1991 to 1995, there were large inventories of raw material at processor facilities. Shortfalls of raw material were made up from these inventories of already mined ore concentrates and tin slag that were kept by processors. From 1998, these inventories have been reduced considerably and lately, demand is closely matched by supply. Since then there has been much less dependence on inventories and raw materials and concentrates must be produced to meet current demand then. This has brought about major expansions of mining operations.

Capacitors store, filter and regulate electrical energy and current flow, and so are essential in all-electronic components. As consumers demand the convenience of smaller units, and the offering of enhanced performance continues its upward trend, the demand for space-efficient high-performance tantalum capacitors increases. Kenmet, the world's largest tantalum capacitor producer, reports that average usage has increased from 3 to 6 tantalum and/or ceramic capacitors for each integrated circuit over the last 20 years. The consumption rate of integrated circuits has increased at an average of 12% per annum over the last 18 years. Consumption of tantalum and ceramic capacitors grew by 34% yearly over the same period.

Consumption of tantalum increased by an average of 120,658 kg per annum, or 11%, between 1993 and 1999. This last year witnessed a dramatic acceleration of growth, with



Source: Tantalum Niobium International Study Center (TIC)

Note: * Pounds of contained tantalum

Figure 2.4 Tantalum Supply/Demand Balance, 1991 – 2000 (Minerals Bureau, 2002).

estimated consumption increasing by 635,040 kg, or 38%, relative to the previous year. The principal growth segment is tantalum powder production used for the manufacture of tantalum capacitors for the electronics industry. Powder represented approximately 65% of tantalum consumption in 2000.

Raw material supply has not been able to keep pace with the explosive growth in demand for tantalum products, with supply falling short of demand by an estimated 226,800 kg Ta_2O_5 in 2000. Consequently, raw material prices increased dramatically during 2000, reaching a peak of US$365 per 0.45 kg Ta_2O_5 in November.

2.2.5.2 *Future tantalum supply and demand outlook*

Supply deficit for 1999-2000 is estimated at 226,800 to 453,600 kg Ta_2O_5. Despite Sons of Gwalia's expansion plans it is evident that significant additional production capacity is required to address the continuing growth in demand. The dramatic supply/demand picture that developed during the course of 2000 serves to underscore the view that additional primary resources of tantalum must be developed in order to meet historical demand growth and offset falling production from old tin slags.

Demand is expected to maintain its upward trend at a growth rate of between 10-20%. Although the electronics sector was experiencing a slowing in the growth rates experienced in 2000, PC sales are forecast to grow by 10% each year, with a 4% increase in capacitor content per unit. Mobile phone sales, although a significantly smaller end-user in tantalum consumption terms, are looking to grow between 12.5 and 25% (Dave, 2002).

Although expansion of production capacity is planned for existing operations, maintenance of the historical demand growth rate will see a continuing tight supply. To put the additional raw material supply requirements into perspective, the production rate of raw material from established producers generally ranges from 68,040 kg Ta_2O_5 to 99,792 kg Ta_2O_5 per mine per annum. In order to meet demand forecasts, it will be required that at least the equivalent of 3-4 new operations of this size come on stream each and every year. Figure 2.5 shows the world tantalum supply from 2005 to 2011, while Figure 2.6 shows the estimated world consumption of tantalum from 2005 to 2011.

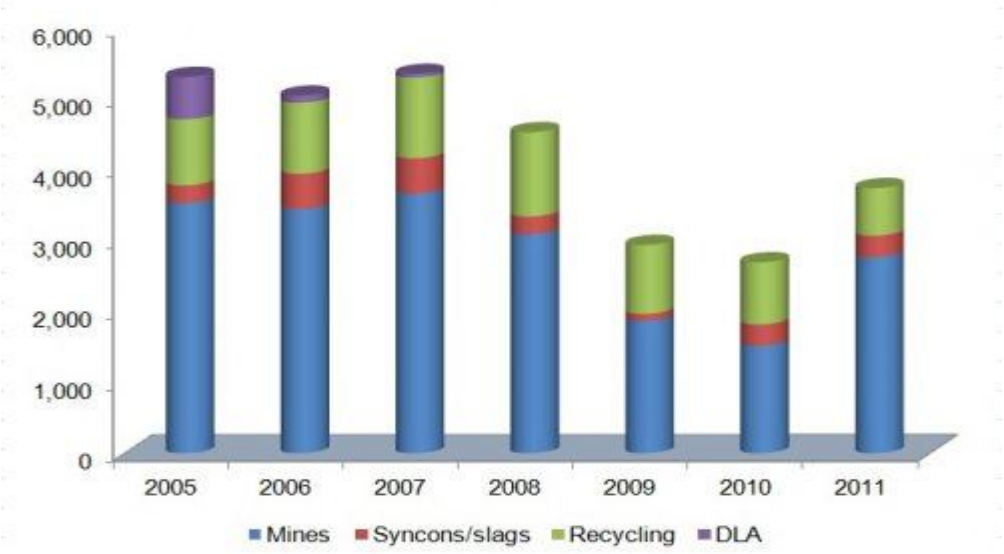


Figure 2.5 World Tantalum Supply 2005 to 2011, (000's lb, Ta_2O_5)
(Stratton and Henderson, 2014)

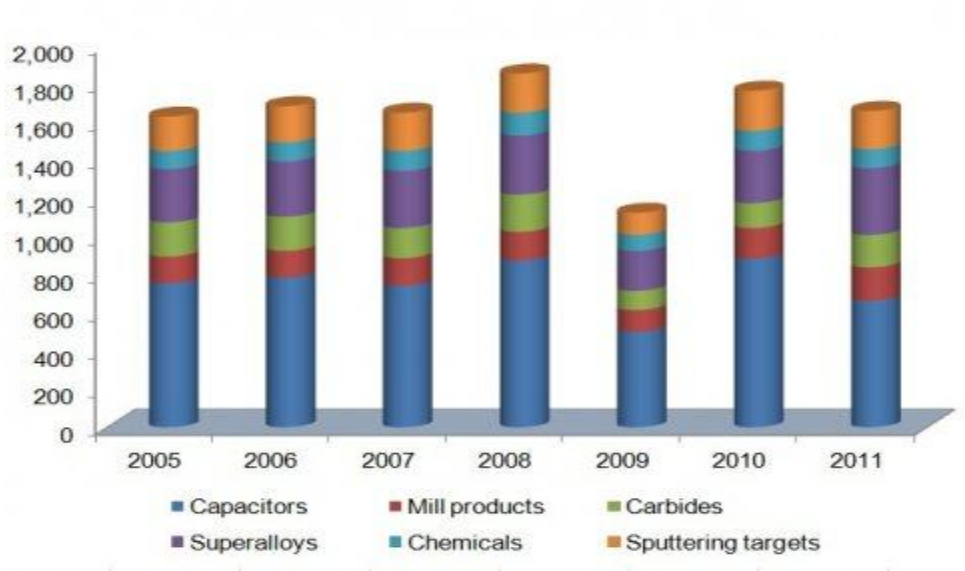


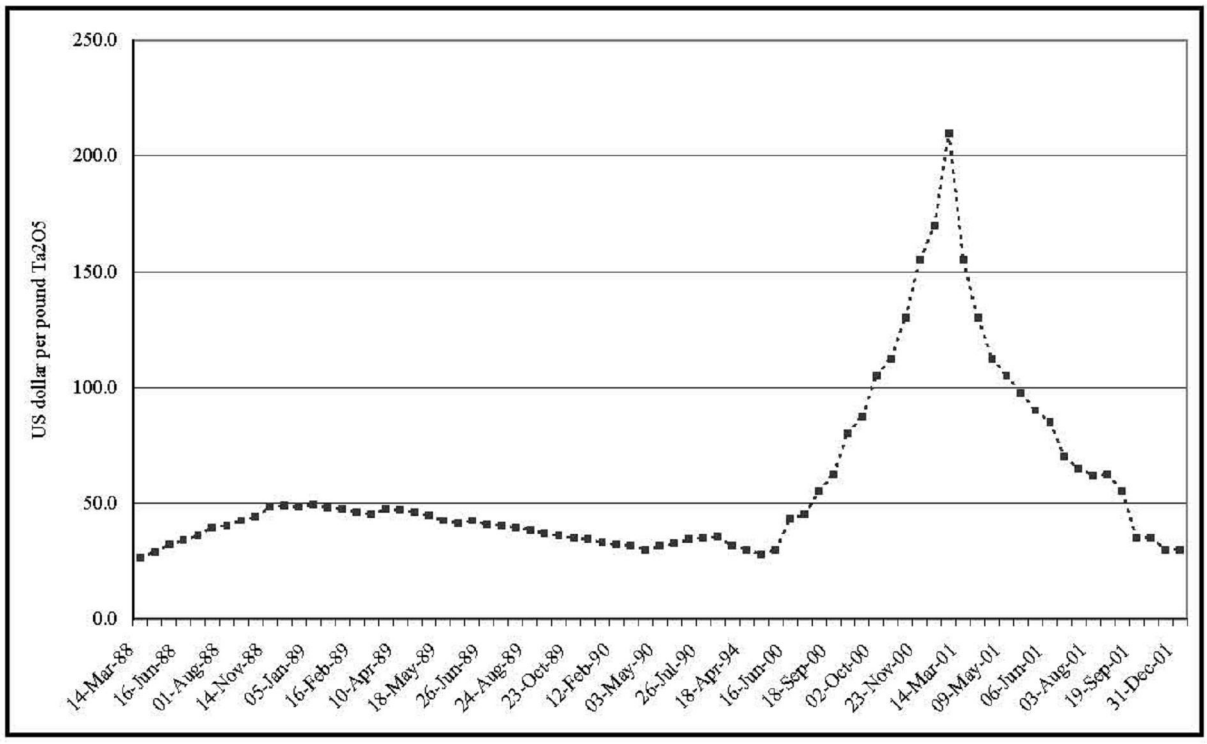
Figure 2.6 Estimated world consumption of tantalum, 2005 to 2011 (t Ta)
(Stratton and Henderson, 2014)

2.2.6 Tantalum price

Pure tantalum of minimum 99.8 % was sold for $400/kg as at February, 2014 in Europe and tantalite; basis of 30 % Ta_2O_5 was sold for about $40/kg. Ta_2O_5 around the same period

(Metal-pages, 2014). Pure tantalum sold for about 63 US$ a kg. in ingot or cap grade powder in 2002. The price of tantalum concentrate during the decade of the 1950s ranged between $1.70 per kilogram to $2.60 per kilogram. It was a quiet period (Dave, 2002). By 1960, tantalum demand increased because of new uses in the chemical, aerospace, electronic, nuclear, and machine tool industries. Tantalum prices during the 1960s experienced erratic behavior because of spurts in demand combined with marginal supplies which, in turn, produced exacerbated price peaks in 1961 and 1966. In both instances resultant overproduction from high cost producers combined with a leveling off of demand took prices back down. For example, in 1961 the price was $5.75/kg, in 1962 it dropped to $2.75/kg, in 1966 it doubled to $6.50/kg, and in 1968 it dropped again to $3.25/kg. The 1960s were the start of a trend in tantalum characterized by wide swings in price because of shortages of supply, rapid inventory drawdowns, and panic buying (Dave, 2002). The 1970s was a decade of increasing tantalum demand, ore shortages, escalating prices, and substitution. Record price levels were set because of panic buying and shortages of adequate supplies. In 1970 the price was $3.57/kg. By the end of the decade the price was over $50/kg. Starting in the1980s tantalum prices exploded. The tantalum concentrate price reached $59 per kilogram by midyear 1980. Once again, prices exhibited erratic behavior because of surges of demand and panic buying only to be followed by dramatic downturns in price. For example, the price dropped to $11.25/kg in 1982 because of hastily and ill-planned inventory buildups by manufacturers accompanied by weakened demand from end users. Since 1990, the price of tantalum has ranged between $13.00/kg and $17.00/kg until late in the decade when the price spiraled to as high as $200/kg in concert with demand from electronic infrastructure requirements, including the Internet, pagers, cell phones, PCs, video cameras, and automobiles (Dave, 2002). The 1990s have experienced steadily

increasing demand for tantalum with acute shortages of raw material occurring during the 1999-2000 period. Figure 2.7 shows tantalite prices from March, 1998 to December, 2001 (Minerals Bureau, 2002). Figure 2.8 shows historical tantalite ore prices from November, 2005 to 2013 (Infomine, 2014). Since the 1950s, the price of tantalum



Note: * Basis 30% Ta_2O_5 cif, max 0,5% U_3O_8 and ThO_2 combined

Figure 2.7 Tantalite Prices*, March 1988 – December 2001 (Minerals Bureau, 2002).

has reacted to periodic shortages of supply, inventory hoarding, and panic buying. In turn, attempts to substitute other metals for tantalum, slackening demand, and the inevitable consequences of panic buying have led to contractions in price. Tantalum does, however, demonstrate the same sensitivity to economic contractions ("recessions") that other industrial metals exhibit in parallel with economic activity, but the degree of tantalum's sensitivity is much more pronounced.



Figure 2.8 Historical Tantalite Ore Prices, November 2005 – 2013 (Infomine, 2014)

Tantalum, based upon approximate quotes of $30 to $40 per kilogram as of September 26, 2001 (with a midpoint of $35/kg used for calculations and based upon spot prices from Africa and Europe), is up 2,253% since 1955 whereas copper at $0.6530, as of September 26, 2001, is up 74% since 1955 (Dave, 2002). This wide disparity in absolute price behavior speaks to the chronic shortage of adequate supply of tantalum and to the growing demand from continual development of new uses in the industrial economy for tantalum. Dissimilar to most common metals like nickel and copper, tantalum is not traded in a central market. The trading market for tantalum is essentially a spot market whereby dealers around the world establish prices via transaction-by-transaction. Dave (2002)

observed that his report on tantalum prices was not aware of any industrial commodity, other than tantalum, that has appreciated by over 2,000% since 1955.

2.3 Solvent Extraction

Separation processes in which two immiscible or partially soluble liquid phases are brought into contact for the transfer of one or more components is referred to as liquid-liquid extraction or, more loosely, as solvent extraction (Habashi, 1970; Perry *et al*, 1997). The processes taking place are primarily physical, since the solutes being transferred are ordinarily recovered without chemical change. On the other hand, the physical equilibrium relationships on which such operations are based depend mainly on the chemical characteristics of the solutes and solvents. Thus, use of a solvent that chemically resembles one component of a mixture more than the other components will lead to concentration of that component in the solvent phase, with the exclusion from that phase of the dissimilar components.

Solvent extraction may be carried out in various ways. In the simplest case, the solvent is added to a liquid mixture, causing a second liquid phase to form. Sometimes, it is desirable to add two liquids, insoluble in each other, permitting the components of the solution being treated to distribute between the two liquid phases. It may be desirable to add salt to an aqueous phase to enhance the activity of a component, causing it to transfer into a non-aqueous phase in which the salt is insoluble. It may be desirable to adjust the pH of an aqueous phase containing organic acidic or basic solutes to depress the ionization of some, causing them to concentrate in the non-aqueous solvent phase. It is often helpful to change

the temperature of the phases in contact to give the most favourable equilibrium at each step of the extraction.

Simple *leaching* of a soluble component away from an inert solid may be regarded as a special case of liquid-liquid extraction (Habashi, 1970; Perry *et al*, 1997). In every case, the successful operation of extraction equipment requires that the solvent phase and the phase being treated be brought into intimate contact so that mass transfer can occur. Then after equilibrium has been approached, the two phases have to be separated mechanically. After one contact-and-separation sequence, it may be desirable to treat each phase further, e.g. in countercurrent fashion. Finally, the solvent laden phases have to be freed of solvent in order to release the enriched components and to recover the solvent for reuse.

2.3.1 Extractants in solvent extraction

An extractant is a liquid used to remove a solute from another liquid. It can also be referred to a liquid or an agent that is used to remove or extract a substance from a mixture or combination of substances.

2.3.1.1 *Requirements of an ideal extractant*

An ideal extractant should fulfil the following requirements (Habashi, 1970):

1) Selectivity
2) High extraction capacity
3) Easily stripped
4) Separates easily from water, i.e.,
    a) Density is appreciably different

b) Low viscosity

c) High surface tension

5) Safe to handle, i.e.,

a) Nontoxic

b) Nonflammable

c) Nonvolatile

6) Stable during storage or when in contact with acids or alkalis; i.e., does not hydrolyze during extraction or stripping

7) Cheap

In practice, however, it is not possible to find an extractant fulfilling all these requirements, and therefore a compromise is usually made. An extractant is seldom used in pure form; it is usually diluted with a cheap organic solvent in order to improve its physical properties, such as its viscosity, density, etc. This organic solvent called diluent, has no capacity to extract metal ions from solution, i.e. it is inert. The solution of the extractant in the organic solvent composes the organic phase and it's often referred to as the solvent. Besides fulfilling most of the requirements of an extractant, a diluent should be insoluble in water. Hydrocarbons and substituted hydrocarbons are therefore the most commonly used diluents.

2.3.1.2 *Solubility of extractants*

While diluents should be insoluble in water, the solubility of extractants in water may vary greatly. Tributyl phosphate, for example, is practically insoluble while a chelating agent such as acetyl acetone is completely soluble. Extraction by chelation is characterized by the

fact that although the extractant (i.e., the chelating agent) may be soluble, yet the metal chelate is insoluble in water but completely soluble in the diluent.

2.3.2 Theory of extraction

2.3.2.1 Mechanism of extraction

Extraction of metal ions

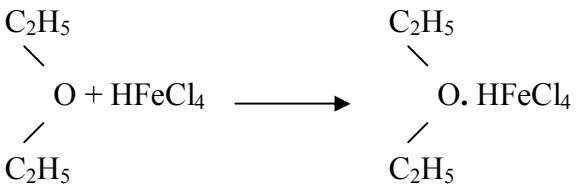
The transfer of metal ions from an aqueous phase to an organic phase is measured by the distribution coefficient D, which is defined as follows:

$$D = \frac{\text{Concentration of Metal in Organic Phase}}{\text{Concentration of Metal in the Aqueous Phase}} \qquad (2.1)$$

The higher the value of D at equilibrium, the higher is the extractability of the metal ions in question by that particular extractant.

Solvent extraction may be physical or chemical in nature. Physical processes are very few and in these, Nernst's distribution law is usually obeyed. In majority of cases, however, solvent extraction is a chemical process and Nernst's distribution law is not obeyed. In these processes metal ions or unchanged species in the aqueous phase enter into interaction with the extractant, and the reaction product is soluble in the organic phase. Interaction takes place in one of the following ways (Habashi, 1970):

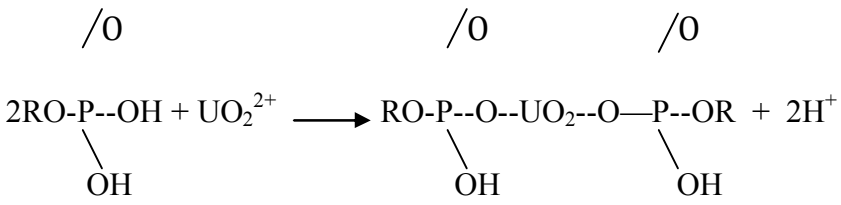
1.) *Ion-pair transfer* In this case, electrically neutral molecules interact with the extractant to form an addition compound. The most suitable extractants for such interaction are those having an oxygen atom with a lone pair of electrons, e.g., ethers, alcohols, and the neutral phosphoric acid esters. For example, diethyl ether extracts iron from hydrochloric acid solution as follows:



(2.2)

2.) *Ion-exchange* In this type, the metal is transferred from the aqueous phase as a simple ion, and at the same time an ion from the extractant is transferred stoichiometrically to the aqueous phase.

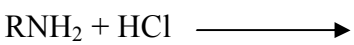
a.) Cation exchange The extracted specie is a positively charged ion and the extractant is an acid, e.g., monoalkyl phosphoric acid, dialkyl phosphoric acid, alkylpyrophosphoric acid, carboxylic acids, naphthenic acids, etc. For example, the extraction of uranium by a monoalkyl phosphoric acid takes place as follows:



(2.3)

It can be seen that one uranyl ion is exchanged for two hydrogen ions.

b.) Anion exchange The extracted species is a negatively charged ion and the extractant is a base, e.g., an amine,



(2.4)



(2.5)

It can be seen that an anion A^- is stoichiometrically exchanged for another anion.

Stripping of the organic phase

In the stripping process, two purposes are achieved:

1) Recovery of the metal values from the organic phase.

2) Regeneration of the extractant for recycle.

Stripping can be carried out in one of the following ways:

a) Back-washing the organic phase

b) Precipitation of metal values directly from the organic phase.

c) Selectively, when the organic phase is loaded with more than one metal ion.

The stripping coefficient is defined by

$$D' = \frac{\text{Concentration of Metal in Aqueous Phase}}{\text{Concentration of Metal in Organic Phase}} \qquad (2.6)$$

The higher the value of D' at equilibrium, the higher is the tendency of the metal ion to be transferred to the aqueous phase. The stripping coefficient is the inverse of the distribution coefficient D. Stripping agents depend on the nature of the extraction mechanism-whether ion-pair transfer or ion exchange. Ethers and neutral organic phosphorous compounds such as TBP are readily stripped by water.

2.3.3 **The organic phase**

2.3.3.1 Solvent loading

A certain weight of an extractant has a limited capacity for extracting a certain metal ion from solution. When this limit is reached the extractant is then saturated with the metal ion and is said to have reached its maximum loading. Maximum loading varies widely from one extractant to the other.

The organic phase increases in viscosity with increasing metal ion loading and sometimes it is necessary to operate at a solvent loading substantially below the maximum loading of the extractant. Saturation concentration can be determined by contacting the organic phase several times with fresh aliquots of the aqueous phase until the amount of metal in the organic becomes constant (Habashi, 1970).

2.3.3.2 Nature of extracted species

Usually at the saturation concentration the molecular ratio of extractant/metal ion extracted is a whole number, as can be expected from a reaction of the type,

$$M^{n+} + nHX ==== MX_n + nH^+ \quad (2.7)$$

Where n is an integer. However, the simultaneous extraction of other species may cause deviation from a whole number. The value of the saturation concentration helps to throw light on the stoichiometry of the reaction and the nature of the extracted species.

The saturated organic phase so obtained can be studied in a variety of ways. The simplest way is by heating it at low temperature and under vacuum to evaporate both the diluent and the uncombined extractant. The residue obtained, which may be a liquid or a crystalline solid, is the extracted species, that is, the compound between the metal and the extractant, and usually has a definite boiling or melting point. Infrared and nuclear magnetic resonance measurements are used extensively to identify the nature of the extracted species in the organic phase.

2.3.3.3 Role of diluents in solvent extraction

The diluents themselves are unable to extract metal ions from the aqueous phase, but they greatly affect the extraction behaviour of the solvent. The reason is the interaction that may

take place between the diluent and the extractant. Further, some diluents favor the polymerization of the extractants while others don't. Calorimetric measurements usually give a good indication about such interactions.

Correlation between the effect of a diluent and its dielectric constant is sometimes feasible. In extraction by cation exchange mechanism, the diluents having the least dielectric constant, e.g. kerosene and CCl_4, lead to the best extractions. This is because such diluents do not favor polymerization of the extractant in the organic phase through hydrogen bridges.

2.3.4 The aqueous phase

2.3.4.1 Effect of metal ion concentration

For the process

$$MY_{(a)} + nX_{(o)} ==== MY.nX_{(o)} \quad (2.8)$$

It was shown that

$$D = K[\ X\ ]^n \quad (2.9)$$

Where [X] is the concentration of free extractants at equilibrium. But

$$[\ X\ ] = [\ S\ ] - [\ MY.\ nX\ ] \quad (2.10)$$

where [S] is the total concentration of extractant, and [MY.nX] is the concentration of the extractant bound to the metal species. This latter concentration increases with increasing metal ion in the aqueous phase. Therefore [X] and consequently D should decrease with increasing metal ion concentration in the aqueous phase (Habashi, 1970).

2.3.4.2 Complex formation in the aqueous phase

Highly charged metal ions are usually complexed in the aqueous phase:

$$\text{Metal ion} + \text{Complexing agent} \;====\; \text{Metal complex} \qquad (2.11)$$

If the complex is electrically neutral, then extraction by ion-pair transfer is favoured. If it is electrically charged (positive or negative), then extraction by ion exchange mechanism (cationic or anionic respectively) is favoured. Complexing agents such as EDTA or ammonium thiocyanate are often added to the aqueous phase to facilitate extraction or separation of metal ions.

2.3.4.3 Effect of pH

Extraction by cationic solvents is greatly affected by the pH of the aqueous phase, since H^+ ions are taking part in the process:

$$M^{2+} + H_2X \;====\; MX + 2H^+ \qquad (2.12)$$

Decreasing the hydrogen ion concentration, that is increasing the pH shifts the equilibrium from left to right thus favouring the extraction. In many other cases the variation of distribution coefficient with pH may be due to the effect of the latter on the stability of the complexes in the aqueous phase.

2.3.5 Engineering aspects of extraction

2.3.5.1 Percent extraction

If the original weight of the solute in the aqueous phase is w, and after extraction it is decreased to w_1, then

$$D = \frac{(w - w_1) / V_o}{w_1 / V_a} \quad (2.13)$$

where V_o is the volume of the organic phase and V_a is that of the aqueous phase. From this equation it follows that

$$\frac{w_1}{w} = \frac{V_a}{V_o D + V_a} \quad (2.14)$$

Therefore

$$\text{Percent extraction} = (w - w_1)/w \times 100 \quad (2.15)$$

$$= (1 - w_1)/w \times 100 \quad (2.16)$$

$$= \frac{D}{D + V_a/V_o} \times 100 \quad (2.17)$$

2.3.5.2 Phase ratio

The volume ratio of the two phase is called the phase ratio. A high aqueous/organic ratio is sometimes undesirable because it may lead to high solvent losses. On the other hand, a high organic/aqueous ratio requires a large inventory of solvent, which may be a financial burden. While the percent extraction is a function of the phase ratio, the distribution coefficient is not.

2.3.5.3 Separation factor in extraction

When two metal ions are to be extracted from an aqueous solution by an organic solvent, the separation factor of the two metal ions is defined by

$$\beta = D_1 / D_2 \tag{2.18}$$

where D_1 and D_2 are the distribution ratios of the two metals. In order that separation is possible β must not equal 1 (Habashi, 1970).

2.3.5.4 Multiple extractions

If V_a = volume of aqueous phase containing w grams of the solute, V_o = volume of organic phase, and after the first extraction w_1 = weight of solute remaining in aqueous phase, then the equilibrium concentration in aqueous phase = w_1/V_a, and the equilibrium concentration in organic phase = $(w-w_1)/V_o$. Therefore

$$D = \frac{(w - w_1)/V_o}{w_1/V_a} \tag{2.19}$$

$$\frac{Dw_1}{V_a} = \frac{w - w_1}{V_o} \tag{2.20}$$

$$Dw_1.V_o = V_a w - V_a w_1 \tag{2.21}$$

$$(V_a + DV_o)w_1 = V_a w \tag{2.22}$$

$$w_1 = \frac{wV_a}{V_a + DV_o} \tag{2.23}$$

$$= w\left(\frac{1}{1 + DV_o/V_a}\right) \tag{2.24}$$

After the second extraction, w_2 = weight of solute remaining in aqueous phase; the equilibrium concentration in aqueous phase = w_2/V_a, and the equilibrium concentration in organic phase = $(w_1 - w_2)/ V_o$.

$$D = \frac{(w_1 - w_2)/V_a}{w_2/V_a} \tag{2.25}$$

$$w_2 = w_1 . \frac{1}{1 + D(V_o/V_a)} \tag{2.26}$$

$$= w \left(\frac{1}{1 + D(V_o/V_a)} \right)^2 \tag{2.27}$$

After n extractions,

$$w_n = w \left(\frac{1}{1 + D(V_o/V_a)} \right)^n \tag{2.28}$$

where w_n = weight remaining in aqueous phase after n extractions, or

$$\frac{w_n}{V_a} = \frac{w}{V_a} \left(\frac{1}{1 + D(V_o/V_a)} \right)^n \tag{2.29}$$

$$C_n = C_i \left(\frac{1}{1 + D(V_o/V_a)} \right)^n \tag{2.30}$$

where C_n = Concentration after n extractions,

C_i = Initial concentration in aqueous phase.

To keep C_n to a minimum, that is, for extracting the substance from the aqueous phase practically completely, it is better to keep V_o small and increase n, rather than the opposite.

2.3.6 Applications of solvent extraction

Solvent extraction is used extensively in the following fields:

1.) Recovery of a metal from a leach solution.

2.) Separation of two or more closely related metals.

3.) Purification of a leach solution, i.e., removal of an unwanted impurity such as iron.

2.3.6.1 Separation

An important application of solvent extraction is its use in separating a number of metals occurring together. This can usually be achieved by selecting the proper pH, adding a complexing agent in the aqueous phase, and above all choosing a solvent that shows more selectivity for one metal than for the other (Habashi, 1970; Perry *et al*, 1997).

2.4. Polyethylene Glycol and Solutions of Polyethylene Glycol

2.4.1. Introduction

Regulatory pressure is increasingly focusing on the use, manufacture, and disposal of organic solvents, and thus the development of nonhazardous alternatives (one of several goals of green chemistry and engineering) is vitally important for the continued and sustainable development of the chemical enterprise (Chen, *et al* 2005). There are many potential advantages to replacing volatile organic compounds (VOCs) with water or various types of aqueous solutions. The most obvious are low cost, reduced flammability, reduced toxicity, and reduced environmental risk as a result of discharges of the supporting phase. Water and aqueous-based solvent systems may represent an increasingly significant choice for the replacement of traditional solvents in synthetic chemistry. Other leading VOC

solvent alternatives include supercritical fluids, ionic liquids, immobilized solvents, solventless conditions, and the use of fluorous solvents (Chen, *et al* 2005).

2.4.2. Aqueous PEG solution properties

Polyethylene glycol, PEG: $HO–(CH_2CH_2O)_n–H$, is available in a variety of molecular weights from 200 to tens of thousands. At room temperature, the water soluble and hygroscopic polymer is a colorless viscous liquid at molecular weight < 600 and a waxy, white solid at molecular weights >800. The numerical designation of PEGs generally indicates the number average molecular weight (e.g., PEG-2000), although typically they are not monodisperse polymers. Liquid PEG is miscible with water in all proportions, and solid PEG is highly soluble in water, for example, PEG-2000 has a solubility of about 60% in water at 20^{o}C. Lower molecular weight liquid PEGs can be used as solvents in their own right with or without addition of water. These we define loosely here as low molecular weight PEG.

Unlike VOCs, low molecular weight liquid PEGs are nonvolatile. The vapor density for low molecular weight PEG is greater than 1 relative to air according to available MSDS data, and this is consistent with the industry standard for selection of alternative solvents to VOCs. PEG also has low flammability, and is biodegradable (Chen, *et al* 2005).

PEG has been found to be stable to acid, base, high temperature, O_2, H_2O_2 high oxidation systems, and $NaBH_4$ reduction systems, although partial oxidation of the PEG terminal –CH_2OH group to –COOH may occur in such systems as $H_2O_2–Na_2WO_4$. In addition, PEG may be recovered from aqueous solution by extraction with a suitable solvent or by direct distillation of water or solvent.

PEG usually has a far higher concentration in the upper (low-density) phase of such solutions in spite of its inherent density being greater than water. This, together with the properties of this PEG phase encourage the belief that it creates a predominantly low-density water environment due to its partially hydrophobic character, in turn mainly determined by the methylene groups. Further proof of this may be seen by use of microwave dielectric measurements, which show the water surrounding PEG to be ordered, whereas that surrounding more hydrophilic polymers is disordered (Chaplin, 2005). Also, the dissolution of PEG is exothermic (and increasingly exothermic with PEG size), in line with a shift in the ES⇌CS equilibrium towards the more ordered ES structure. It is interesting and perhaps not simply fortuitous that the diameter (4.9 Å) of the favored PEG helix (formed by trans, gauche, trans links across the C-O-C-C, O-C-C-O, C-C-O-C bonds) is the same as the diameter of the spines of the ES water cluster (4.7 Å) formed by pentagonal boxes, the ether (O-C-C-O) distances (2.88 Å) are close to the O···O distances (2.84 Å) in water and the next ether (O-C-C-O-C-C-O) (5.6 Å) distances are close to the next vertex distance on opposite sides of the pentagonal boxes (5.4 Å). Model building shows that optimum hydrogen bonding would tend to distort this PEG helix, however. The strongly-held hydration, as determined by viscosity, increases from two molecules of water per PEG monomer at very low polymerization (tetramer) to 5 molecules of water per PEG monomer for 45-mer (Chaplin, 2005), showing that the extent of water clustering increases with PEG size.

An interesting and revealing phenomenon occurs in PEG solutions as the temperature is raised; the solution at low temperatures separates into two phases (PEG-rich and PEG-poor) at higher temperature (separating at the cloud-point) and reverts to a single phase at even

higher temperatures. This may be explained as the PEG creating a low-density water environment with decreased entropy (Chaplin, 2005). At low temperatures a solution is formed due to the enthalpy of hydrogen bonding between the PEG and the water more than compensating for the entropy lost in forming the low-density water. This entropy loss is required, due to the hydrophobicity of the methylene groups, but is not great as the water is somewhat ordered already at lower temperatures. At the cloud point, the entropy cost is greater as the water is no longer naturally as structured, and two phases develop. At higher temperatures still, the water possesses excess energy and cannot be structured by the PEG. This reduces the entropic cost, so allowing a solution to form once more. Anions have a distinct effect on the cloud point in line with the Hofmeister series (cloud point lowering: I^- < Br^- < Cl^- < F^- < OH^- < SO_4^{2-} < HPO_4^{2-} < CO_3^{2-} < PO_4^{3-}); the greater lowering of the cloud point is in line with greater surface charge density (Chaplin, 2005), stronger hydration, greater tendency to avoid low-density water and the greater destruction of the natural structuring of the water. Cations have a lesser but opposite effect with chaotropes (*e.g.* NH_4^+) tending to lower the cloud point but kosmotropes (*e.g.* Li^+) raising it. Exceptionally, however, some di- and trivalent cations such as Mg^{2+} and Zn^{2+} act counter to their normal Hofmeister behavior, due presumably to their specific chelation to oxygen atoms in the PEG molecules (Chaplin, 2005).

Anions and cations distribute themselves differently between the phases depending on their affinity for low or higher density water but with the requirements that the phases be electrically neutral and iso-osmotic, so producing an interfacial potential difference, which may aid the partitioning of charged molecules. Preference for the PEG-rich or PEG-poor phase is related to the Hofmeister series for the structuring ability of the salts, particularly

the anions (*e.g.* preference for PEG-rich phase: $I^- > Br^- > Cl^- > F^- > SO_4^{2-}$; $Cs^+ > Na^+ > Ba^{2+} > Ca^{2+}$; preference for PEG-poor phase: $SO_4^{2-} > F^- > Cl^- > Br^- > I^-$)]. A similar Hofmeister series effect is noticed intensifying the incompatibility between two polymers such as polyethylenimine-PEG, or dextran-PEG, by increasing the concentration of strongly hydrated (CS-forming) anions, such as sulfate (Chaplin, 2005).

Note that the polymers formed with either one (-O-C-O-C-O-) or three (-O-C-C-C-O-C-C-C-O-) methylene groups between the oxygen atoms are both insoluble in water. The reason however is not so much that the O···O distances (2.18 Å and 4.79 Å respectively) fit less well with the water cluster spacing but rather that the molecules form almost-linear extended (rather than helical) chains with a pronounced hydrophobic character that have strong intra-molecular attraction.

2.4.2.1. *Phase separation*

Aqueous solutions of PEG display a miscibility gap characterized by lower and upper critical solution temperatures (LCST and UCST, respectively) in which the polymer and water segregate into polymer-rich and polymer-poor phases. The physical basis of this behavior is dependent upon the amphipathic nature of the polymer chain with its hydrophobic methylene groups interspersed with ether groups which can compliment the hydrogen bonded structure of water. Hydration/dehydration of these groups promotes the observed behavior. Similar phase incompatibility may be found in a number of different polymers such as PEG–PPG co-polymers, polyvinylpyrrolidone, poly-N-isopropylacrylamide, and in the clouding of non-ionic surfactants. Additionally, aqueous solutions of PEG phase separate in the presence of other, incompatible, but still water

soluble polymers. The exact nature of phase separation here is incompletely understood, but appears to be an UCST phenomenon perhaps based on incompatible hydrogen bonded structures, or on an excluded volume mechanism (Chen, *et al* 2005). PEG-based biphasic systems are generally formed by the addition of PEG and other water soluble polymers such as Dextran, above critical concentrations, however, many other pairs of polymers show incompatibility (and not only in aqueous solution); the phase separation of Ficoll and Dextran is an important example. Thus, aqueous PEG solutions may display phase separation under controlled conditions. Such phase separated solutions are known as ABS (Aqueous Biphasic Systems) or alternatively, ATPS (Aqueous Two-Phase Systems), and have been exploited in bioseparation for nearly fifty years since their discovery by Albertsson. Differences in phase preference between species can be adjusted by controlling the ABS system composition. The fact that PEG, and other polymers, form biphasic systems, having tunable phase properties is an important advantage that allows the development of versatile reactive extraction systems; a property of PEG solutions which has yet to be fully exploited (Chen, *et al* 2005).

2.4.2.2. *Solution polarity*

The poor solubility of organic reactants and their intermediates in water is the main limitation to the widespread application of water as a reaction solvent. Enhancement of the solubility of organic solutes in aqueous solutions, including the use of supercritical water, surfactants, co-solvents, and complexants, is an important aspect of the application of aqueous solutions as alternative solvents. For example, supercritical water is characterized by a reduced dielectric constant and a weaker hydrogen bonded network, which greatly increases the solubility of organic compounds. Eckert *et al* (1996) have pointed out that this

unusual combination of physical properties can provide environmentally benign separation and reaction processes (Chen, *et al* 2005). The water soluble polymer PEG can be considered a cosolvent in water which leads to an apparent decrease of the aqueous solution polarity. The consequent increase in solubility of organic molecules has led to the application of PEG as a solvent and a phase transfer catalyst (PTC) in organic synthesis. PEG, in aqueous solution, acting as a co-solvent, significantly changes many of the properties of water. Solutions of PEG in water may be viewed as monophasic, consisting of two homogeneously mixed components, or as biphasic, having large hydrated polymer molecules separated by regions of free water. Zaslavsky (1992) has made the argument that the latter viewpoint invites comparison of the resultant solution properties to the effects ascribed to vicinal water, i.e. water adjacent to solid interfaces, which has significantly different properties from pure water (Chen, *et al* 2005). In comparison to bulk water, vicinal water shows a decrease in density and dielectric relaxation, and an increase in viscosity and ionic conductance. Perhaps of even more significance to a discussion of PEG solutions as reaction media, is the effect of PEG on the polarity of aqueous solutions. Solution polarity is frequently measured by reference to the solvatochromatic properties of certain polarity sensitive dyes, in particular to Reichardt's betaine, from which is derived the molar electronic transition energy (ET) scale of polarity (Chen, *et al* 2005).

2.4.2.3. *PEG–metal ion complexes*

PTCs are usually used to transport an aqueous reagent into an organic phase in an activated state, so that the reaction can proceed as a consequence of bringing the aqueous reagent and organic reagent together. PEG has the ability to serve as a PTC since the polyethylene oxide chains can form complexes with metal cations, similar to crown ethers (Chen, *et al*

2005). To maintain electroneutrality, such PEG–metal cation complexes must bring an equivalent anion into the organic phase, thus making the anion available for reaction with the organic reactants. Many factors affect phase catalytic activity, such as PEG molecular weight, chain end effects, and the nature of the associated cations and anions. PEGs certainly have the ability to form complexes with metal cations. This property may be of some importance in the application of PEGs as alternative PTCs and in aqueous biphasic reactive extraction (ABRE) processes. Crown ether metal ion complexation depends on the fixed size of the cavity in the center of the crown. However, fixed molecular weight PEGs show more flexible selectivity in the binding of different size metal cations due to changes in helical conformation. During the phase-transfer process, PEG may transfer metal cations from the aqueous phase to the organic phase by complexation and partition. The corresponding anion is also forced to transfer to maintain electroneutrality, thus the inorganic or organic solvated anion may be activated in the organic phase for participation in the chemical reaction.

2.4.3. Liquid PEG as reaction solvent

PEG and its aqueous solutions represent interesting solvent systems for solvent replacement, and may stand comparison to other currently favored systems such as ionic liquids, supercritical carbon dioxide, and micellar systems. Recently, Sheftel (2000) has reviewed the general toxicological action of PEG such as acute toxicity, the mean lethal doses of all molecular weights of PEG, short and long-term, reproductive toxicity, and the mutagenicity in vitro or vivo. Additionally, relevant laws or regulations governing use in the European Union and from the US FDA were also included. One important difference between using PEG and other ‘neoteric solvents’ is that all of the toxicological properties,

the short and long-term hazards, and the biodegradability, etc., are established and known. For many of the other alternative solvent systems, lengthy investigations will be required to establish the necessary background safety and toxicological information. PEG is a hydrophilic polymer, easily soluble in water and many organic solvents including: toluene, dichloromethane, alcohol, and acetone, but it is not soluble in aliphatic hydrocarbons such as hexane, cyclohexane, or diethyl ether. The non-polar and hydrophobic hexane, slightly polar 2-octanone, and mildly polar heptanol, all showed some solubility in 70% PEG-300(aq), giving solutions of 0.01, 0.1, and 0.8 M, respectively (Chen, *et al* 2005).

2.4.4. PEG as phase-transfer catalyst (PTC)

PEGs and their many derivatives have been extensively investigated as PTCs, and are used in many commercial processes to replace expensive, and environmentally-harmful PTCs. Of the commonly used PTCs, linear PEGs are much cheaper than analogous macrocyclic crown ethers and cryptands (Chen, *et al* 2005). PEGs are also more stable at high temperatures, up to 150–200^{o}C, and show higher stability to acidic and basic conditions than quaternary onium salts.

2.4.5. Aqueous biphasic reactive extraction (ABRE)

The term aqueous biphasic reactive extraction (ABRE) has been used to describe the use of ABS as biphasic reaction media in which controlled partitioning of reactants, catalysts, and products, by choice of phase systems and manipulation of tie-line length (TLL), can be used to enable higher reaction yields, greater product selectivity, and simultaneous separation of reactants, products, and catalysts. ABS has been used for separations primarily relating to biological solutes and particles for almost half a century (Chen, *et al*

2005). Recent extension of this technology has been directed toward application as green separation media including, separation of organic hydrocarbon species and metal ions.

ABRE has three main characteristics: (1) phase separation benefiting separation of reactants and products, and providing a reaction driving force; (2) the PEG-rich top phase in PEG–salt ABS has organic solvent-like properties as a medium for reaction; (3) ABS components, PEG and metal salts, may be included in the form of PTCs and metal-catalysts. Two types of ABRE have been noted. One takes the form of a three-phase reaction, (Chen, *et al* 2005) and the other a two-phase reaction. The three-phase reaction results from adding organic reactants with or without corresponding supporting organic solvent into an ABS, thus, the system forms three phases initially as shown in Figure 2.9. The three phases are usually composed of the light organic phase, and the typical PEG–salt ABS made of the PEG-rich top phase and salt-rich bottom phase. The two-phase reaction results from the chemical or enzyme catalyzed reaction supported only by the normal ABS biphases as demonstrated in Figure 2.10.

2.4.5.1. *Three-phase reactions*

In order to enhance reaction rate and yield, PEG–salt ABS were formed to increase the organic reactant solubility and PEG concentration in the PEG-rich top phase, which has been described as an ABRE process applied to catalytic oxidation, substitution, and isomerization reactions. The currently rather limited number of investigations of ABRE processes, suggest that the role of ABS may be very important for increasing the reaction yield, however, the underlying mechanism is still largely unexplored. For the reactions shown in Figure 2.9, ABS formation results in a PEG rich top phase, which facilitates an increase in the solubility of some organic reactants (Chen, *et al* 2005). Secondly, phase

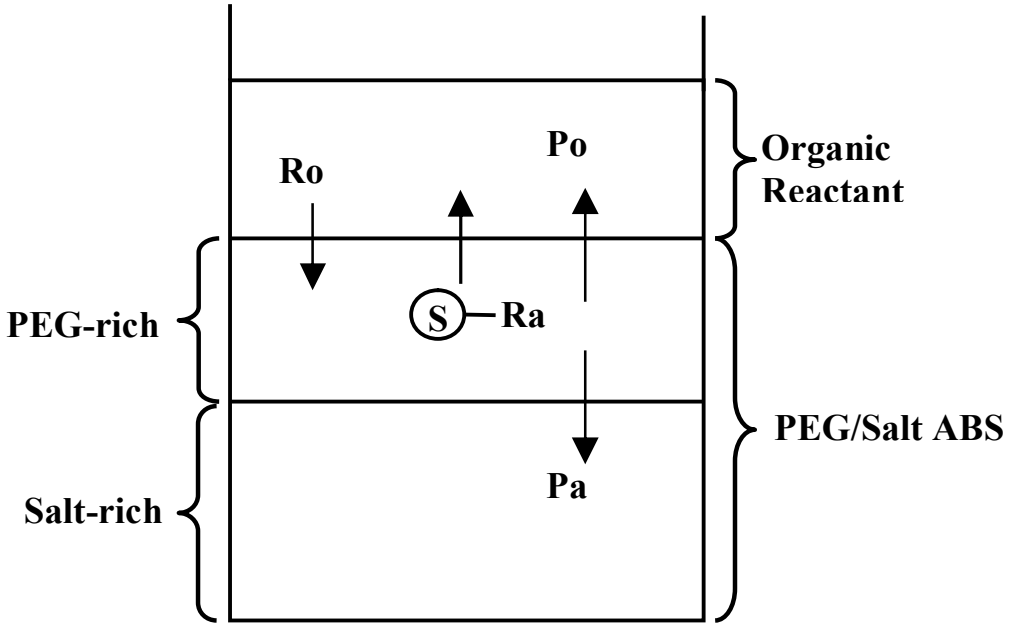


Figure 2.9 Three-Phase ABRE: Ro = organic reactant; Ra = aqueous reactant; Po = organic product; Pa = aqueous product; S = PTC

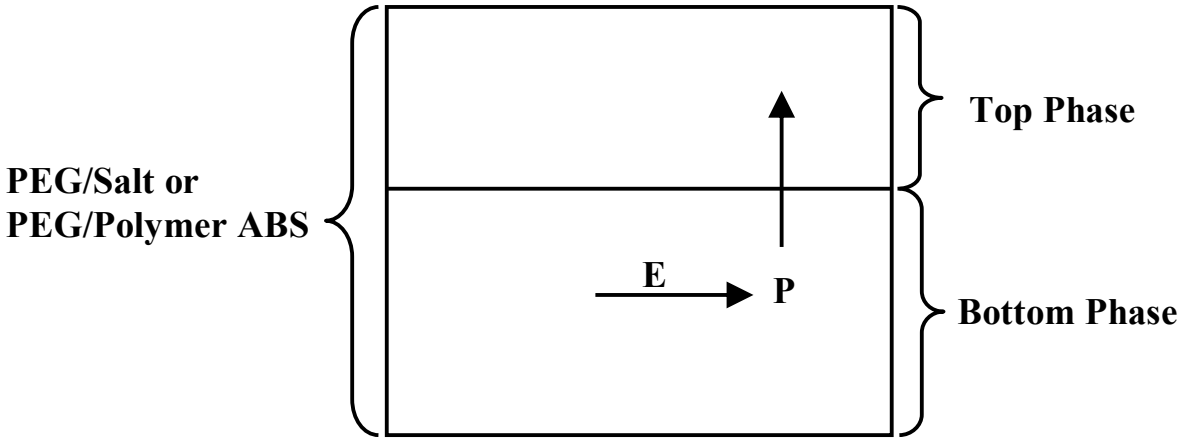


Figure 2.10 Typical enzyme hydrolysis reaction in ABS: S = substrate; E = enzyme; P = product

separation is useful for reactant and product separation, and thirdly, alteration of the reactant, product or catalyst distribution may be used to manipulate the reaction rate. In three-phase reactions, many solvophilic and solvophobic reactants may display some solubility in and partition, at least to some extent, to the PEG-rich top phase and the reaction may occur in this phase.

2. 5. Aqueous Biphasic Systems (ABS)

Aqueous biphasic systems (ABS) consist of two immiscible phases formed when certain water-soluble polymers are combined with one another or with certain inorganic salts in specific concentrations (Rogers, *et al* 1996, Graber, *et al* 2000, Zeng and Osseo-Asare, 2003, Liu, *et al* 2006 and Kamalika and Lahiri, 2006). They are formed when a water soluble polymer, [e.g., poly (ethylene glycol), PEG] is mixed with certain water – structuring salts [e.g., $(NH_4)_2SO_4$, K_2CO_3, K_3PO_4] (Rogers and Griffin, 1998; Graber, *et al* 2000). Poly (ethylene glycol) – based aqueous biphasic systems (PEG – ABS) can be utilized to separate and recover metal ions in environmental and hydrometallurgical applications. The related aqueous biphasic extraction chromatographic resins (ABEC), comprised of poly (ethylene glycol) covalently bonded to an inert support, may represent relatively benign systems for extractive processes for the separation of metal ions and organic molecules in industrial separations as well as environmental applications (Rogers and Griffin, 1998; Kamalika and Lahiri, 2006). Separation processes are ubiquitous in industry and systems employed in liquid-liquid separations processes frequently involve the use of toxic and volatile organic compounds (Rogers, *et al* 1998). Beijerinck first noted, in 1896, the 'incompatibility' of certain polymers in aqueous solution. In this case, two phases

were formed when agar was mixed with soluble starch or gelatin. Since then, many immiscible biphasic aqueous systems have been found utilizing hydrophilic polymers in aqueous solution; for example, poly(ethylene glycol) (PEG, HO-(CH_2-CH_2-O)$_n$-H where n is the degree of polymerization). The most thoroughly investigated of these is the aqueous dextran-PEG system, where dextran forms the more hydrophilic, denser, lower phase and PEG the more hydrophobic, less dense, upper phase (Chaplin, 2005). The basis of partitioning in these two phases depends on the surface properties of the particles, which include size, charge and hydrophobicity (Kamalika and Lahiri, 2006). A number of different chemical and physical interactions are involved for example hydrogen bonds, charge interactions, van der waals' forces, hydrophobic interactions, steric effects etc. (Kamalika and Lahiri, 2006).

Phases form when limiting concentrations of the polymers are exceeded. Both phases contain mainly water (typically 70-90% w/w water) and are enriched in one of the polymers. The limiting concentrations depend on the type and molecular weight of the polymers and on the pH, ionic strength and temperature of the solution (Chaplin, 2005). Some polymers form a two-phase system by themselves; PEG forming the upper more-hydrophobic phase in the presence of fairly concentrated solutions of citrates, phosphates or sulfates or at higher temperatures. Although sometimes perceived as due to polymer incompatibilities, the properties of these biphasic systems can be mainly attributed to incompatibility between aqueous pools of low and higher density water. Each phase may be considered as a different, although aqueous, solvent with properties determined by its structuring (Chaplin, 2005).

As two-phase systems they are suitable for carrying out liquid-liquid separations of various solutes such as biomolecules, metal ions, and particulates (Rogers, *et al* 1996, Zeng and Osseo-Asare, 2003 and Liu, *et al* 2006). The ability to utilize a number of different diluents, extractants, and aqueous phases makes solvent extraction a powerful separations method possessing a number of favorable characteristics including rapid extraction kinetics for many separations, the adaptability of the method to a wide variety of solutes, and back extraction or stripping of the solute and recycling of the solvent and/or diluent are often feasible (Rogers, *et al* 1996). Further, liquid-liquid extraction is capable of large volume throughput and is amenable to large-scale separations, and can be engineered for high selectivity and efficiency by the use of multistage contactors. In spite of these numerous advantages, there are several drawbacks to traditional oil-water solvent extraction. Even with today's environmental standards a number of extraction systems still utilize toxic and flammable organic diluents. When the diluent is coupled with a highly selective extractant the cost of the solvent system can become very expensive. (Not to mention the costs of safely designing a system to operate with a volatile or flammable diluent.) Finally, partitioning of a polar or charged solute from an aqueous phase into an organic medium requires dehydration, the extent of which depends upon the organic solvent. In some separations schemes this is trivial, while in others, particularly for the separation of metal ions, it is of paramount importance.

In ABS the major component in each of the two phases is water, (Rogers, *et al* 1996; Rogers and Griffin, 1998) and because of this non-denaturing environment these systems have been widely employed in biological separations for over 40 years. Prior to the work of Rogers, *et al* (1996), only a limited number of papers reporting metal ion separations in

aqueous biphasic systems were published with a single review comprehensively summarizing these results (Rogers, *et al* 1996). Compared with the traditional organic solvent extraction, an aqueous biphasic extraction system has the following advantages: less poisoning (nontoxic), non-flammable, quicker separation, easier operation, more clear phase boundary and no emulsification; and are biodegradable in nature (Pai, *et al* 2000, Zhang, *et al* 2001, Willauer, *et al* 2002, Liu, *et al* 2006 and Kamalika and Lahiri, 2006). To date, this method has been widely used to separate and purify proteins because it is gentle and does not denature fragile biomolecules and it can also serve as an extraction technology for metal ions (Liu, *et al* 2006). Recently, it was found that the mixture of alcohol and water also could form an aqueous biphasic extraction system by adding some inorganic salts (Liu, *et al* 2006).

A number of different water-soluble polymers may be utilized in ABS, with polyethylene glycols (PEGs), dextrans, and ficolls receiving the most attention. An even wider variety of polymer-salt combinations exists usually with Na^+, K^+, or NH_4^+ salts of mono- through trivalent anions like OH^-, CO_3^{2-} , SO_4^{2-}, and PO_4^{3-}. The partitioning of solutes in ABS is affected by numerous variables. The type and molecular mass of the polymer(s) and the type of salt (both the cation and anion are important) are amongst the most important variables, as are their respective concentrations. The phase-forming components must be present in sufficient quantities to create heterogeneous aqueous phases. Other important variables include system pH, temperature, and the addition of neutral and charged species which may be used to modify partitioning character. ABS retains all of the practical advantages of liquid-liquid extraction and also has a number of unique advantages due, in large part, to their aqueous nature. Polyethylene glycol-based aqueous biphasic systems

(PEG-ABS) are virtually nontoxic and non-flammable; all components are commercially available in bulk quantities and are inexpensive, and the systems have reasonable phase separation characteristics and can even be used with traditional solvent extraction equipment (Rogers, *et al* 1996). One of the most important advantages of aqueous biphasic systems is that partitioning takes place between two aqueous phases, therefore the effects of solute dehydration on the extraction process are diminished. When metal ions distribute to the PEG-rich phase only a subtle reorganization of the hydration sphere may be required, whereas in traditional solvent extraction near-complete dehydration may be necessary. Metal ion extraction in aqueous biphasic systems usually fits into one of three major categories (Zhang, *et al* 2001; Rogers, *et al* 1996; Rogers and Griffin, 1998): (1) extraction by the PEG-rich phase alone; (2) extraction of negatively charged metal complexes of inorganic anions; and (3) extraction using a water-soluble complexant. The majority of metal ion separations carried out thus far are from category three, and examples from category one are extremely rare, with TcO_4^- as the primary example (Rogers, *et al* 1996). Use of thiocyanate and halide anions to form anionic metal complexes has received scattered attention in aqueous two-phase separations.

As in conventional liquid–liquid extraction (Zeng and Osseo-Asare, 2003), the partition of particles in aqueous biphase systems is dependent upon the physicochemical interaction between the solid surface and the liquid solution, rather than the bulk properties of the solid or solution, such as density. Therefore, the selective partition of particles in different systems can be realized by controlling the surface chemistry of the solids or by carefully choosing aqueous biphase systems with specific interaction between liquid phase components and the solids (Zeng and Osseo-Asare, 2003).

Solute partitioning depends only on the composition of the phase-forming components PEG and salt (Willauer, *et al* 2002). The composition of the phases is the result of the salting-out ability of the salt and the number of ethylene monomers comprising the PEG. A solute added to ABS partitions between the phases, and its partition coefficient, K_{part} *(D)*, is defined as the solute concentration in the upper (top) phase divided by the solute concentration in the lower (bottom) phase (Fontana and Ricci, 2000 and Gupta, *et al* 2006).

$$K_{part\ (D)} = C_{top}/C_{bottom}. \tag{2.31}$$

The ability of a certain substance to partition in such a phase system maybe described as the sum of different factors which can be expressed as (Gupta, *et al*, 2006):

$$\ln K_{part} = \ln K_{el} + \ln K_{hydrophobic} + \ln K_{hydrophilic} + \ln K_{conformation} + \ln K_{of\ other\ factors} \tag{2.32}$$

where K_{el}, $K_{hydrophobic}$, $K_{hydrophilic}$, and $K_{conformation}$ denote partition factors due to electrical, hydrophobic, hydrophilic and conformation effects respectively. Thus, different factors of the system can be manipulated in order to achieve the desired effect. The two aqueous phases can be fine tuned to achieve excellent phase separation characteristics which are often quite similar to widely used oil-water systems. Heavy metal ions require a different approach for extraction: in traditional oil-water solvent extraction, complexing ligands are often necessary to coordinate the metal ion and give it a hydrophobic shell before partitioning to an organic solvent. To utilize this approach in PEG – ABS, water-soluble complexing ligands are required, because in the absence of ligands, the distribution ratios are often very low (Fontana and Ricci, 2000 and Zhang et al, 2001).

In ABS, the major component in each of the two immiscible phases is water, and thus a liquid/liquid extraction technology can be envisioned which completely eliminates the use of volatile organic compounds (VOCs). Elimination of VOCs has the potential to revolutionize many industrial processes by reducing potential downstream pollution while increasing safety. The goal of "Technology Vision" 2020 (Rogers, 2005) is to enable the chemical industry to continue to lead in technology development, manufacturing and profitability, while optimizing health and safety and ensuring environmental stewardship. One area of opportunity for new chemical science and engineering technology which will help meet this goal is the development of new separation technologies that eliminate the use of flammable, toxic VOCs such as solvents. Used in conjunction with, or instead of appropriate current manufacturing processes, such technologies would help to prevent pollution and increase safety. New separations technologies developed for pollution prevention may also find application in pollution remediation, helping to clean up the already contaminated sites.

Traditional solvent extraction employs partitioning of a solute between two immiscible phases, typically an organic solvent and an aqueous solution.

2.5.1. Phase diagrams, systems and properties

Phase diagrams are used for the characterization of aqueous two-phase systems. A phase diagram graphically depicts the phase behavior, thereby delineating the potential working area, of an aqueous two-phase system. Phase diagram consists of binodal curve and tie lines. Binodal curve divides a region into component concentrations that form two

immiscible phases. Tie line is a straight line that connects two nodes on the binodal curve, which represents the equilibrium concentration between both top and bottom phase (Srinivas and Regupathi, 2011).

Aqueous two phase systems (ATPS) or ABS have a unique phase diagram under a particular set of conditions such as pH and temperature (Raja *et al*, 2011). The phase diagram provides information about concentration of phase forming components required to form a two-phase, the concentration of phase components in the top and bottom phases, and the ratio of phase volumes. In Figure 2.11, the binodal curve TCB divides a region of component concentrations that will form two immiscible aqueous phases (above the curve) from those that will form one phase (below the curve). The three systems X, Y and Z differ in their initial compositions and in the volume ratios. However, they all have the same top phase equilibrium composition (T_{PEG}, T_{Salt}) and the same bottom phase equilibrium composition (B_{PEG}, B_{Salt}). This is because they are lying on the same tie-line (TB), whose end points determine the equilibrium phase compositions and lie in a convex curve called as the binodal curve. This curve represents the separation between the two immiscible phases. The binodal data is required for the design of ATPS extraction processes and development of models that predict partitioning of biomolecules, metal ions etc.

The tie line length (TLL) has units of %w/w, same as the component concentrations. The length of the tie line is related to the mass of the phases by the equation $V_t\rho_t/V_b\rho_b = XB/XT$ where V and ρ are the volumes and densities of the top (t) and bottom (b) phases and XB & XT are the segment lengths of the tie line as shown in Figure 2.11.

TLL and the slope of the tie-line (STL) can be related to the equilibrium phase composition as follows (Raja *et al*, 2011):

$$TLL = \sqrt{[B_{salt} - T_{salt}]^2 + [T_{PEG} - B_{PEG}]^2} \tag{2.33}$$

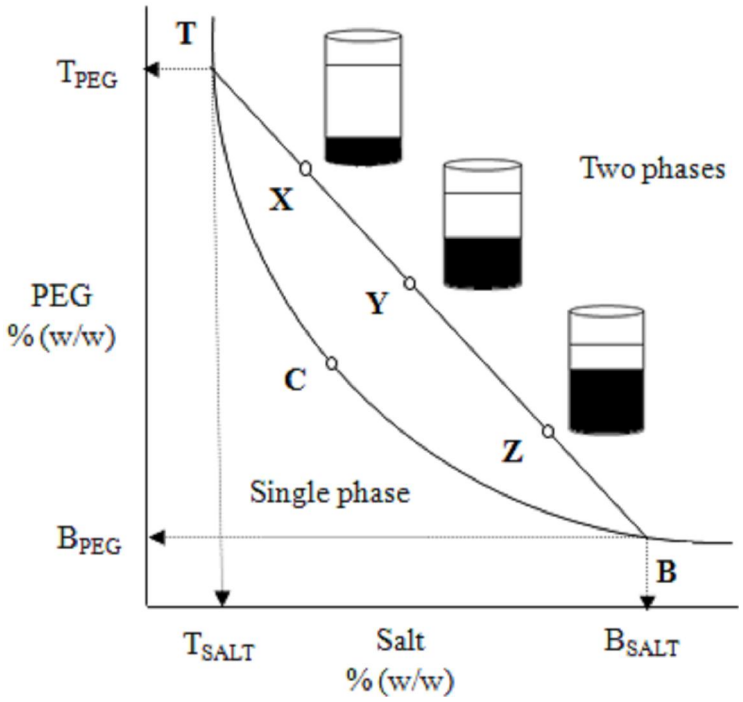


Figure 2.11. Binodal curve. In the figure, TCB = Binodal curve, C = critical point, TB = Tie line, T = composition of the top phase, B = composition of the bottom phase, and X, Y and Z = total composition of ATPS (Raja *et al*, 2011).

Tie lines are commonly parallel and hence the STL can be calculated by the following formula thus facilitating the construction of further tie lines.

$$STL = [T_{PEG} - B_{PEG}] / [B_{salt} - T_{salt}] = \Delta PEG / \Delta salt \quad (2.34)$$

As tie-lines decrease in length, they ultimately approach a critical point (C) on the binodal curve, where the TLL = 0. At this point the composition and volume of the two phases theoretically become equal.

2.6 Methods of Separating Tantalum and Niobium

Most of the methods used in separating Tantalum and niobium in tantalite entail using organic solvents (VOCs). To date no aqueous biphase separation has been attempted in this regard. The following review will cover some of these separations as geared ABS systems.

Stevenson and Hicks (1953) investigated the possibility of a tantalum-niobium separation based on the phenomenon that tantalum and niobium have been found to extract into certain polar organic solvents from aqueous solutions containing hydrofluoric and hydrochloric acids (Stevenson and Hicks, 1953). Diisopropyl ketone was chosen as a solvent for examination. In addition to the system tantalum-hydrochloric acid-hydrofluoric acid, the systems tantalum-sulphuric acid-hydrofluoric acid, tantalum-nitric acid-hydrofluoric acid, and tantalum-perchloric acid-hydrofluoric acid were investigated in their work. However, the system sulphuric acid-hydrofluoric acid seemed to offer the most nearly specific solvent-extraction separation and purification of tantalum and niobium.

Ellenburg, *et al* (1954) in their study, tribenzylamine, TBA, was of particular interest. It is water-insoluble and was known to form the corresponding amine acid salts which were also water-insoluble but, in general, soluble in various organic solvents (Ellenburg, *et al* 1954). Quantitative separation of niobium from tantalum was effected by extracting 11M HCl acid solution of the sample with 8% solution of TBA in chloroform or methylene chloride. Chloroform and methylene chloride were the only satisfactory solvents for TBA among those tested.

Fletcher, *et al* (1956) gave an outline of solvent extraction process for the purification of niobium from ores or from ferroniobium. They investigated two possible solvent extraction systems, based on the use of tributyl phosphate (TBP). The two systems involved

hydrofluoric acid-nitric acid and hydrofluoric acid-sulphuric acid solutions respectively (Fletcher, *et al* 1956). The extraction by TBP of iron, manganese, titanium and tin-which are frequently associated with niobium- is considerably less than that of niobium and tantalum.

Soisson, *et al* (1961) modified the classical Marignac method- the oldest method for separating tantalum and niobium. The Marignac method was based on the difference between the solubilities of K_2TaF_7 and K_2NbOF_5 in water containing a slight excess of hydrofluoric acid. The Marignac process and modification of it, used for many years, gradually gave way to the modified liquid-liquid (solvent) extraction method (Soisson, *et al* 1961). In the early liquid-liquid extraction process, tantalum fluoride was extracted from acid solution with aliphatic and aromatic ketones. The most used ketone was methyl isobutyl ketone (MIBK).

In the work of Butters, (1967) at the research department of Murex Ltd, UK, solvent extraction was applied to process for tantalum production. Reference was made to the work of Higbie and Werning who pointed clearly the choice of methyl isobutyl ketone as the solvent and HF or HF/H_2SO_4 as the aqueous medium (Butters, 1967).

In the work presented by Bureau of Mines (1975), reference was made on extraction of tantalum from mineral concentrates by dissolving the concentrate in hydrofluoric acid following by leaching with water and hydrochloric acid to remove impurities. Anhydrous hydrogen fluoride and potassium hydroxide were added to the solution and heated. The

resulting potassium-tantalum fluoride was separated from potassium-columbium oxyfluoride by solvent extraction with methyl isobutyl ketone. It was also mentioned that tantalum compounds can be extracted from concentrates by fusion with hot sodium hydroxide followed by acid treatment to remove impurities and separated from columbium compounds by fractional crystallization (Bureau of Mines, 1975).

Mayorov and Nikolaev (1996) described an investigation of the influence of macro-concentrations of impurity elements (Ti and Si) on Nb and Ta solvent extraction by tributyl phosphate (TBP) from fluoride solutions when mineral acids are absent, as well as Nb and Ta separation and purification from fluorotitanium acid solutions (Mayorov and Nikolaev 1996).

Yang and Hlavacek (1999), in their work, considered the carbochlorination reactions of tantalum and niobium pentoxides as representing an interesting route of extraction of tantalum and niobium from ores or minerals. In the chlorination process, the solid metal oxide reacts with a gaseous chlorinating agent in the presence of a reductant such as C or CO, to form metal chlorides. The chlorides are volatile at the operating temperatures, and are carried away by the gas stream, condensed, and then separated by rectification (Yang and Hlavacek 1999).

Welham, (2001), ball-milled a tantalum/niobium concentrate for up to 50 h in a laboratory mill without apparent phase change, other than a decrease in unit cell symmetry and some

amorphisation. The author therefore, examined in detail the effect of extended milling of a Ta/Nb concentrate on the rate of dissolution in a solution of sodium fluoride in hydrochloric acid. A number of mineral systems have shown that the leaching rate can be enhanced by milling, the enhancement being greater than that expected from the increase in surface area. This enhancement has been assigned to the increase in strain in the mineral and the formation of steps and kinks on the surface. It has been noted that the smaller crystallites formed during milling dissolve more rapidly than larger crystallites and this is considered due to the increased surface energy of smaller crystallites compared with larger crystallites (Welham, 2001).

Mayorov and Nikolaev (2002), presented the results of investigation into conditions of Ta and Nb separation and purification with the production of pentoxides of these elements. The extraction was done by octyl alcohol (octanol) from fluoride and fluoride-sulphuric acid solutions. It was mentioned that the efficiency of Octanol is shown to be comparable with methyl isobutyl ketone (MIBK). However, octanol was preferred in their work since MIBK is fire- and explosion-hazardous and readily soluble in aqueous solutions (Mayorov and Nikolaev, 2002).

Rodriguez, *et al* (2004), studied the effects of adding carboxylic acid to the leaching media upon the extraction of niobium and tantalum from a ferrocolumbite. The addition of carboxylic acids was also to introduce improvements in the process currently in use for the treatment of these minerals, which consists of the digestion with 70% hydrofluoric acid in open containers (Rodriguez, *et al* 2004).

El Hussaini and Rice (2004), leached niobium-tantalum ore using sulphuric acid. Niobium and tantalum were extracted from the leach liquor by a tertiary amine, Alamine 336, using kerosene and xylene as diluents and n-decanol as a modifier. The separation factor was greater for kerosene diluent (El Hussaini and Rice 2004).

CHAPTER THREE

MATERIALS AND METHODS

3.1 Materials and Reagents

The following materials and chemical reagents were employed for the project:

a) Tantalite ore $(Fe,Mn)(Ta,Nb)_2O_6$ 3 kg

b) Sulphuric acid (H_2SO_4) (Conc. 98%) 1L

c) Sulphuric acid (H_2SO_4) (95 - 97%) 2.5L

d) Hydrofluoric acid (HF) (48% & 47-51%) 1L

e) Poly ethylene glycol (PEG) 3350 500g

f) Poly ethylene glycol (PEG) 4000 500g

g) Poly ethylene glycol (PEG) 6000 250g

h) Poly ethylene glycol (PEG) 8000 500g

i) Poly ethylene glycol (PEG) 7000-9000 500g

j) Poly ethylene glycol (PEG) 10000 500g

k) Poly ethylene glycol (PEG) 12000 1 kg

l) Poly ethylene glycol (PEG) 20000 1 kg

m) Sodium sulphate 500g

n) Sodium hydroxide 500g

o) Potassium carbonate 500g

p) Ammonium sulphate 500g

q) Hydrochloric acid 0.5 L

r) Nitric acid 0.25 L

3.2 Methodology

3.2.1 General outline of methodology

In order to achieve the set objective of this study, the experiments were carried out as shown in the block diagram of Figure 3.1:

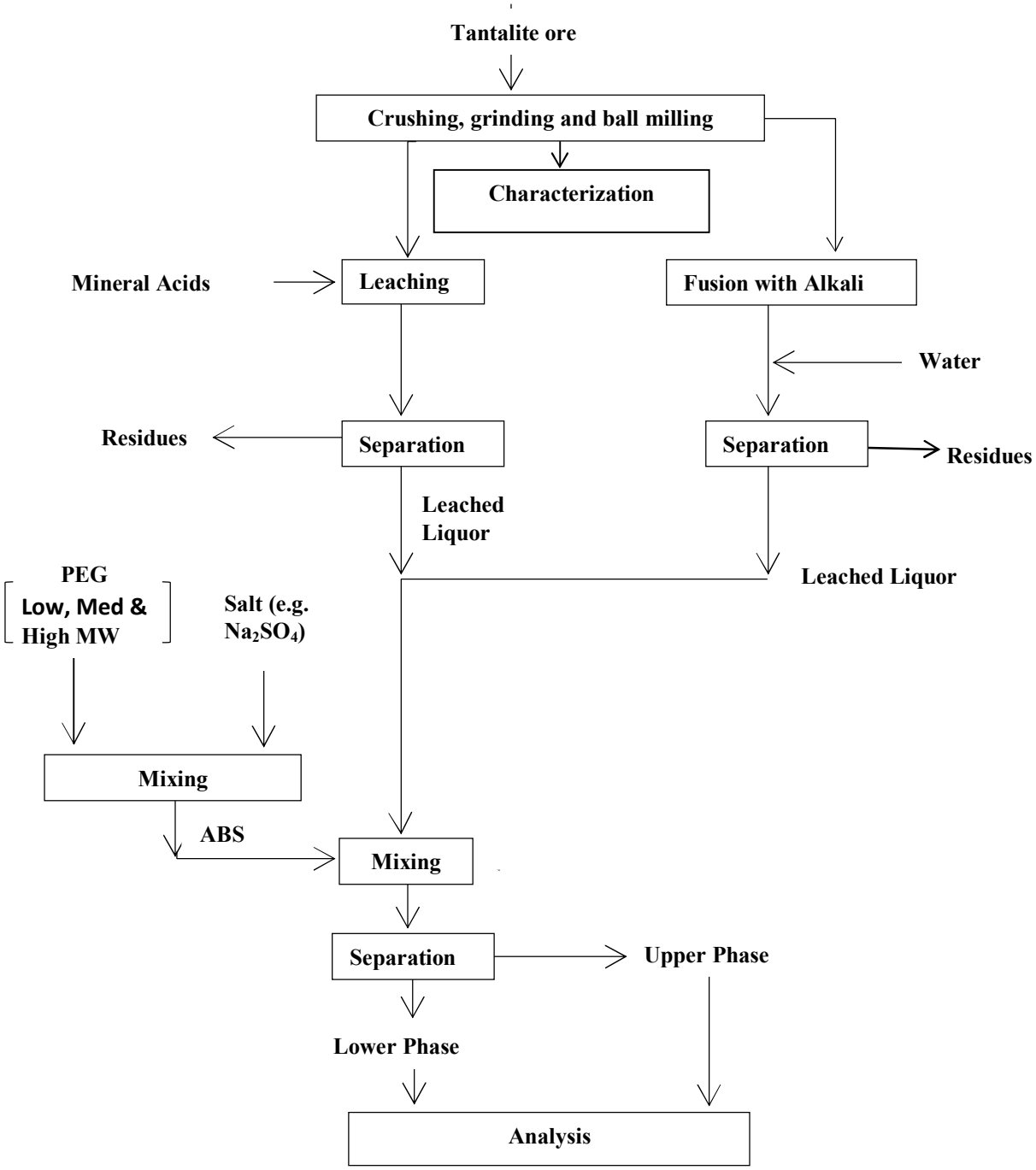


Figure 3.1 The Flow Diagram of the Experimental Procedure

3.2.2 Preparation and analysis of feed material

3.2.2.1 *Crushing and grinding of ore*

Three different samples of the tantalite ore were procured from three different sources. The first sample was procured from Jos market in Plateau State. The second and third samples were procured from Niger and Nasarawa States, respectively. The ore samples were crushed and ground to give a particle size range of 120 μm to 200 μm sieve size, using a Retsch, Type BB1 Masch No.70992 crushing machine.

3.2.2.2 *Ball milling and analysis of ore*

The crushed ores were ball milled for 6 h using a ball mill (KERA b.v. Soesterberg, Machine number 16083) to a particle size range of 120 μm to 74 μm. The ball milled samples were then sieved to particle size of -74 μm (200 mesh) using sieve (Test Sieve B.S 410/43, Endecotts filters Mesh No 72 PAT). Elemental analysis of the samples was carried out at the Center for Energy Research and Training (CERT), Ahmadu Bello University Zaria, using energy dispersive X-ray florescence (EDXRF) method. From the EDXRF result it was found that the tantalum content of the ore from Plateau state was the highest among the three ore samples. Hence, attention was focused on the ore from Plateau State. XRD (Pan analytical X' Pert MPD) and SEM (Carl Zeiss MA-10) were used to further analyze the ore sample from Plateau State.

3.2.3 Protocol for digesting samples

3.2.3.1 *Mineral acid leaching of the tantalite ore sample*

Standard solutions of the mineral acids were prepared as follows: i) 10.8M solution of 98% H_2SO_4 and ii) 15M solution of 48% HF. Fifty grams of the 74 μm ball-milled sample was

placed in a conical flask and then mixed with 150 g (≈ 81.6 ml) of 10.8M 98% H_2SO_4 acid at an acid/ore ratio of 3:1 and then with 81.6 ml 15M HF acid in order to improve on the dissolution of Ta and Nb; at an acid/acid ratio of 1:1 (Markland, 1974, El-Hussaini and Rice, 2004 and Maina *et al*, 2007). The mixture was stirred with a glass rod and the conical flask was placed on a magnetic heating plate. A magnetic stirrer was also placed inside the mixture, to enable stirring continuously as it was heated for 3 hr at 80 ^oC. This was to improve on the dissolution process in the conical flask. After the three-hour heating, the flask was removed from the magnetic plate and the magnetic stirrer removed. The mixture was left to stand for three minutes and decanted. The residue was then washed twice with deionized water. A general laboratory centrifuge (GLC – 2) was used to separate the solids from the water. This cycle was repeated until the pH of the solution was near neutral. After the final decantation, the residue was dried in an oven at 80 ^oC and weighed. The leached liquor (i.e. the decanted leached liquid) was kept for subsequent aqueous biphasic extraction.

Samples of the dried residue and leached liquor were taken for elemental/compositional analysis at Center for Energy Research and Training, Ahmadu Bello University Zaria. As noted earlier, the laboratory employed X-ray fluorescence and energy dispersive X-ray fluorescence methods. The results obtained from the analysis are presented in chapter four. A number of leaching processes were carried out by varying the molar concentration of the HF used. The various results with respect to the aforementioned leaching are also presented in chapter four. However, in view of the variance in the leaching results, a new set of mineral acids were purchased from Germany, through Zayo Chemicals Ltd. in Jos. A new set of standard solutions of the mineral acids were prepared. The leaching procedure described above was repeated with the new standard solution prepared with mineral acids

purchased from Germany. To check for reproducibility, a second leaching test was carried out with the new standard solutions.

Samples of the dried residues and those of the leached liquors were taken for elemental/compositional analysis at Center for Energy Research and Training, Ahmadu Bello University Zaria. The laboratory employs X-ray fluorescence methods, hence XRF (Mini pal 4 PW4025 Phillips Analytical) was used for analysis. The results obtained from the analysis are presented in chapter four.

3.2.3.2 *Alkali fusion of the tantalite ore sample*

Two grams of the tantalite ore ground to 74µm was weighed and mixed with 10 g of potassium hydroxide (KOH), which was earlier crushed with ceramic hand mortar and pestle, in the ratio of 1:5. It was labeled as sample 1. Another 2 g of tantalite ore was weighed and mixed with 10 g of crushed sodium hydroxide; and labeled as sample 2. The fusion experiments were performed in a high temperature furnace (Nabertherm GmbH LH120/14 Nr. /No. 182487) using ceramic crucibles. Both samples were placed inside the furnace and heated to 400 ^{o}C and allowed to fuse for one hour. After the reaction, the fused mass was taken out of the furnace and allowed to cool. Figure 5.3 show the fused mass obtained with the two alkali.

After cooling the fused mass, each sample was mixed with 100 ml of de-ionized water at room temperature for the leaching of tantalum and niobium. After the leaching, unreacted residues were separated by filtration. The resulting leachate and residues were analyzed for Ta and Nb by XRF and ICP–AES (OES Perkin Elmer Precisely, Optima 5300DV). The leachate was used in the subsequent aqueous biphase separation.

3.2.4 Preparation of aqueous biphase system solutions

Polyethylene glycol (PEG) of various molecular weights (PEG3350, PEG4000, PEG6000, PEG8000, PEG7000-9000, PEG10,000, PEG12,000 and PEG20,000) were purchased from Aldrich in Germany, through Zayo Chemicals Ltd. Jos and used as received. The PEGs were divided into three groups: Low MW PEG comprising 600 – 5,000 MW, Mid MW PEG comprising 6,000 – 8,000 MW and High MW PEG comprising 9,000 – 20,000 MW. The salts used in the aqueous biphase separation were: (i) sodium sulphate (a product from UK) purchased at Steve More's in Zaria and used as received; (ii) ammonium sulphate ($(NH_4)_2SO_4$) and (iii) potassium carbonate (K_2CO_3) obtained from the Department of Chemical Engineering, ABU, Zaria. To produce the aqueous biphase system, two stock solutions were prepared. 33.3 g of PEG was dissolved in 100 ml of water to yield the organic aqueous solution. The inorganic stock solution was prepared by dissolving 16.7 g of salt (e.g. $NaSO_4$) in 100 ml of deionized water. The ratio of PEG to salt used to form the ABS stock solutions by weight was 2:1 according to Zhang, *et al* (2001). However earlier, a PEG: Salt ratio of 1:1 by weight was tried in preparing the ABS stock solutions, but there was no clear separation into two phases. The ABS was formed by mixing equal volumes of PEG and salt stock solutions in the ratio of 1:1. Therefore, for the study 8 ml of PEG stock solution and 8 ml of salt stock solutions were mixed to form the ABS for each set of experiments. Meanwhile, a number of experiments were carried out to determine the formation of the ABS by varying the volume of PEG stock solutions from 1 ml upwards to the point when the biphase is formed; when keeping the volume of the salt stock solution constant. This was done to actually know the point at which the ABS was formed; and also to see the effect of the PEG molecular weight on the formation of the ABS. Thereafter, the volume of the PEG stock solution was kept constant, while the salt stock solution was

varied from 1 ml upwards to the point of biphase formation. A number of experiments were also carried out with $(NH_4)_2SO_4$ and K_2CO_3 salts stock solutions to determine the point at which the biphase is formed by varying the volume of the PEG stock solutions from 1 ml upwards, keeping the salt stock solutions constant. This was also done in order to see the effect of the PEG molecular weight. Thereafter, the PEG stock solutions were kept constant and the salt stock solutions varied from 1 ml upwards to the point of ABS formation.

The binodal curves were determined by the cloud point method (Ramyadevi *et al*, 2012). Initially the stock solution of PEG and salts of 33.3% and 16.7% respective concentration by weight were prepared and used for phase diagrams determination. A known amount of the salt solution was taken and titrated against PEG. To ensure the end point, PEG was added in drops till the appearance of turbidity. The first appearance of turbidity indicates that the system is about to enter the two-phase area. Water was then added until the disappearance of turbidity. The procedure was repeated to get the other binodal points. Thus, PEG concentration and the quantity of added salt were known and it was possible to calculate the percentage composition or fraction of a point of the binodal curve.

3.2.5 Separation of tantalum and niobium in the aqueous biphase

The leached liquors from the fusion process with NaOH and KOH were used for the extraction of tantalum and niobium in the aqueous biphase systems formed. Ten millilitres of each leached liquor was diluted with 10 ml of de-ionized water in the ratio of 1:1. Thereafter, 1 ml each of the diluted samples was added to the ABS formed earlier. Each sample was shaken vigorously for a few seconds (5 to 10) to ensure proper mixing; and

then allowed to settle down to enable the separation into the two-phase. The upper phase (PEG-rich phase) was separated from the lower phase (salt-rich phase). 1 ml each of the PEG-rich phase and salt-rich phase from the leached liquor with NaOH were diluted with 10 ml ethanol; while 1 ml each of the PEG-rich phase and salt-rich phase from the leached liquor with KOH were diluted with 10 ml de-ionized. The change in diluent was due to the shortage of the pure ethanol. The other ones used were not pure, as such formed precipitates. The two sets of samples were analyzed for tantalum (Ta) and Niobium (Nb) by Inductively-coupled plasma atomic emission spectroscopy (ICP–AES) [OES Perkin Elmer Precisely (Optima 5300DV)] at Pennsylvania State (PennState) University, U.S.A.

Another fresh sample of tantalum/niobium liquor was prepared and mixed with a freshly prepared ABS solutions of the various PEG molecular weights and sodium sulphate salt. This process was repeated in view of the long storage before analysis and effect of losses through precipitates of the PEGs and probably salts, in the earlier samples. Thereafter, the upper (PEG-rich) phase was separated from the lower (salt-rich) phase. The phases were not diluted with deionized water, this time around before sending for analysis. The samples were, once again analyzed for tantalum and niobium by Inductively-coupled plasma atomic emission spectroscopy (ICP–AES) [OES Perkin Elmer Precisely (Optima 5300DV)] at Pennsylvania State (PennState) University, U.S.A. The summary of the ABS sets of experiments carried out and the results of analyses are presented in chapter four.

CHAPTER FOUR

RESULTS

4.1 Introduction

This chapter presents the results of the data generated during the course of this work. The data was evaluated and statistical analysis was done to establish relationships.

4.2 Preparation and Analysis of Feed Materials

4.2.1 Characterization of the feed materials

Table 4.1 presents the chemical composition of the three tantalite ore samples procured from Plateau, Nassarawa and Niger States

Table 4.1 EDXRF analysis from CERT showing Chemical Composition of the three Tantalite Ore Samples procured.

Element/ compound	Ball milling time (6h) Sample from Plateau State	Sample from Nassarawa State	Sample from Niger State
MnO %	2.59	7.69	2.7
TiO_2 %	11.88	4.02	27.71
Fe_2O_3 %	11.86	14.9	27.33
Ta_2O_5 %	29.06	25.4	14.1
Nb_2O_5 %	15.31	47.78	27.8
Y (ppm)	640	389	-
Th (ppm)	-	2959	75
Zr (ppm)	2910	-	-
U (ppm)	980	-	-

4.3 Protocol for Digesting Samples

4.3.1 Mineral acid leaching of the tantalite ore sample

Table 4.2 presents the XRF analysis of the ore from Plateau State before and after leaching with mineral acids.

Table 4.2 XRF analysis of Tantalite ore from Plateau State before leaching and residue after leaching for 0.2M HF and 15M HF respectively in 10.8M H_2SO_4.

Compounds	Composition (wt. %)		
	Before Leaching	Residue 0.2M HF	15M HF
TiO_2	7.79	9.51	14.07
MnO	2.83	2.58	4.57
Fe_2O_3	9.46	9.0	13.84
Ta_2O_5	25.64	27.35	48.11
WO_3	5.09	5.4	10.58
ThO_2	0.22	0.16	0.37
U_3O_8	0.11	0.06	NA
ZrO_2	0.58	0.58	0.99
Nb_2O_5	22.89	23.92	40.63
ZnO	ND	ND	0.42
SiO_2	ND	ND	ND
CaO	ND	ND	ND
V_2O_5	ND	ND	ND
Cr_2O_3	ND	ND	ND

NA = Not available; ND = Not detected

Table 4.3 presents the XRF analysis of the ore from Plateau State before and after leaching with mineral acids.

Table 4.3 XRF analysis of Tantalite ore from Plateau State before leaching and residue after leaching for 20M HF, 15M HF and 2M HF respectively in 10.8M H_2SO_4.

Compounds	Composition (wt. %)			
	Before Leaching	Residue		
		20M HF	15M HF	2M HF
TiO_2	4.61	7.16	6.61	4.62
MnO	1.90	1.93	1.47	1.90
Fe_2O_3	6.51	6.28	6.18	6.25
Ta_2O_5	23.39	29.3	29.55	24.66
WO_3	5.94	3.99	4.33	5.84
ThO_2	0.26	0.36	0.30	0.20
U_3O_8	NA	NA	NA	NA
ZrO_2	0.81	0.99	0.95	0.76
Nb_2O_5	34.05	30.9	30.61	33.76
ZnO	0.24	0.32	0.31	NA
SiO_2	ND	ND	ND	ND
CaO	ND	ND	ND	ND
V_2O_5	ND	ND	ND	ND
Cr_2O_3	ND	ND	ND	ND

NA = Not available; ND = Not detected

Table 4.4 presents the XRF analysis of the ore from Plateau State before and after leaching with mineral acids.

Table 4.4 XRF analyses of Tantalite ore from Plateau State before leaching and residue after leaching for 2M HF in 10.8M H_2SO_4.

Compounds	Composition Before Leaching	(wt. %) Residue 2M HF
TiO_2	12.17	10.45
MnO	3.61	2.60
Fe_2O_3	11.81	10.23
Ta_2O_5	28.82	28.33
WO_3	ND	ND
ThO_2	0.22	0.14
U_3O_8	ND	ND
ZrO_2	0.32	0.32
Nb_2O_5	12.45	12.10
ZnO	ND	ND
SiO_2	ND	ND
CaO	ND	ND
V_2O_5	ND	ND
Cr_2O_3	ND	ND

ND = Not detected

Table 4.5 presents another XRF analysis of the ore from Plateau State before and after leaching with mineral acids.

Table 4.5 XRF analysis for 2M HF and 0.2M HF residues after leaching in 10.8M H_2SO_4.

Compounds	Composition (wt. %) Residue	
	2M HF Mean ± SD	0.2M HF
TiO_2	7.54 ± 4.12	9.51
MnO	2.25 ± 0.5	2.58
Fe_2O_3	8.24 ± 2.81	9.0
Ta_2O_5	26.5 ± 2.6	27.35
WO_3	5.84	5.4
ThO_2	0.17 ± 0.04	0.16
U_3O_8	NA	0.06
ZrO_2	0.54 ± 0.31	0.58
Nb_2O_5	22.93 ±15.3	23.92
SiO_2	NA	NA
CaO	NA	NA
V_2O_5	NA	NA
Cr_2O_3	NA	NA

NA = Not available

Table 4.6 presents the XRF analysis of the ore from Plateau State before leaching with mineral acids.

Table 4.6 XRF analysis for Tantalite ore sample from Plateau State before leaching.

Compounds	Composition (wt. %) Before Leaching CERT (Mean ± SD)
TiO_2	8.19 ± 3.8
MnO	2.78 ± 0.9
Fe_2O_3	9.26 ± 2.7
Ta_2O_5	25.95 ± 2.7
WO_3	5.52 ± 0.6
ThO_2	0.23 ± 0.02
U_3O_8	0.11
ZrO_2	0.57 ± 0.3
Nb_2O_5	23.13 ± 10.8
SiO_2	ND
CaO	ND
V_2O_5	ND

NA = Not available; ND = Not detected

Table 4.7 presents another XRF analysis of the ore from Plateau State after leaching with mineral acids.

Table 4.7 XRF analysis for 15M HF residues after leaching in 10.8M H_2SO_4.

Compounds	Composition (wt. %) Residue CERT (Mean ± SD)
TiO_2	10.34 ± 5.3
MnO	3.02 ± 2.2
Fe_2O_3	10.01 ± 5.4
Ta_2O_5	38.83 ± 13.1
WO_3	7.46 ± 4.4
ThO_2	0.34 ± 0.04
ZrO_2	0.97 ± 0.03
Nb_2O_5	35.62 ± 7.08
ZnO	0.37 ± 0.08
SiO_2	ND
CaO	ND
V_2O_5	ND
Cr_2O_3	ND

NA = Not available; ND = Not detected

Table 4.8 presents the XRF analysis of the ore from Plateau State before leaching with mineral acids.

Table 4.8 XRF analysis for Tantalite ore from Plateau State before leaching (Each analysis was repeated as shown).

Compounds	Composition (wt. %) Before Leaching	
TiO_2	10.2	11.0
MnO	4.76	4.95
Fe_2O_3	14.49	15.0
Ta_2O_5	31.4	32.5
WO_3	8.13	8.34
ThO_2	ND	ND
U_3O_8	ND	ND
ZrO_2	ND	ND
Nb_2O_5	16.3	19.4
ZnO	ND	ND
SiO_2	5.9	4.2
CaO	0.61	0.57
V_2O_5	0.24	0.29
Cr_2O_3	0.15	0.082
NiO	0.17	0.061
Y_2O_3	ND	ND
SnO_2	1.5	2.7
PbO	ND	0.70

NA = Not available; ND = Not detected

Table 4.9 presents the XRF analysis of the ore residues from Plateau State after leaching with mineral acids.

Table 4.9 XRF analysis for 2M HF and 15M HF residues after leaching of the Tantalite ore in 10.8M H_2SO_4. (Each analysis was repeated as shown).

Compounds	Composition (wt. %)	
	Residue	
	2M HF (Mean ± SD)	15M HF (Mean ± SD)
TiO_2	10.95 ± 0.5	9.9 ± 0.1
MnO	5.08 ± 0.04	4.32 ± 0.01
Fe_2O_3	13.51 ± 0.2	11.68 ± 0.06
Ta_2O_5	35.2 ± 0.57	35.7 ± 0.71
WO_3	8.15 ± 0.08	8.55 ± 0.18
ThO_2	ND	ND
U_3O_8	ND	ND
ZrO_2	ND	ND
Nb_2O_5	19.85 ± 2.76	21.65 ± 0.92
ZnO	ND	ND
SiO_2	4.0	2.15 ± 0.21
CaO	0.45 ± 0.06	0.52 ± 0.47
V_2O_5	0.27 ± 0.06	0.28
Cr_2O_3	0.1 ± 0.06	0.08 ± 0.02
NiO	0.1 ± 0.08	0.09 ± 0.04
Y_2O_3	ND	ND
SnO_2	3.13 ± 0.89	4.71 ± 0.42
PbO	0.85 0.21	0.74

ND = Not detected

Table 4.10 presents the XRF analysis of the leached liquors with mineral acids.

Table 4.10 XRF analysis of leached liquors for 2M HF and 15M HF in 10.8M H_2SO_4.

Compounds	Composition (wt. %)	
	Leached Liquor	
	2M HF	15M HF
	Mean ± SD	Mean ± SD
TiO_2	4.03 ± 0.46	2.57 ± 0.63
MnO	2.07 ± 0.5	1.81 ± 0.66
Fe_2O_3	11.17 ± 3.24	4.2 ± 0.94
Ta_2O_5	8.16 ± 0.66	7.17 ± 0.11
WO_3	2.94 ± 0.29	2.19 ± 0.01
ThO_2	ND	ND
SO_3	52.9 ± 2.12	60.3 ± 1.56
ZrO_2	ND	ND
Nb_2O_5	-	-
ZnO	0.1 ± 0.04	0.07 ± 0.03
SiO_2	1.35 ± 0.91	-
CaO	0.35 ± 0.01	0.36 ± 0.12
V_2O_5	0.14 ± 0.02	0.07 ± 0.02
Cr_2O_3	0.08 ± 0.04	0.03 ± 0.02
NiO	0.07 ± 0.04	0.02 ± 0.01
SnO_2	ND	ND
PbO	ND	0.37 ± 0.13

ND = Not detected

Figure 4.1 presents the XRD patterns of tantalite ore from Plateau State before leaching.

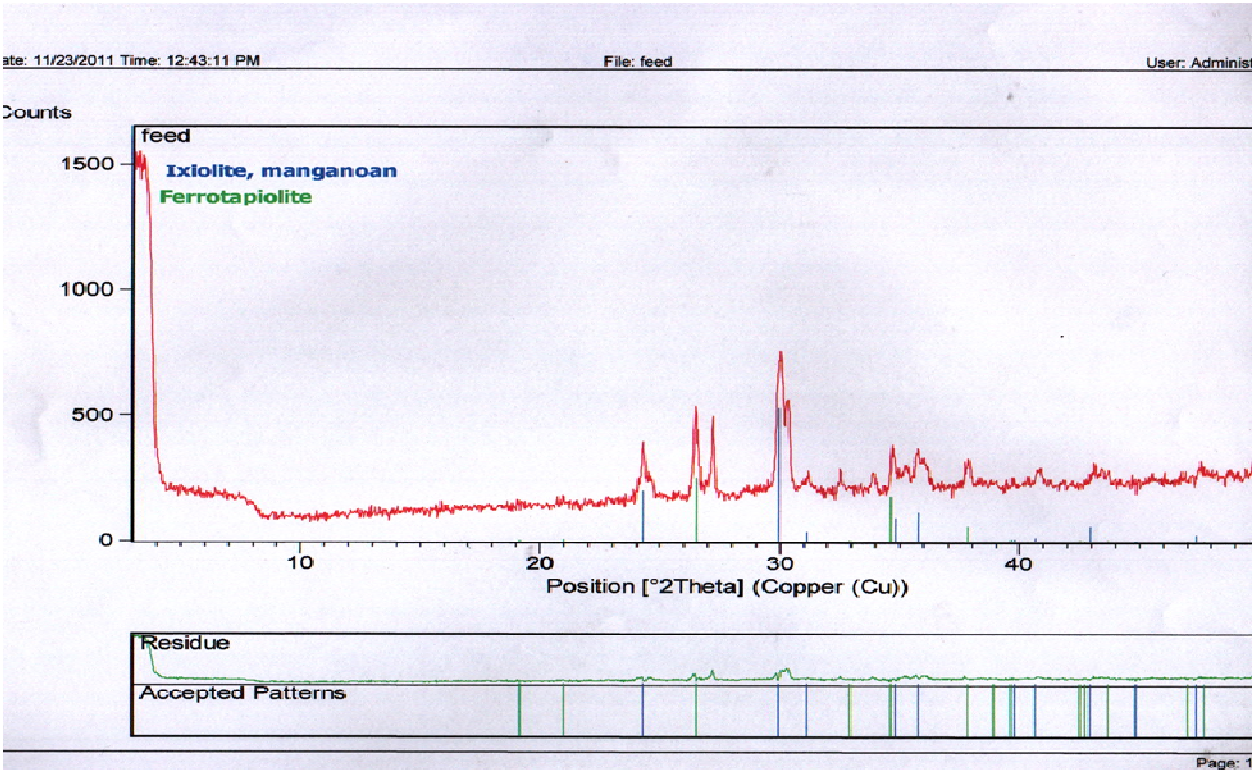


Figure 4.1 XRD Analysis of the Tantalite ore from Plateau State before leaching

Figure 4.2 presents the XRD pattern of the leached tantalite ore residues from Plateau State.

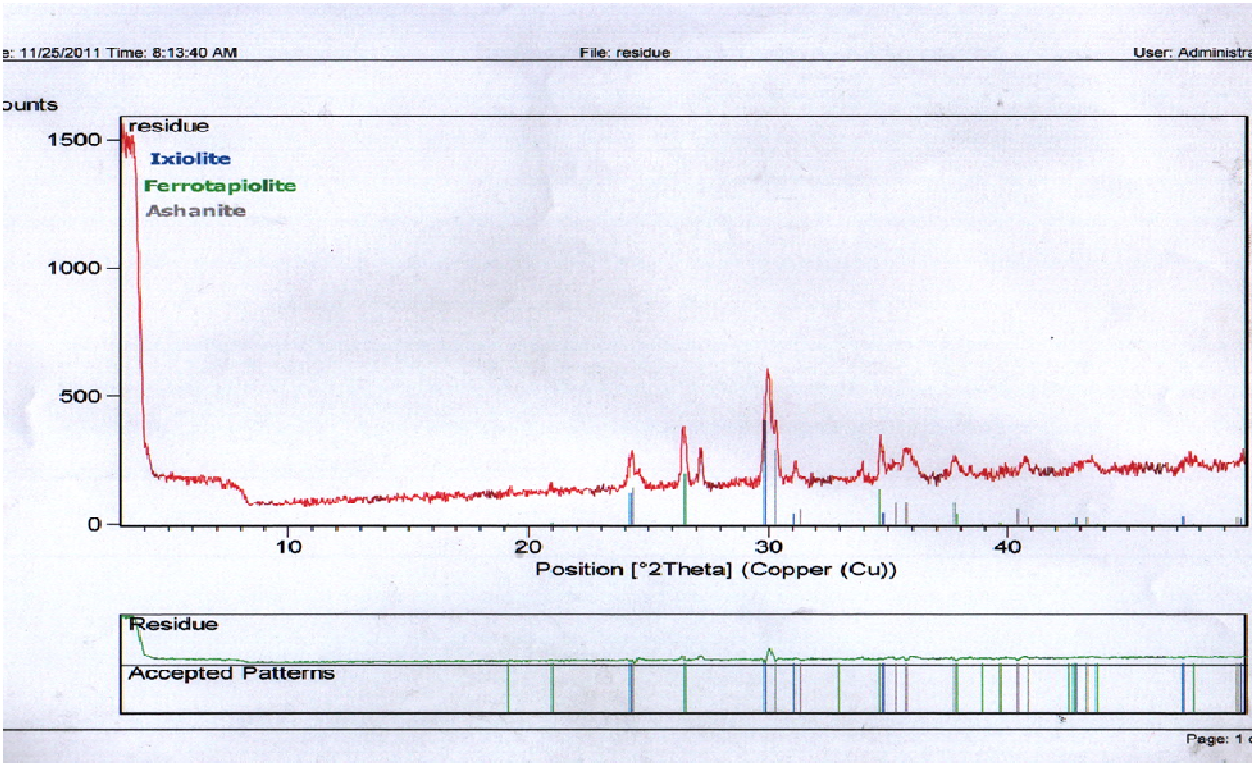


Figure 4.2 XRD Analysis of the leached Tantalite ore residues from Plateau State

Figure 4.3 present the SEM images of the Tantalite ore from Plateau State before leaching at 10 µm and Mag at 1.00 K X

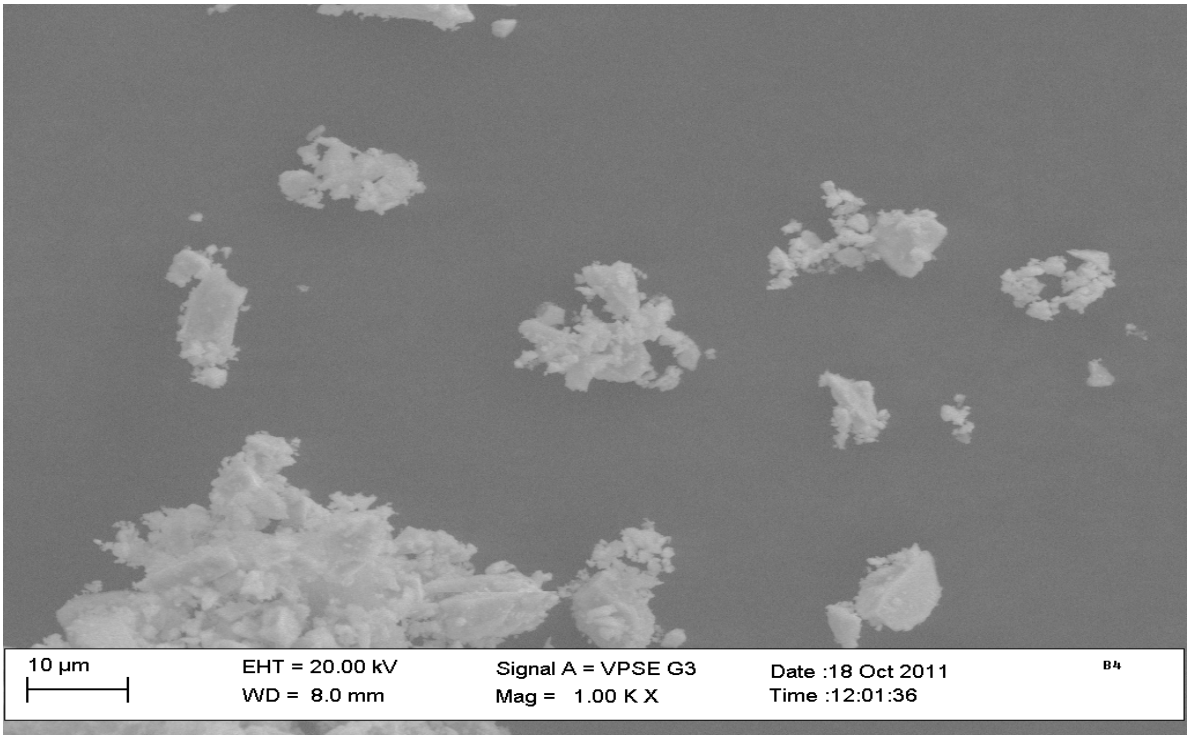


Figure 4.3 SEM images of the Tantalite ore from Plateau State before leaching at 10 µm and Mag at 1.00 K X

Figure 4.4 presents the SEM images of the Tantalite ore from Plateau State before leaching at 20 µm and Mag at 200 X

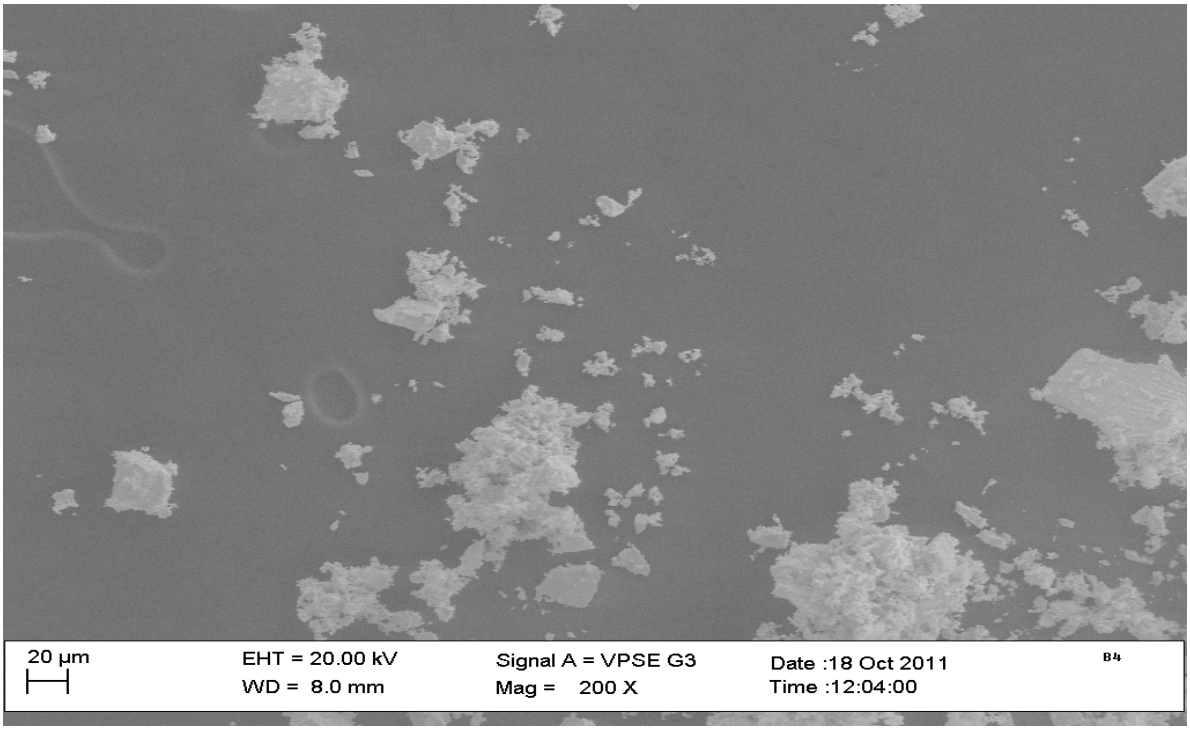


Figure 4.4 SEM images of the Tantalite ore from Plateau State before leaching at 20 µm and Mag at 200 X

Figure 4.5 presents the SEM images of the Tantalite ore from Plateau State before leaching at 2 μm and Mag at 2.03 K X

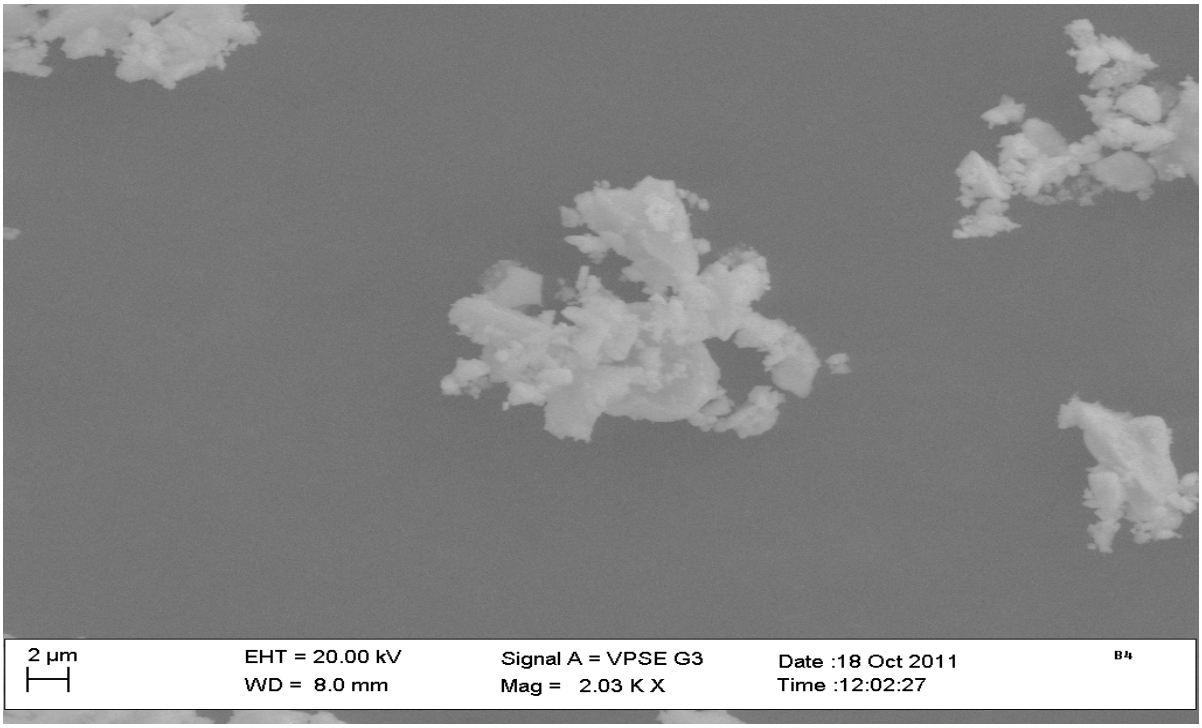


Figure 4.5 SEM images of the Tantalite ore from Plateau State before leaching at 2 μm and Mag at 2.03 K X

Figure 4.6 presents the SEM images of the Tantalite ore from Plateau State before leaching at 30 µm and Mag at 500 X

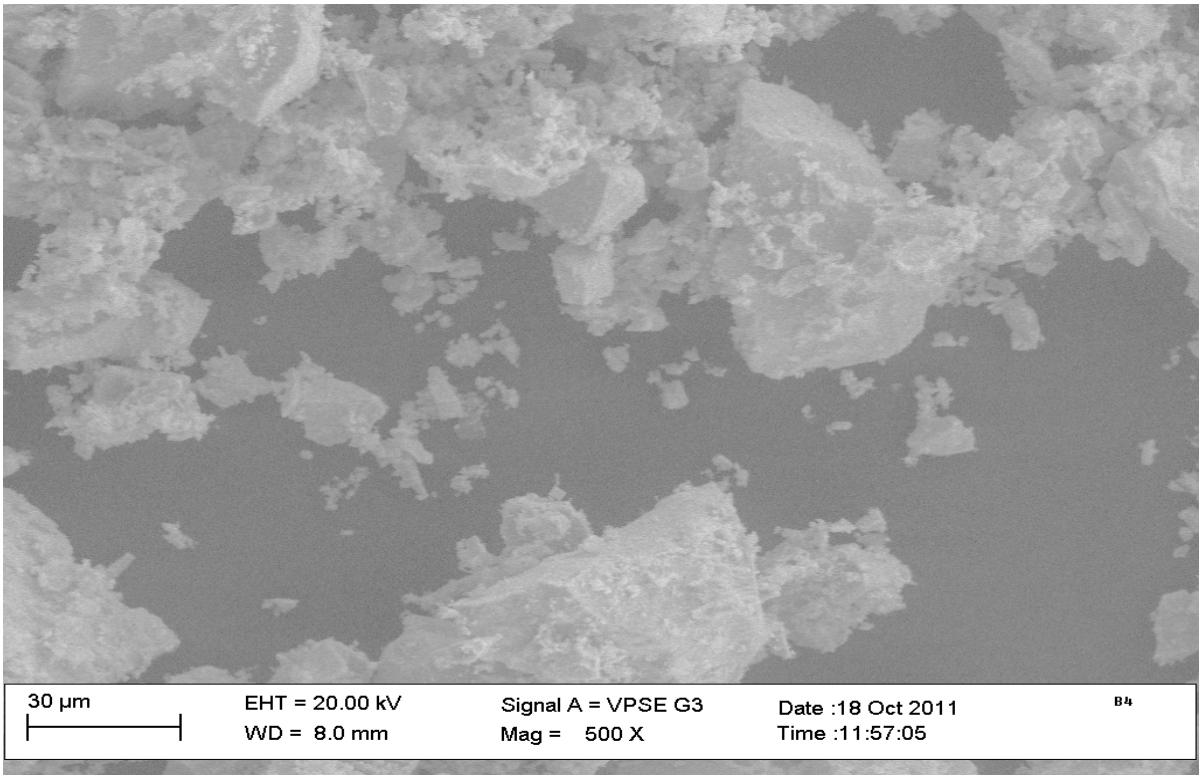


Figure 4.6 SEM images of the Tantalite ore from Plateau State before leaching at 30 µm and Mag at 500 X

Figure 4.7 presents the SEM images of the Tantalite ore from Plateau State before leaching at 20 µm and Mag at 500 X

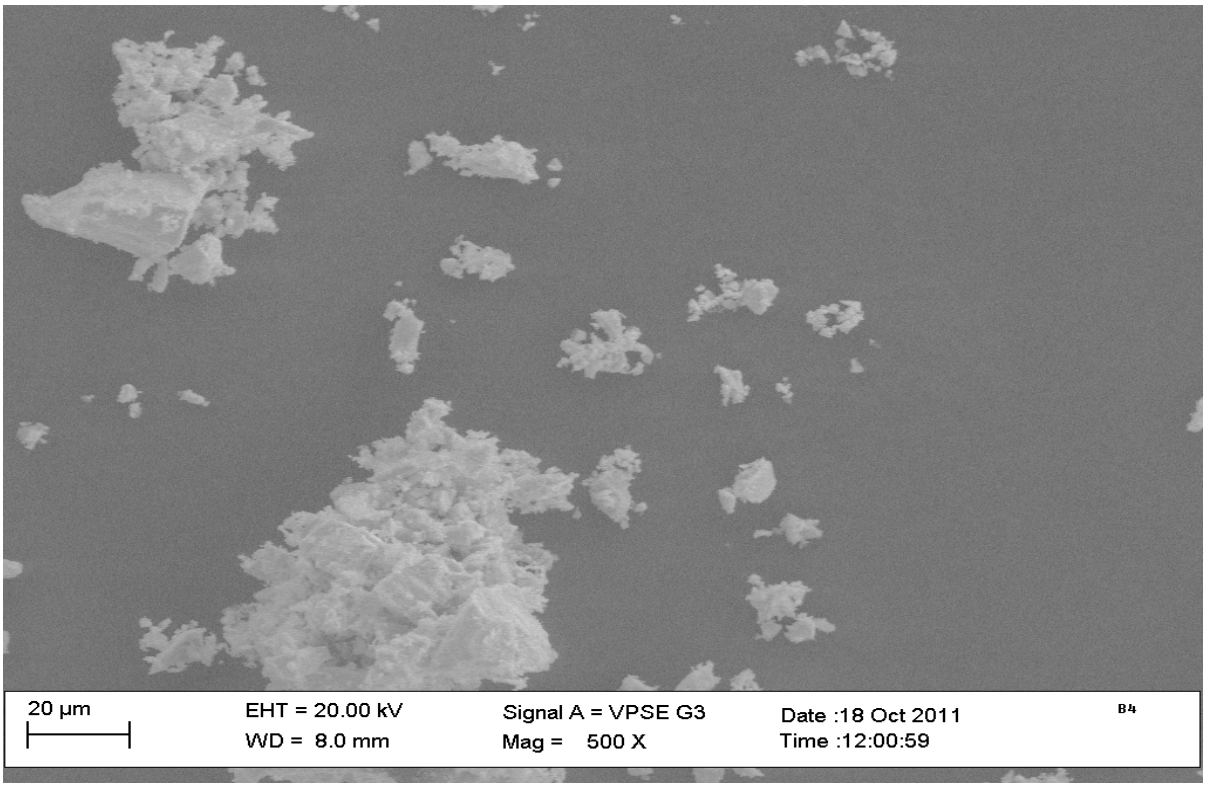


Figure 4.7 SEM images of the Tantalite ore from Plateau State before leaching at 20 µm and Mag at 500 X

Figure 4.8 presents the SEM images of the Tantalite ore from Plateau State before leaching at 2 μm and Mag at 5.00 K X

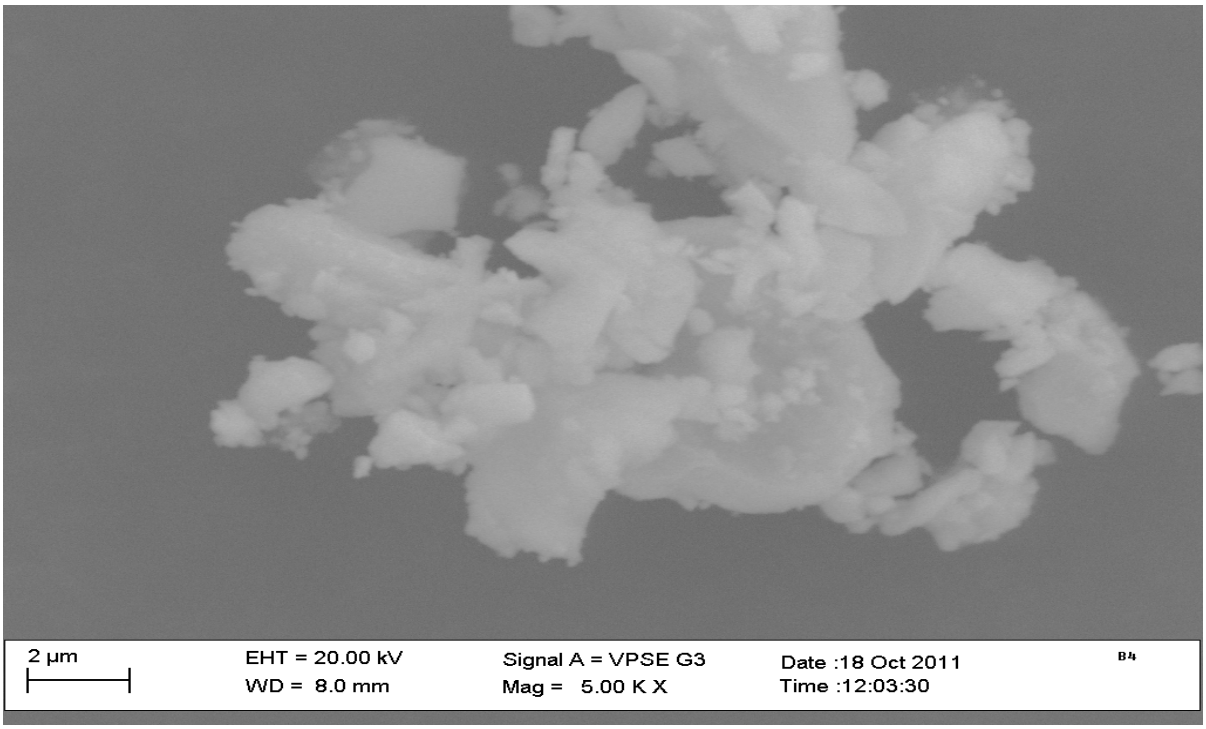


Figure 4.8 SEM images of the Tantalite ore from Plateau State before leaching at 2 μm and Mag at 5.00 K X

Figure 4.9 presents the SEM images of the Plateau State residues after leaching at 10 µm and Mag at 1.01K X

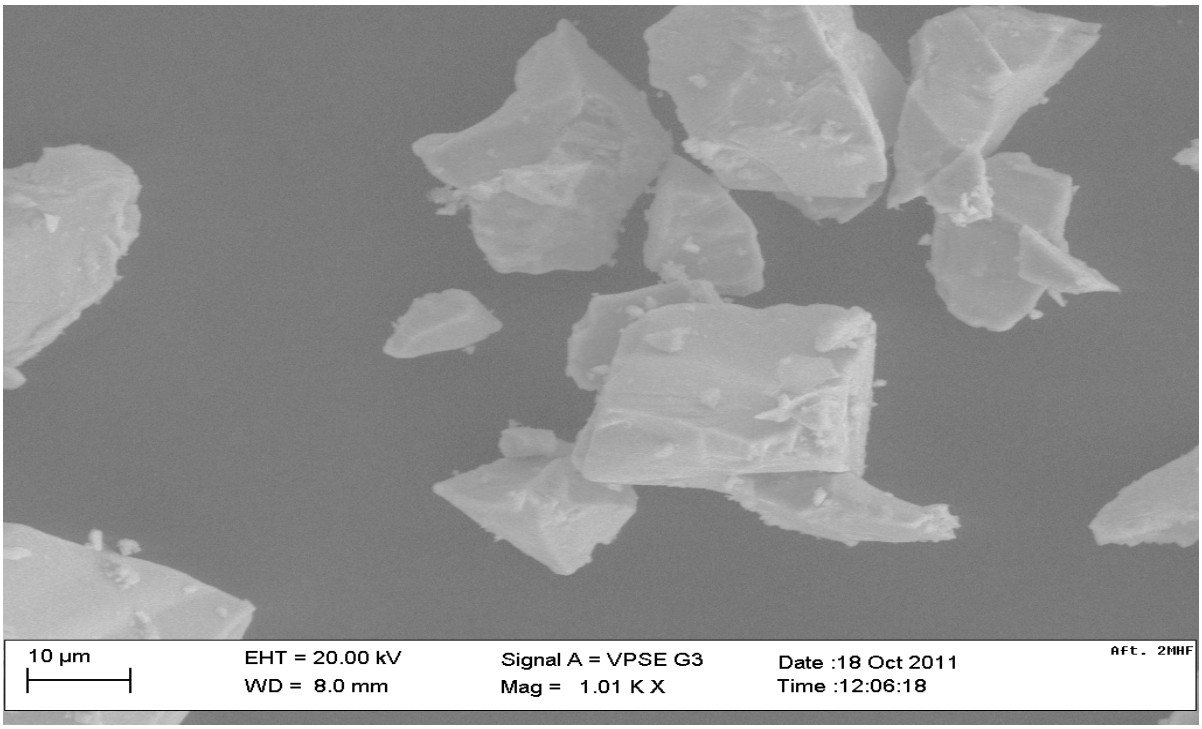


Figure 4.9 SEM images of the Plateau State residues after leaching at 10 µm and Mag at 1.01K X

Figure 4.10 presents the SEM images of the Plateau State residues after leaching at 2 µm and Mag at 2.00 K X

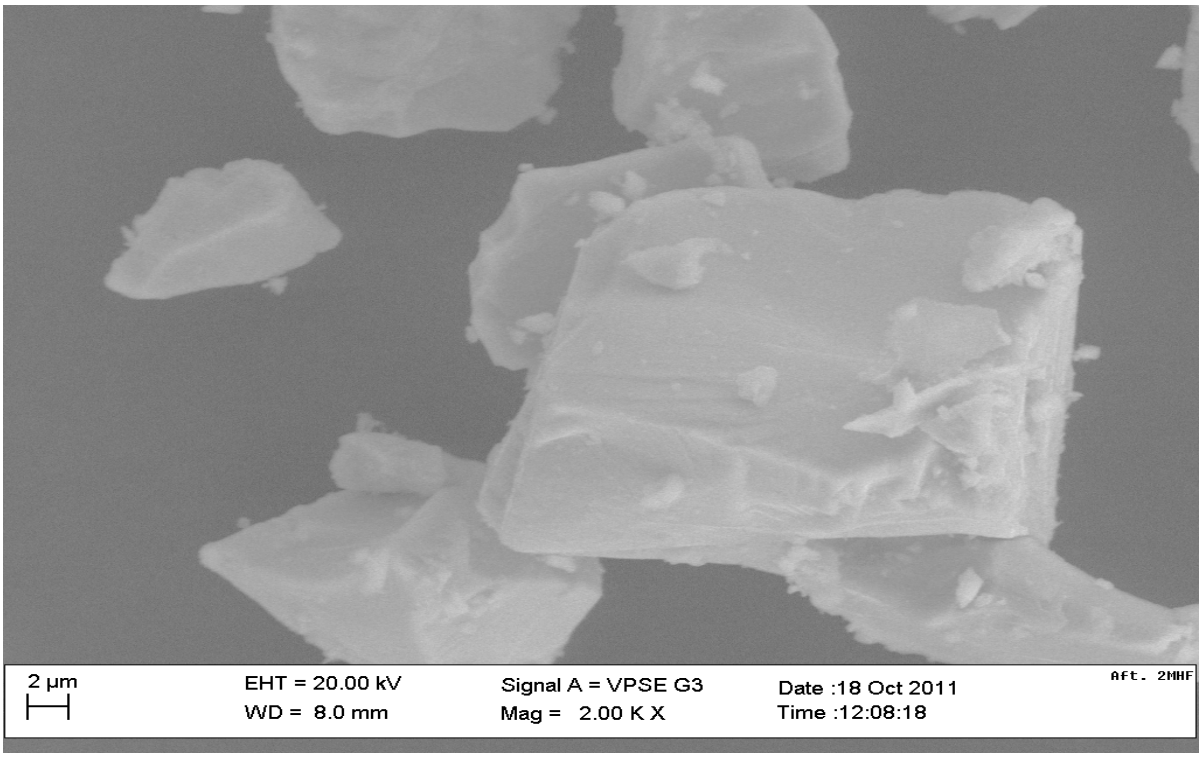


Figure 4.10 SEM images of the Plateau State residues after leaching at 2 µm and Mag at 2.00 K X

Figure 4.11 presents the SEM images of the Plateau State residues after leaching at 20 µm and Mag at 200 X

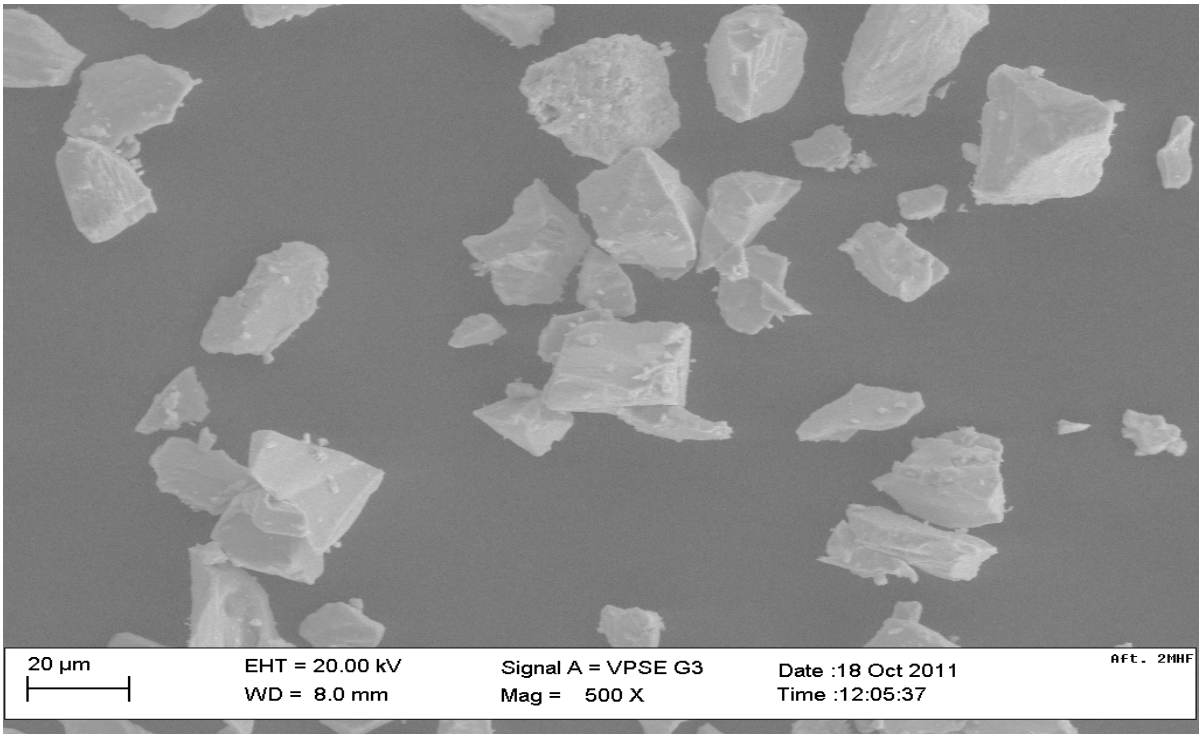


Figure 4.11 SEM images of the Plateau State residues after leaching at 20 µm and Mag at 200 X

Figure 4.12 presents the SEM images of the Plateau State residues after leaching at 2 µm and Mag at 5.00 K X

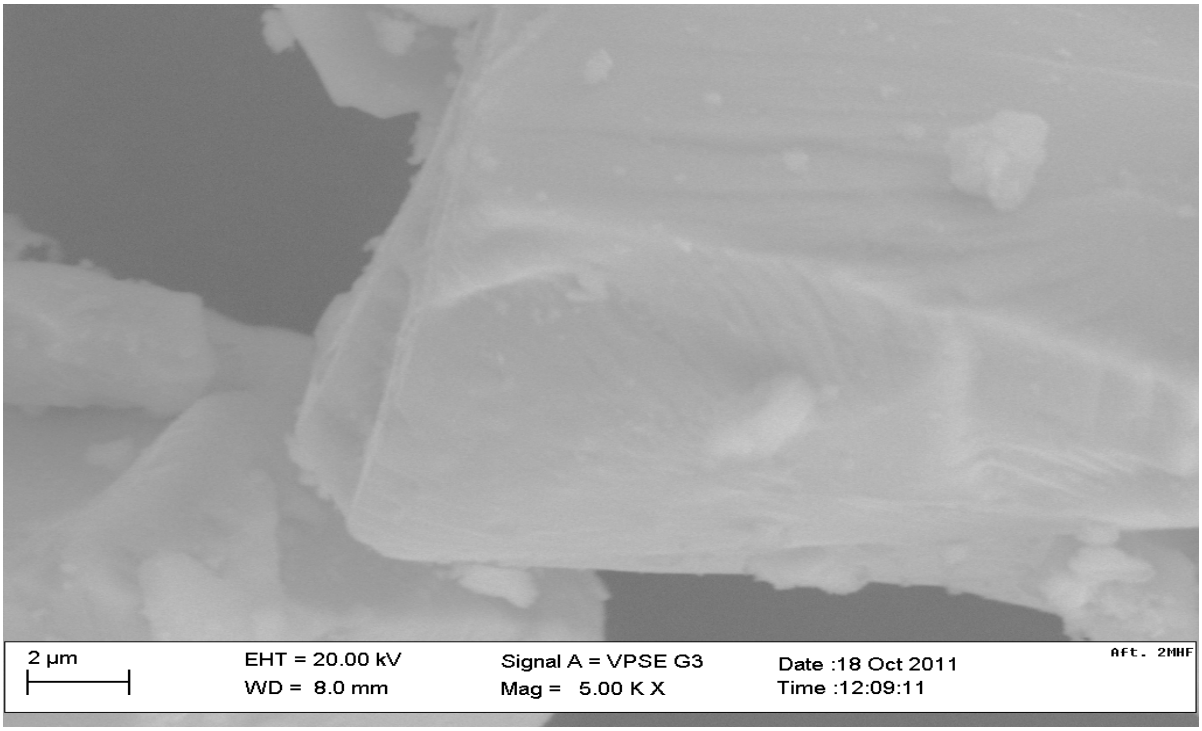


Figure 4.12 SEM images of the Plateau State residues after leaching at 2 µm and Mag at 5.00 K X

4.3.2 Alkali fusion of the tantalite ore sample

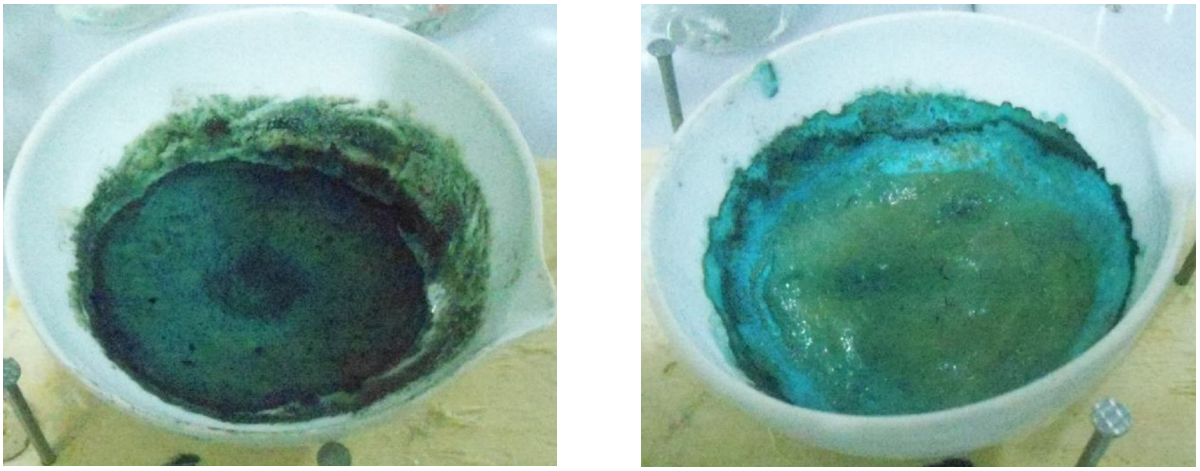
4.3.2.1 *Characterization of fused masses after fusion with alkali*

Table 4.11 XRF analysis of Tantalite ore from Plateau State and residues after fusion with KOH and NaOH

Compounds	Composition (wt. %)		
	Tantalite ore	Residues	
		Fused with KOH	Fused with NaOH
SiO_2	9.7	22.0	11
CaO	0.38	ND	3.83
TiO_2	10.2	7.59	11.7
V_2O_5	0.29	0.24	0.30
Cr_2O_3	0.024	ND	0.036
MnO	4.42	3.19	7.32
Fe_2O_3	14.2	18.4	21.32
Nb_2O_5	20.4	2.7	10.4
Ag_2O	2.02	ND	2.63
SnO_2	3.66	ND	3.04
Ta_2O_5	27.1	9.08	23.6
WO_3	7.53	ND	ND
K_2O	ND	31.2	ND
PdO	ND	4.87	ND
Rb_2O	ND	ND	4.6
Nd_2O_3	ND	0.23	ND
ZnO	ND	0.095	0.10

ND = Not detected

Figure 4.13 presents the fused masses after alkali fusion with KOH and NaOH.



a) Scale 1:1.2 cm b) Scale 1:1.2 cm

Figure 4.13 Fused mass after alkali fusion a) with KOH and b) with NaOH

4.4 Preparation of Aqueous Biphase Systems Solutions

Table 4.12 presents the summaries of the ABS sets of experiments carried out.

Table 4.12 Summary of the ABS sets of experiments carried out

Table 4.12.1 Two-phase formed from ABS and liquor from fusion with NaOH

Upper phase	BA 1Up	BA 2Up	BA 3Up	BA 4Up	BA 5Up	BA 6Up	BA 7Up	BA 8Up
Set 1 samples	1	2	3	4	5	6	7	8
Lower phase	BA 1L	BA 2L	BA 3L	BA 4L	BA 5L	BA 6L	BA 7L	BA 8L

Table 4.12.2 Two-phase formed from ABS and liquor from fusion with KOH

Upper phase	DE 1Up	DE 2Up	DE 3Up	DE 4Up	DE 5Up	DE 6Up	DE 7Up	DE 8Up
Set 2 samples	1	2	3	4	5	6	7	8
Lower phase	DE 1L	DE 2L	DE 3L	DE 4L	DE 5L	DE 6L	DE 7L	DE 8L

Table 4.12.3 Two-phase formed from ABS and fresh tantalum/niobium liquor

Upper phase	1Up	3Up	4Up	5Up	6Up	7Up	8Up	S15
Samples	1	3	4	5	6	7	8	
Lower phase	1L	3L	4L	5L	6L	7L	8L	S16

Legend:

Up – Upper phase

L – Lower phase

Samples – 1, 2, 3, 4, 5, 6, 7 and 8 represent the PEG molecular weight which are:

3350, 4000, 6000, 8000, 7000-9000, 10000, 12000 and 20000 respectively.

BA1Up – Upper phase of sample 1 (PEG 3,350 MW) in set 1.

BA1L – Lower phase of sample 1 (PEG 3,350 MW) in set 1.

LL1 = Leached liquor after fusion with KOH (undiluted)

LL2 = Leached liquor after fusion with NaOH (undiluted)

BA = Diluted Leached liquor after fusion with NaOH

DE = Diluted Leached liquor after fusion with KOH

Figure 4.14 presents the binodal curves and the tie lines for PEG of varying molecular weight + sodium sulphate + water

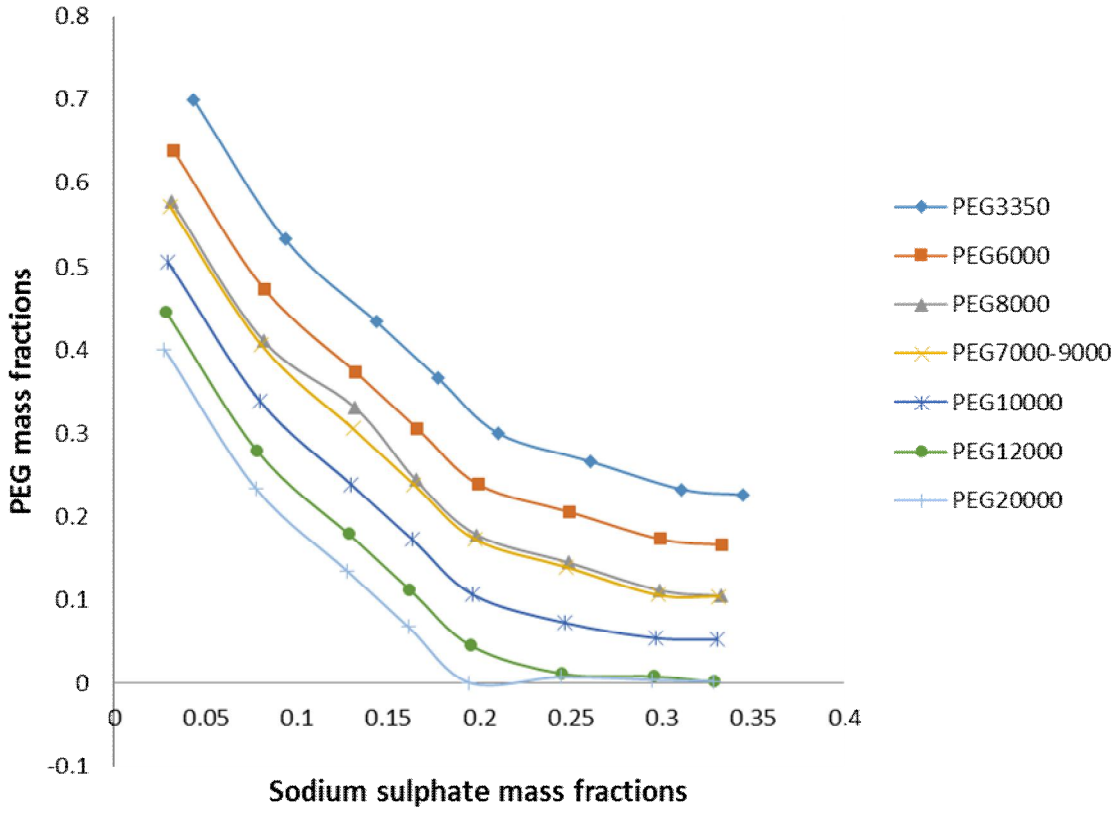


Figure 4.14 Binodal curves and the tie lines for PEG of varying molecular weight + sodium sulphate + water

Figure 4.15 presents the binodal curves and the tie lines for PEG of varying molecular weight + potassium carbonate + water

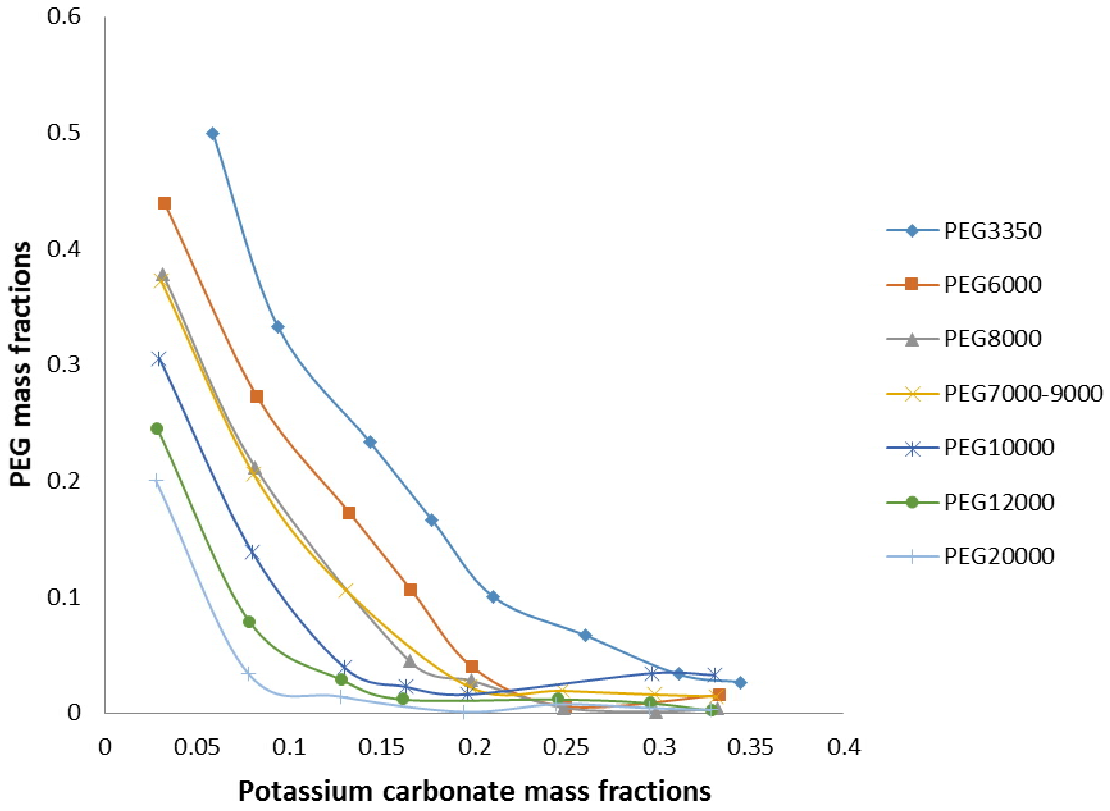


Figure 4.15 Binodal curves and the tie lines for PEG of varying molecular weight + potassium carbonate + water

Figure 4.16 presents the binodal curves and the tie lines for PEG of varying molecular weight + ammonium sulphate + water

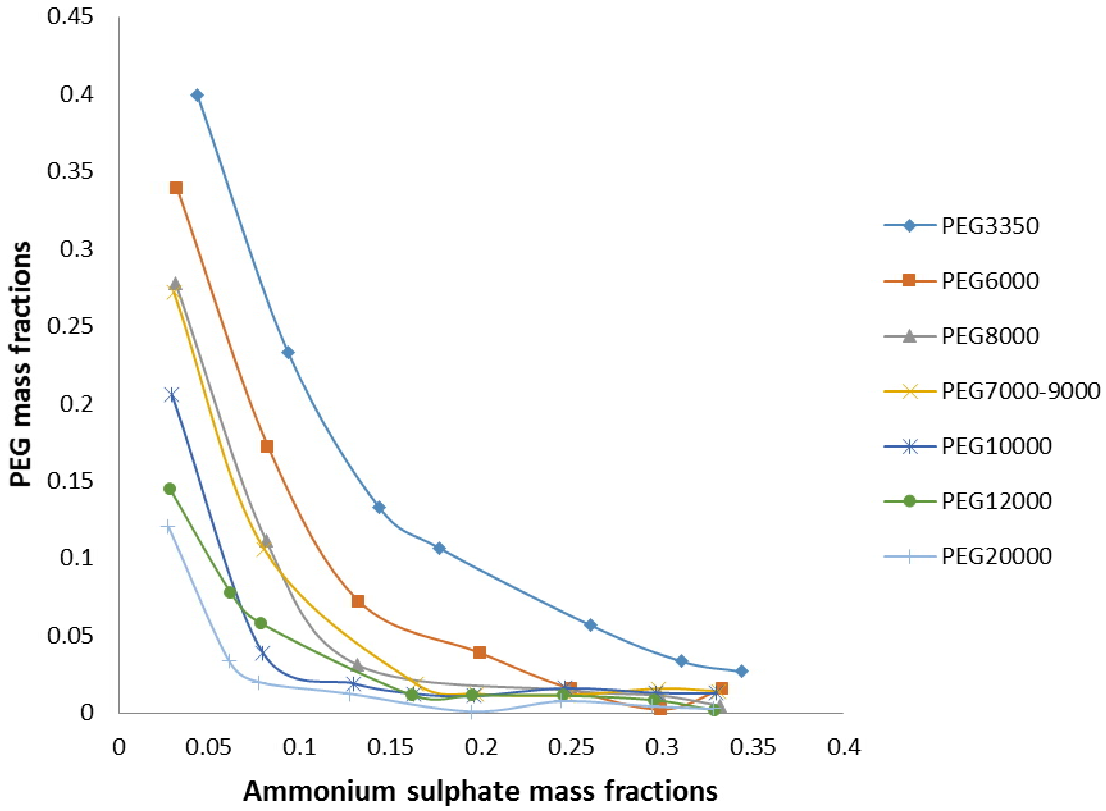


Figure 4.16 Binodal curves and the tie lines for PEG of varying molecular weight + ammonium sulphate + water

4.5 Separation of Tantalum and Niobium in Aqueous Biphase Systems

Table 4.13 presents the ICP-AES results of the PEG –rich phase and Salt-rich phase (I)

Table 4.13 ICP - AES analysis of the PEG –rich phase and Salt-rich phase (I)

Sample reference	Nb (µg/ml)	Ta (µg/ml)
ba 1l	0.169	0.376
ba 3l	0.21	0.302
ba 4l	0	0.231
ba 5l	0	0.242
ba 6l	0	0
ba 7l	0	0
ba 8l	0	0
ba 1up	0	0
ba 3up	0	0
ba 4up	0	0
ba 5up	0	0
ba 6up	0	0
ba 7up	0	0
ba 8up	0	0
de 3l	3.003	1.618
de 4l	19.742	4.252
de 5l	13.095	2.764
de 6l	6.382	2.966
de 7l	9.577	4.071
de 8l	2.436	1.449
de 3up	0.502	0.496
de 4up	0.997	0.647
de 5up	2.559	1.302
de 6up	0.781	0.462
de 7up	0.456	0.376
de 8up	2.637	1.456
ba	5.567	3.032
de	132.792	24.052
ll1	360.682	215.497
ll2	26.947	22.987

Table 4.14 presents the distribution coefficients for Niobium, Tantalum and Molybdenum from sample BA (leached liquor from fusion with NaOH)

Table 4.14 Distribution coefficients for Niobium, Tantalum and Molybdenum from sample BA (leached liquor from fusion with NaOH)

Sample reference BA	PEG Molecular Weight	Upper phase Nb Conc. (µg/ml)	Sample reference	Lower phase Nb Conc. (µg/ml)	Distribution Coefficient
ba 1up	3350	0	ba 1l	0.17	0
ba 3up	6000	0	ba 3l	0.21	0
ba 4up	8000	0	ba 4l	0	UD
ba 5up	7000-9000	0	ba 5l	0	UD
ba 6up	10,000	0	ba 6l	0	UD
ba 7up	12000	0	ba 7l	0	UD
ba 8up	20000	0	ba 8l	0	UD
		Upper phase Ta Conc. (µg/ml)		Lower phase Ta Conc. (µg/ml)	
ba 1up	3350	0	ba 1l	0.38	0
ba 3up	6000	0	ba 3l	0.30	0
ba 4up	8000	0	ba 4l	0.23	0
ba 5up	7000-9000	0	ba 5l	0.24	0
ba 6up	10,000	0	ba 6l	0	UD
ba 7up	12000	0	ba 7l	0	UD
ba 8up	20000	0	ba 8l	0	UD

UD = Undefined

Table 4.15 presents the distribution coefficients for Niobium and Tantalum from sample DE (leached liquor from fusion with KOH).

Table 4.15 Distribution coefficients for Niobium and Tantalum from sample DE (Leached liquor from fusion with KOH)

Sample reference DE	PEG Molecular Weight	Upper phase Nb Conc. (µg/ml)	Sample reference	Lower phase Nb Conc. (µg/ml)	Distribution Coefficient
de 3up	6000	0.502	de 3l	3.003	0.17
de 4up	8000	0.997	de 4l	19.742	0.05
de 5up	7000-9000	2.559	de 5l	13.095	0.20
de 6up	10,000	0.781	de 6l	6.382	0.12
de 7up	12000	0.456	de 7l	9.577	0.05
de 8up	20000	2.637	de 8l	2.436	1.08
		Upper phase Ta Conc. (µg/ml)		Lower phase Ta Conc. (µg/ml)	
de 3up	6000	0.496	de 3l	1.618	0.31
de 4up	8000	0.647	de 4l	4.252	0.15
de 5up	7000-9000	1.302	de 5l	2.764	0.47
de 6up	10,000	0.462	de 6l	2.966	0.16
de 7up	12000	0.376	de 7l	4.071	0.09
de 8up	20000	1.456	de 8l	1.449	1.01

Table 4.16 presents the total mass from sample BA (leached liquor from fusion with NaOH).

Table 4.16 Total mass from sample BA (leached liquor from fusion with NaOH)

BA	Nb Conc. (µg/ml)	Ta Conc. (µg/ml)	Upper phase vol., ml	Nb Conc. (µg/ml)	Ta Conc. (µg/ml)	Lower phase vol., ml	Total mass µg
1up	0	0	9.2	0.17	0.38	7.8	4.3
3up	0	0	7.4	0.21	0.30	8.9	4.5
4up	0	0	7.4	0	0.23	8.9	2.1
5up	0	0	7.0	0	0.24	9.3	2.2
6up	0	0	7.0	0	0	9.3	0
7up	0	0	7.0	0	0	9.3	0
8up	0	0	6.6	0	0	9.7	0

Table 4.17 presents the total mass from sample DE (leached liquor from fusion with KOH).

Table 4.17 Total mass from sample DE (leached liquor from fusion with KOH)

DE	Nb Conc. (µg/ml)	Ta Conc. (µg/ml)	Upper phase vol., ml	Nb Conc. (µg/ml)	Ta Conc. (µg/ml)	Lower phase vol., ml	Total mass µg
3up	0.502	0.496	8.0883	3.003	1.618	9.2883	51.0
4up	0.997	0.647	7.7207	19.742	4.252	8.9207	226.7
5up	2.559	1.302	7.7207	13.095	2.764	8.9207	171.3
6up	0.781	0.462	7.7207	6.382	2.966	8.9207	93.0
7up	0.456	0.376	7.353	9.577	4.071	9.2883	132.9
8up	2.637	1.456	7.353	2.436	1.449	9.656	67.6

Table 4.18 presents the separation factor (ß) of tantalum and niobium from sample DE.

Table 4.18 Separation factor (ß) of tantalum and niobium from sample DE

Sample reference	PEG Molecular Weight	Ta D1	Nb D2	ß D1/D2
3	6000	0.306551	0.167166	1.83
4	8000	0.152164	0.050501	3.01
5	7000-9000	0.471056	0.195418	2.41
6	10,000	0.155765	0.122375	1.27
7	12000	0.092361	0.047614	1.94
8	20000	1.004831	1.082512	0.93

Table 4.19 presents the ICP-AES results of the PEG –rich phase and Salt-rich phase (II)

Table 4.19 ICP - AES analysis of the PEG –rich phase and Salt-rich phase (II)

Our #	Your #	Na (µg/ml)	Nb (µg/ml)	Ta (µg/ml)
14-1511	1 U	17,029	7.6	1.4
14-1512	1 L	32,583	7.4	4.7
14-1513	3 U	10,978	9.8	1.1
14-1514	3 L	34,839	8.7	4.1
14-1515	4 U	9,781	7.9	0.9
14-1516	4 L	35,350	7.6	6.7
14-1517	5 U	10,133	8.4	0.5
14-1518	5 L	34,943	7.8	5.0
14-1519	6 U	10,600	10.3	2.0
14-1520	6 L	35,302	8.8	6.0
14-1521	7 U	10,276	10.3	2.7
14-1522	7 L	34,731	8.7	5.9
14-1523	8 U	8,573	9.4	1.9
14-1524	8 L	35,476	8.4	4.8
14-1525	15	45,801	0.0	1.8
14-1526	16	46,185	13.1	-0.1

Table 4.20 presents the distribution coefficients for Niobium and Tantalum from table 4.19

Table 4.20 Distribution coefficients for Niobium and Tantalum from table 4.19

Upper phase	Ta (µg/ml)	Lower phase	Ta (µg/ml)	D
1 U	1.4	1 L	4.7	0.3
3 U	1.1	3 L	4.1	0.3
4 U	0.9	4 L	6.7	0.1
5 U	0.5	5 L	5.0	0.1
6 U	2.0	6 L	6.0	0.3
7 U	2.7	7 L	5.9	0.5
8 U	1.9	8 L	4.8	0.4
	Nb (µg/ml)		Nb (µg/ml)	
1 U	7.6	1 L	7.4	1
3 U	9.8	3 L	8.7	1.1
4 U	7.9	4 L	7.6	1
5 U	8.4	5 L	7.8	1.1
6 U	10.3	6 L	8.8	1.2
7 U	10.3	7 L	8.7	1.2
8 U	9.4	8 L	8.4	1.1
	Na (µg/ml)		Na (µg/ml)	
1 U	17,029	1 L	32,583	0.5
3 U	10,978	3 L	34,839	0.3
4 U	9,781	4 L	35,350	0.3
5 U	10,133	5 L	34,943	0.3
6 U	10,600	6 L	35,302	0.3
7 U	10,276	7 L	34,731	0.3
8 U	8,573	8 L	35,476	0.2

Table 4.21 presents the separation factor (ß) of tantalum and niobium from table 4.20

Table 4.21 Separation factor (ß) of tantalum and niobium from table 4.20

Sample reference	PEG Molecular Weight	Nb D2	Ta D1	ß D2/D1
1	3350	1.03	0.3	3.43
3	6000	1.12	0.27	4.15
4	8000	1.04	0.13	8.0
5	7000-9000	1.07	0.1	10.7
6	10,000	1.17	0.33	3.55
7	12000	1.18	0.45	2.62
8	20000	1.12	0.39	2.87

Table 4.22 presents the total mass of tantalum and niobium in the upper and lower phases.

Table 4.22 Total mass of tantalum and niobium in the upper and lower phases

	Ta (µg/ml)	Nb (µg/ml)	Upper phase vol., ml		Ta (µg/ml)	Nb (µg/ml)	Lower phase vol., ml	Total mass, µg
1 U	1.4	7.6	27.6	1 L	4.7	7.4	24.0	536.7
3 U	1.1	9.8	22.8	3 L	4.1	8.7	28.0	606.7
4 U	0.9	7.9	22.4	4 L	6.7	7.6	28.8	610.1
5 U	0.5	8.4	22.4	5 L	5.0	7.8	28.4	563.8
6 U	2.0	10.3	22.4	6 L	6.0	8.8	28.4	695.9
7 U	2.7	10.3	22	7 L	5.9	8.7	29.2	711.3
8 U	1.9	9.4	20.8	8 L	4.8	8.4	29.6	626.6

CHAPTER FIVE

DISCUSSION

5.1 Introduction

This chapter presents the discussion of the results of each segment of the work presented in chapter four.

5.2 Preparation and Analysis of Feed Material

5.2.1 Crushing, Grinding, Ball-milling and Analysis of Feed Material

Table 4.1 shows the elemental analysis of the tantalite ore. From the table, it can be seen that tantalum pentoxide (Ta_2O_5) was the predominant constituent of the Tantalite ore procured from Plateau. However, the other ores from Nasarawa and Niger have low Ta_2O_5 content and high Nb_2O_5 content. Thus the ore from Plateau can be referred to as tantalite since it contains more tantalum pentoxide than niobium pentoxide. There were also traces of yttrium, zirconium and uranium in the ores. Similar results within the same range were obtained by Maina *et al* (2007) and Maina and Basu (2008). It was noted that Funtua *et al* (1999) determined the Ta content in the pegmatite region around Jos, Nassarawa and Jama'a areas of central Nigeria at between 21 and about 30% (Adetunji *et al*, 2005). The difference between ore samples could probably be explained in terms of the diversity in the ore contents from site to site and from one ore vein to another. Therefore, among the three tantalite ore samples, the ore from Jos was used for the project since it had more tantalum pentoxide.

5.2.2 Effect of Ball Milling Time

The tantalite ores were ball milled for 6 h. This time was selected since previous studies by Maina *et al* (2007) and Maina and Basu (2008) showed that the particle size distribution of the product did not change significantly after milling for the duration longer than 6 h. Welham (2001) has also reported that with dry milling, size reduction is typically completed within 2 h. A number of mineral systems have shown that the leaching rate can be enhanced by milling, the enhancement being greater than that expected from the increase in surface area. This enhancement has been attributed to the increase in strain in the mineral and the formation of steps and kinks on the surface (Welham, 2001). It has been noted that the smaller crystallites formed during milling dissolve more rapidly than larger crystallites and this is probably due to the increased surface energy of smaller crystallites compared with larger ones.

5.3 Protocol for Digesting Samples

5.3.1 Mineral Acid Leaching of the Tantalite Ore Sample

Tables 4.2 – 4.4 show the X-ray fluorescence analysis for the Tantalite ore before leaching and residue after leaching for various molar concentrations of HF ranging from 0.2M, 2M, 15M and 20M. All these molar concentrations of HF were mixed with 10.8M H_2SO_4 for leaching process according to El Hussaini *et al*, (2004). The extraction depends mainly on the leaching of the Tantalite ore and the better the leaching the higher the quantity of tantalum to be extracted. The difficulty of tantalum and niobium extraction from the ore is due to the fact that only few acids can leach the ore and only in the presence of fluoride ion (Maina *et al*, 2007). The degree of leaching by this solvent is not high and is achieved at

high temperatures. Leaching is concerned with the extraction of soluble constituent from a solid by the means of solvent (Coulson, 2002), or it is the removal of a soluble fraction in the form of a solution from an insoluble, permeable solid phase with which it is associated. The separation usually involves the selective dissolution, with or without diffusion (Perry and Green, 1997).

From Table 4.2, it can be seen that leaching at 0.2M HF and 15M HF did not give a good result as the amount of residue for Ta_2O_5 and Nb_2O_5 were not reduced as compared to the sample before leaching. Ordinarily, if leaching had taken place there should be reduction in the concentration of Ta_2O_5 and Nb_2O_5 in the residue. The percentage in the residue is also in relation to the other compounds in it. Table 4.3 shows another set of leaching carried out for molar concentration of 20M HF, 15M HF, and 2M HF in 10.8M H_2SO_4. A similar observation could be made also, that the leaching was not effective since a reduction in the concentration of Ta_2O_5 and Nb_2O_5 were expected. Table 4.4 also shows the leaching for 2M HF in 10.8M H_2SO_4. It can be observed also that not much was leached. In the light of the foregoing, it is plausible that either the XRF equipment is faulty and/or the HF used was not pure, since fluoride ions play critical role in the dissolution of tantalum and niobium in ores.

Tables 4.5 – 4.7 show XRF analyses for 2M HF and 0.2M HF residues after leaching in 10.8M H_2SO_4. The leached samples were analyzed again, as shown from the standard deviation analysis. In Table 4.5, it can be seen that for some elements, the results agree with each other, or are close from the standard deviation. The reasons for this are not clear at present, but may probably be due to sampling errors during pellet preparation in XRF at

CERT. Table 4.6 similarly shows the XRF for only the Tantalite ore samples, which was done more than once. From the result, it can be seen that there is considerable variation on the data. Table 4.7 shows the XRF analysis for 15M HF residues after leaching in 10.8M H_2SO_4. It can be seen also that the results are not similar because of the variation in the standard deviation.

The observed inadequacies or trends in the results in Tables 4.2 to 4.7 could be attributed to three major aspects - 1) The nature of chemicals used and uncertainty with respect to their purity. 2.) The human errors that could occur at the analyzing labs. and 3.) The nature of the equipment used for the analysis whether the calibrations are correct. In view of these observations, new set of chemicals had to be purchased from Germany, through Zayo chemicals Ltd, Jos. While awaiting for the arrival of the chemicals, the Centre for Energy Research and Training (CERT) A.B.U. purchased new XRF equipment. Therefore, the subsequent analyses were done using the new XRF.

Tables 4.8 to 4.10 show the XRF analysis of the tantalite ore before leaching, residues and leached liquor after using the new mineral acids from Germany, through Zayo Chemicals Ltd., Jos. The XRF result showed possible reproducibility of the results as seen in the closeness.

Table 4.8 shows the XRF analysis from CERT for tantalite ore before leaching. Tantalum pent oxide (Ta_2O_5) had the highest percentage in the ore (31.4 – 32.5%) and remains tantalite. Niobium pentoxide content was 16.3 – 19.4%. Adetunji *et al* (2005) had noted that concentrates suitable for further processing to recover Ta should contain at least 25%

Ta_2O_5, with 50% combined Ta_2O_5 and Nb_2O_5. Primary ore with these Ta_2O_5 and Nb_2O_5 contents would only need cleanup operations for Ta extraction processes. The cleanup operation results in the removal of associated minerals and impurity elements to a tolerable extent. Typical associated minerals from Table 4.8 are TiO_2, MnO, Fe_2O_3, WO_3, SiO_2, which are major impurities. Other impurities are in traces.

Table 4.9 shows the XRF analysis at CERT for 2M HF and 15M HF residues after leaching of the tantalite ore in 10.8M H_2SO_4 . Each analysis was carried out twice. It can be seen that for each molar concentration the reproducibility was reasonably good. For a good leaching process, the percentages of the compound should have reduced in the residues. From Tables 4.8 and 4.9 it can be seen that Ta_2O_5 and Nb_2O_5 content of the residue did not change significantly after leaching. Therefore, it can be said that the mineral acids were not able to extract the Nb_2O_5 and Ta_2O_5 from the ore.

Table 4.10 shows the XRF analysis of the leached liquors for 2M HF and 15M HF in 10.8M H_2SO_4. The analyses were done twice as indicated for 2M HF and 15M HF. The results show some agreement in the analysis. In addition, the reproducibility was also good. Actually they should have been the same; since, in this table we are looking at the leached liquor which should have been a homogeneous mixture. The measured concentration of Ta_2O_5 in the leached liquor varied from 7.09% to 8.62%. However, Nb_2O_5 was not detected in the analysis. This can also be seen from Table 4.8 and Table 4.9 which showed the composition of the tantalite ore before leaching and that of leached residues, respectively.

For Ta_2O_5, in Table 5.8 the composition is 31.4 – 32.5% and in the residue Table 4.9, 34.8 – 35.6% which show no significant difference. But for Nb_2O_5 in Table 4.8 it ranged between 16.3 and 19.4%, while in Table 4.9 it ranged between 17.9% and 21.8% which also indicated that there wasn't much extracted. These percentages here reported are also in respect to other minerals or compounds present in the tantalite ore and also in the leached residue. From Table 4.10, it can also be seen that the amount of SO_3 is high, about 51.4% to 54.4% for 2M HF and about 61.2% to 61.4% for 15M HF. This is because the leached liquor was still in acidic state. Further treatment and extraction process was expected to bring it to alkaline state.

Figure 4.1 Shows the XRD analysis of the tantalite ore from Plateau state before leaching. It can be seen that the major peaks of the crystals are ixiolite, manganon and ferrotapiolite. The ixiolite is the crystal structure of tantalite; with the chemical formula (Ta, Nb, Sn, Fe, Mn) O_2. The manganon is a variety of calcite rich manganese, which gives the mineral a pink colour. Its chemical composition is (Ca, Mn)O_3. The name is manganese calcium carbonate. The ferrotapiolite is a crystal usually well developed, short prismatic or equant, with several forms. It's chemical formula is (Fe, Mn, Ta, Nb)$_2O_6$ with a composition of Nb_2O_5 – 1.32 %, Ta_2O_5 – 85.21 %, TiO_2 – 0.46 %, FeO – 9.67 % and Mn O-4.17 % (Mineral Data, 2013).

Figure 4.2 shows the XRD analysis of the residues after leaching with mineral acids. It can be seen that the major peaks of crystals are ixiolite, ferrotapiolite and ashanite. The ashanite originally thought to be the Nb-dominant analogue of ixiolite; the type of material

is now believed to be a mixture of several minerals including Ixiolite, samarkite – (Y) and uranmicrolite. The chemical formula is $(Nb, Ta, U, Fe, Mn)_4O_8$.

From the two XRD patterns of Figures 4.1 and 4.2, it can be seen that there's not much change in the height of the crystals peak for ixiolite and ferrotapiolite which are the major Ta and Nb containing crystals. This basically implied that the leaching with the mineral acids were not really effective. This could be due to the escape of the HF fumes in the process of dissolution, just as Xiao-hui *et al*, (2009 and 2010) and Yang *et al*, (2012) attributed such to the strong volatility, about 6 % - 7 % of hydrofluoric acid is lost during decomposition process. Such effects could also be seen in the XRF analysis of Tables 4.2 to 4.4.

Figures 4.3 to 4.8 show the SEM images for the tantalite ore before leaching with mineral acids at different magnifications. It can be seen that the images, looked scattered in granular form or shape and cleaved together in groups. Figures 4.9 to 4.12 show the SEM images for the residues after leaching with mineral acids. The images appeared more compact and structured in shape. The images are shown for different size magnification. The images before and after leaching with acid did not reveal quantitative differences, but it can be seen that there is some change in the shape and form of the samples.

5.3.2 Alkali Fusion of the Tantalite Ore Sample

Figure 4.13 shows the fused mass after alkali fusion with potassium hydroxide and sodium hydroxide. The pictures were taken after cooling the mass by hand fanning. The sample fused with KOH looked dried and the colour change looked darker than the sample fused with NaOH. Both samples look greenish-blue. The sample fused with NaOH had some shiny-yellowish paste on the surface.

Table 4.11 show the XRF analysis of the ore before fusion and the residues after fusion with KOH and NaOH, and then with water leaching. From the results, it can be seen that the KOH fusion gave a better result than the NaOH fusion. This can be seen in the reduction of Ta_2O_5 and Nb_2O_5 from 27.1 % and 20.4 % in the ore to 9.08 % and 2.7 % in the residues respectively. While for the NaOH fusion, the reduction of Ta_2O_5 and Nb_2O_5 is from 27.1 % and 20.4 % in the ore to 23.6 % and 10.4 % in the residues respectively. The reduction in the residues implied that the water-leaching was effective and more of the elements were present in the leached liquors. This can also be seen in Table 4.13, the ICP-AES analysis of the leached liquors LL1 for KOH and LL2 for NaOH. The essence of the fusion was to get the leached liquor containing tantalum and niobium, which in turn was needed for the aqueous biphase study.

5.4 Preparation of Aqueous Biphase Systems Solutions

Aqueous biphasic systems consist of two immiscible phases formed when certain water-soluble polymers are combined with one another or with certain inorganic salts in specific concentrations. In this study a number of polyethylene glycols (PEGs) with molecular weight from 3350 to 20,000 were investigated. Three types of salts-Na_2SO_4, $(NH_4)_2\ SO_4$

and K_2CO_3 were used. The individual PEG and salt solutions were prepared individually before the two solutions were mixed at certain ratios to form the aqueous biphase systems (ABS).

Table 4.12 presents the summaries of the ABS sets of experiments carried out. Table 4.12.1 shows the two-phase formed from ABS and liquor from fusion with NaOH. Table4.12.2 shows the two-phase formed from ABS and liquor from fusion with KOH. Table 4.12.3 shows the two-phase formed from ABS and freshly prepared tantalum/niobium liquor. These tables show how the upper and lower phases were separated and labelled before their analyses.

Phase diagrams comprise a binodal curve and different parallel tie-lines. While the binodal represents the borderlines between the one-phase and the two-phase regions, the tie-line describes the compositions of the two phases in equilibrium.

Figure 4.14 shows the binodal curves and the tie lines for PEG of varying molecular weights + sodium sulphate + water. As the mass fractions of the sodium sulphate increases, the mass fractions of the PEG were reducing. The binodal curve describes the borderline between the single-phase area and the two-phase area. The area above the binodal describes all compositions giving rise to two phase systems. It can be seen that as the polymer molecular weight increases, the binodal curve shifts down and close to the origin; indicating a clear increase in the two-phase region. Raja *et al* (2011), noted that if there's increase in PEG molecular weight, thus requires lower concentrations for phase separation.

This may be caused by the increase in the incompatibility between the system components due to the more hydrophobic character of PEGs of higher molecular weights.

Figure 4.15 shows the binodal curves and the tie lines for PEG of varying molecular weights + potassium carbonate + water. It was observed that more of the PEGs tend to shift towards the origin that is towards zero. This could be attributed to the salt used to form the ABS, because in Figure 4.14 sodium sulphate formed better ABS as shown on the binodals.

Figure 4.16 shows the binodal curves and the tie lines for PEG of varying molecular weights + ammonium sulphate + water. The trend observed here seemed similar to that of Figure 4.15. As the PEG molecular weight increased, the curves tend to shift towards the origin. That is, the binodal curves tend to move away from the two-phase region. This also implied that lower concentrations are adequate for the two phase formation.

The composition of the two phase system is characterized by the tie-line length. Interfacial tension between the phases increases with increasing tie-line length (Srinivas and Regupathi, 2011). Tie line length represents the variation in the composition of the top and bottom phase. The larger the tie line length, the higher the difference between top phase and bottom phase composition. Tie lines are commonly parallel and as they decrease in length, they ultimately approach a critical point on the binodal curve, where the tie-line length becomes zero (Raja *et al*, 2011). At this point the composition and volume of the two phases theoretically become equal.

Effect of PEG molecular weight

The molecular weight of the PEG used influences the partitioning of the metal ions. The higher the molecular weight of the polymers, the lower is the polymer concentration required for phase separation. As polymer concentration increases, differences in density and viscosity between the phases increase (Raja *et al*, 2011). Binodal curves shift towards the origin with increase in PEG molecular mass, stating that lower concentrations are adequate for the two phase formation thereby, resulting in the expanded area of two phase region. This variation can be explained in terms of excluded volume effect in which the increase in molecular weight of PEG reduces the volume available to bind up the water molecules thereby, increases the incompatibility between the system components (Ramyadevi *et al*, 2012).

5. 5 Separation of Tantalum and Niobium in Aqueous Biphase Systems

Table 4.13 shows the ICP–AES analysis of the PEG–rich phase and the salt–rich phase (I) carried out at the Pennsylvania State (Penn State) University, USA. The sample reference ba was from the leached liquor of the fusion process with NaOH. The numbering 1, 3, 4, 5, 6 , 7 and 8 represent the molecular weight of the PEG, while the letters up and l represent the upper phase (PEG–rich phase) and the lower phase (salt–rich phase) respectively. The samples reference de was from the leached liquor of the fusion process with KOH. The ba and de liquors were diluted in the ratio of 1:1. LL1 represents the undiluted leached liquor of the fusion with KOH and LL2 represents the undiluted leached liquor of the fusion process with NaOH. As for Tantalum and Niobium concentrations in the ba samples, only few and lower concentrations were detected and in the lower (salt–rich) phase. No

concentrations were detected in the upper (PEG–rich) phase. This could be attributed to a number of factors suspected: 1.) It can be observed that the concentration of Ta and Nb in the undiluted leached liquor of the fusion with NaOH (LL2) were very low; 2.) The upper and lower phases of sample ba were diluted after separation with ethanol. It was learnt that, at the ICP–AES lab at Penn State University, USA, the organics present in the ba samples were putting-off the flames as such were diluted further with nitric acid. However on doing that, it was observed thereafter that a lot of precipitates were formed which prompted us to suspect the little or no concentrations detected; and 3.) After separating the upper phase from the lower phase, it was also observed that precipitates were formed around the lids of the sample bottles; especially if allowed to stand for a number of days or weeks. The best option is to analyze the samples immediately after separation.

On the other hand, the upper and lower phases of the de samples were diluted with de-ionized water before sending them to the ICP–AES lab. From the de samples, it can be observed that molybdenum was not detected in the upper or lower phase; though they were detected in the main leached liquors LL1 and LL2. Tantalum and Niobium were detected and can be seen from the ICP–AES analysis. This is good indication that the ABS can be effectively used to separate tantalum and niobium. However, it can be noticed that more niobium was detected in the samples more than the tantalum. Furthermore, it was observed that more of the elements were within the lower (salt–rich) phase. Well, all the trends could also be attributed to some losses within the PEG–rich (upper) phase due to precipitates formed around the lids or cover of the sample bottles. It was suspected that some of the elements could have been taken up along with the precipitates. The most important thing here is that tantalum and niobium were detected in the upper and lower phases. According

to Zhang *et al* (2001) and Rogers *et al* (1996) most metal ions tend to stay in the salt – rich phase with distribution ratio of much less than 1.0 without any added extractant since they are highly hydrated and interact strongly with water. However, in the case of tantalum and niobium they may not necessarily interact with water because of their high resistance to so many reactions. Hence, there's need to further enhance the partitioning of tantalum and niobium to the upper phase by adding inorganic anions like halide anions and also water-soluble extractants.

Tables 4.14 and 4.15 show the distribution coefficients for Nb and Ta from samples BA and DE. Distribution coefficient (D) is the ratio of the concentration of element in the upper phase to that of the concentration of the same element in the lower phase. In Table 4.14, it is observed that D for Ta and Nb are zero. This implied that no concentration of Ta and Nb were detected or found in the upper (PEG-rich) phases of the BA sample. Some concentrations of Ta and Nb were however, detected in the lower (salt-rich) phases. Almost the same amount of Nb was detected in the PEG3350 and PEG6000 average molecular weights. Ta was detected in PEGs of molecular weights 3350 to 7000-9000.

In Table 4.15 it is observed that D for Ta and Nb are less than one for PEG6000 to PEG12000 average molecular weights and about one for PEG20000. This implied that for D lower than one, that there was separation between the upper and lower phases, but however most of the concentrations of elements were found in the lower phase. For PEG20000 average molecular weight with D of about one, signified that there was no separation of Ta and Nb elements between the upper and lower phases, that is almost the same concentrations of both elements were found in the upper and lower phases. While it is not necessary that distribution coefficient be larger than 1, large values are very desirable

since less solvent will then be required for the extraction (Treybal, 1981). It can be generally observed from Tables 4.14 and 4.15 that Ta and Nb are present in the solution to be separated, Ta and Nb were sparingly separated into the organic (PEG-rich) phase while more of the Ta and Nb were concentrated in the aqueous (salt-rich) phase.

The aqueous biphasic systems utilized for metal ion partitioning have been classified into three categories (Zhang *et al*, 2001 and Rogers *et al*, 1996). In the first category, the metal ion is transferred directly into the PEG – rich phase from the salt – rich phase without any added extractant. A second category produces a metal complex that partitions to the PEG – rich phase from the salt – rich phase with the addition of an inorganic anion such as halide anions or SCN^-. The third category utilizes water-soluble extractants that coordinates the metal ion. In this study of Tantalum and Niobium separation, the partitioning of Ta and Nb has been investigated in the PEG/ salt aqueous biphase systems without any added extractant.

Tables 4.14 and 4.15 show the distribution coefficients for Ta and Nb from samples ba and de, respectively. It could be observed that the distribution coefficients were low for Ta and Nb. The reasons for these are not far-fetched and are attributed to some of the issues or factors mentioned above, that could have prevented us from seeing higher concentrations of Ta and Nb in the ICP – AES analysis.

Tables 4.16 and 4.17 show the total masses from the two sets of samples ba and de. The total masses for the ba samples are within certain range; but for the de samples the total mass seemed scattered. All these variations could be attributed to some of the losses

suffered, like through reduction in concentrations through precipitations or loses due to evapouration of parts of the liquid samples or due to some minor spillage. Another important factor has to do with the issue of long storage of samples for several months before sending to Pennsylvania State for analysis.

Table 4.18 shows the separation factor (β) of tantalum and niobium from sample DE. The separation factor shows how effective the tantalum and niobium have been separated. It was observed that the separation factor for PEG8000 and PEG7000-9000 average molecular weight gave better separation with values 3.01 and 2.41, respectively. This implied that despite the effect of long storage of the samples before analysis, it was possible to separate tantalum and niobium in the ABS.

Separation factor, or selectivity, β is analogous to the relative volatility of distillation. For all useful extraction operations the selectivity must exceed unity, the more the better. If the selectivity is unity, no separation is possible (Treybal, 1981).

Meanwhile, in view of the long storage of the earlier samples before analysis, another set of experiments were carried out with freshly prepared tantalum/niobium liquor and ABS.

Table 4.19 shows the ICP-AES analysis result of the PEG-rich phase and salt-rich phase (II) for the freshly prepared tantalum/niobium liquor. The numbering 1, 3, 4, 5, 6, 7, and 8 represent the PEG molecular weight, while the letters U and L represent the upper (PEG-rich) phase and the lower (salt-rich) phase, respectively. However, 15 and 16 represent the sodium sulphate solution alone, that was mixed with the freshly prepared tantalum/niobium

liquor. The major elements from the results are sodium (Na), Nb and Ta. It was observed that more of the Na was found in the lower salt-rich phase. For the Nb, it can be noticed that at lower PEG molecular weight, more of it was found in the lower salt-rich phases, but as the PEG molecular weight increased, more of it was found in the upper PEG-rich phase. In the case of Ta, it was observed that all through the PEG molecular weights, most of it remained in the lower salt-rich phase.

Table 4.20 shows the distribution coefficients (D) for niobium and tantalum from Table 4.19. It was observed that D for tantalum ranged from 0.1 to 0.5, while that of niobium ranged from 1 to 1.2. The D for tantalum showed that most of it was found in the lower salt-rich phase and the D for niobium showed that most of it was found in the upper PEG-rich phase. These statements already, are pointing to the fact that, tantalum and niobium have been separated. Treybal (1981) pointed out that, 'while it is not necessary that distribution coefficient be larger than 1, large values are very desirable since less solvent will then be required for the extraction'.

Table 4.21 shows the separation factor of tantalum and niobium from Table 4.20. The separation factor shows how effective the tantalum and niobium were separated from each other. Treybal, (1981) pointed out that, 'Separation factor, or selectivity, β is analogous to the relative volatility of distillation. For all useful extraction operations the selectivity must exceed unity, the more the better. If the selectivity is unity, no separation is possible'. It was observed from the separation factor that, as the PEG molecular weight increased, from PEG3350 to PEG7000-9000, the separation factor increased from 3.43 to 10.7. However, there was decrease in the separation factor from PEG10,000 to PEG20,000 with values

from 3.55 to 2.87. There was a sharp drop in separation factor from 10.7 to 3.55 for PEG7000 to PEG 10,000.

Table 4.22 shows the total mass of tantalum and niobium in the upper and lower phases. The total mass was calculated as the total concentration of Ta and Nb in upper phase times the volume, plus the total concentration of Ta and Nb in the lower phase times the volume. It can be observed that the total mass ranged between 536.7 μg and 711.3 μg. However, it was expected that the total mass should be within a certain range or close. The variation could be attributed, probably to experimental errors.

The suitability of using solvent extraction for a given separation is determined by thermodynamic and kinetic considerations. The main thermodynamic parameter is the solute distribution ratio, D, between the organic (PEG) and the aqueous (salt) phase.

Various PEG molecular weights were investigated in the work. PEG8000 average molecular weight gave a separation factor of 8.0 and PEG7000-9000 average molecular weight gave a separation factor of 10.7. The separation factor is the ratio of distribution ratio of tantalum to the distribution ratio of niobium. In all the PEG molecular weights used, tantalum and niobium were separated, with separation factors above 1.0. However, within the ambient temperature that the experiment was investigated, PEG7000-9000 average molecular weight gave the optimum design parameter, with separation factor of 10.7; meaning that at this point, more niobium is found in the upper (PEG-rich) phase and more tantalum is found in the lower (salt-rich) phase.

The result of this work provided the optimum condition, that using PEG7000-9000 average molecular weight, at which niobium may be most effectively separated from tantalum; which may also be used for design, especially in a batch system.

Other parameters such as extraction rate, residence time and flow rates will have to be considered in the design of a continuous process.

CHAPTER SIX

CONCLUSIONS AND RECOMMENDATIONS

6.1 Conclusions

1. ABS was formed using various water–structuring salts–Na_2SO_4, K_2CO_3 and $(NH_4)_2SO_4$ and PEG of various molecular weights, especially PEG10,000, PEG12,000 and PEG20,000.

2. ABS formed with Na_2SO_4 gave better binodal curves, compared with K_2CO_3 and $(HN_4)_2SO_4$.

3. The fusion process of tantalite ore with KOH and subsequent water leaching gave a better result than that with NaOH within the same experimental conditions.

4. Tantalum and niobium were effectively extracted from Nigerian tantalite ore and separated using ABS.

5. The calculated distribution coefficients (D) were from 0.1 to 0.5 for Tantalum and 1.0 to 1.2 for Niobium with separation factors of 3.43, 4.15, 8.0, 10.7, 3.55, 2.62 and 2.87 for the PEGs used.

6. The separation factor was highest, 10.7 for PEG of average molecular weight 7000-9000 among the PEGs investigated.
7. The separation factor of 10.7 shows that in a solution Niobium can be effectively separated from Tantalum using ABS. Niobium will be partitioned to the PEG-rich phase and then Tantalum will remain in the salt-rich phase.

8. A solvent has been developed for extracting Tantalum and Niobium using ABS.

6.2 Recommendations

1. Extraction with ABS should be carried out when the equipment for analysis is readily available. This is necessary to avoid some of the problems associated with long storage times for recovered samples and differences in analytical protocols in the different laboratories.
2. Water-soluble extractants could also be used to see if it could enhance the salting–out effect of the PEG in the extraction of metal ions (Zhang *et al*, 2001; Rogers *et al*, 1996).
3. The leached liquor from the fusion process should be tested directly for the ABS separation without dilution to see how it partitions between the bi-phase systems.
4. The effect of alkali-to-ore mass ratio, fusion temperature and fusion time on the decomposition behavior of tantalum-niobium ore should be further investigated.
5. The addition of an inorganic anion such as halide anions (I^-, Br^- or SCN^-) should be tried or tested to see if more of the tantalum and niobium could be partitioned to the PEG-rich phase from the salt-rich phase.
6. Water-soluble extractants should also be tried on the tantalum and niobium to see if more of the elements could be partitioned to the PEG-rich phase.

REFERENCES

Adetunji, A.R., Siyanbola, W.O., Funtua, I.I., Olusunle, S.O.O., Afonja, A.A. and Adewoye, O.O. (2005), Assessment of Beneficiation Routes of Tantalite ores from key locations in Nigeria, *Journal of Minerals & Materials Characterization & Engineering*, Vol. 4 No. 2 p. 67 – 73.

Angus and Ross (2003), Tantalum. Retrieved from http://www.angusandross.com

British Columbia Institute of Technology (2005), Tantalum, BCIT Chemistry Resource Center. Retrieved from http://www.nobel-scas.bcit.ca/resource

Bureau of Mines, (1975) U.S. Bureau of mines, Bulletin "Tantalum", Mineral Facts and Problems, 697, p. 1093-1102

Burt, R. (2003), Beneficiation of Tantalum ore – How is it achieved and could it be better? Retrieved from http://www.austehc-unimelb.edu.au/2003

Butters, P.A. (1967), The Separation of Tantalun and Niobium by Solvent Extraction, *Chemistry & Industry*. April p. 613-615.

Chaplin, M. (2005), Aqueous biphasic Systems. Retrieved from http:// www.isbu.ac.uk/water/biphasic.html p. 1-3.

Chen, J., Spear, S.K., Huddleston, J.G. and Rogers, R.D. (2005), Polyethylene glycol and solutions of polyethylene glycol as green reaction media, *Green Chemistry*, Volume, No. 7 p. 64-82. Retrieved from http://www.rsc.org/greenchem

Chen, Y., Meng, Y., Tang, J., Sun, T., Sun, F. and Liang, S. (2010), Extraction of Unicase from Candida utilis by applying PEG/(NH4)2SO4 ATPS, *African Journal of Biotechnology*, Vol. 9 (30) p. 4788-4795, 26 July.

Coulson and Richardson's Chemical Engineering (2002), Volume 2, 5th Edition (In Imprint of Elsevier Replika Press Pvt. Ltd. India (2003 India).

Dave, H. (2002), Tantalum Price. Lipmann Forum. Retrieved from http://www.lipmann.co.uk

Eagle Alloys (2008), Tantalum. Retrieved from http://www.eaglealloys.com/t-TantalumProperties.aspx

Ellenburg, J.Y., Leddicotte, G.W. and Moore, F.L. (1954), Separation of Niobium and Tantalum by Liquid-liquid Extraction, *Journal of Analytical Chemistry*, Volume 26, No. 6 June p. 1045-1047.

El Hussaini, O.M. and Rice, N.M. (2004), Liquid-liquid Extraction of Niobium and Tantalum from aqueous sulphate/fluoride solutions by a Tertiary Amine, *Journal of Hydrometallurgy*, Volume 72 p. 259-267

Fletcher, J.M., Morris, D.F.C. and Wain, A.G. (1956), Outline of a Solvent Extraction Process for the Purification of Niobium from Ores or from Ferroniobium, Bulletin Institute of Mining and Metallurgy, Volume 597 p. 487- 489.

Fontana, D. and Ricci, G. (2000), Poly (ethylene glycol)-based Aqueous Biphasic System: effect of temperature on phase equilibria and on partitioning of 1,10-phenanthroline-copper (II) sulphate complex, *Journal of Chromatography* B, 743 p. 231-234.

Forest, M. (2002), Tantalum – Sources and Properties of Tantalum. Materials World, vol. 10 No. 10, p. 14 – 16. Retrieved from http://www.azom.com

Glinka, N.L. (1981), *General Chemistry* Vol. II, Mir Publishers, Moscow.

Gupta, R., Bradoo, S. and Saxena, R.K. (2006), Aqueous two phase systems: An attractive technology for downstream processing…p.1-7. Retrieved from http://www.ias.ac.in/currsci/aug25/articles19.htm

Graber, T.A., Andrews, B.A. and Asenjo, J.A. (2000), Model for the partition of metal ions in aqueous two phase systems, *Journal of Chromatography* B 743 p. 57-64.

Habashi, F. (1970), *Principles of Extractive Metallurgy* Volume 2 Hydrometallurgy, Gordon Breach, Science Publication Inc. New York p. 332-392

Huddleston, J.G., Willauer, H.D., Scott, T.G. and Robin, D.R. (1999), Aqueous Polymeric Solutions as Environmentally Benign Liquid/Liquid Extraction Media, Applied Chemistry. *Journal of Industrial & Engineering Chemistry Research,* 38, p. 2523-2539.

Huddleston, J.G., Willauer, H.D., Scott, T.G. and Robin, D.R. (1998), Partitioning of Small Organic Molecules in Aqueous Biphasic Systems, *Journal of Chromatography* B, 711 p.255-263.

Huddleston, J.G., Willauer, H.D., Scott, T.G. and Robin, D.R. (2000), Solvatochromic Studies in Polyethylene glycol-salt Aqueous Biphasic Systems, *Journal of Chromatography* B, 743 p.137-149.

Huddleston, J.G., Willauer, H.D., Scott, T.G. and Robin, D.R. (2002), Solute Partitioning in Aqueous Biphasic Systems Composed of Polyethylene Glycol and Salt: The Partitioning of Small Neutral Organic Species, *Journal of Industrial & Engineering Chemistry Research*, 41, p.1892-1904.

Humphrey, J.L. (1995), Separation Processes: Playing a Critical Role, Chemical Engineering Progress, 91(10) p. 31-41.

Infomine (2014) Historical Tantalum Prices and Price Chart. Retrieved from http://www.infomine.com/investment/metal-prices/tantalite-ore/all/

Isono, Y. and Nakajima, M. (1999), Application of hydrophobic membrane for alcohol separation from alcohol/aqueous biphase mixture, *Journal of Separation and Purification Technology* 17 p. 77-82.

Kamalika, R. and Lahiri, S. (2006), A green method for synthesis of radioactive gold nanoparticles, *Journal of Green Chemistry*, (Royal Society of Chemistry) volume 8 p. 1063-1066.

Lenntech (2008), Tantalum/Niobium. Retrieved from http://www.lenntech.com

Liu, X., Gao, Y., Tang, R. and Wang, W. (2006), On the extraction and separation of iodide complex of cadmium (II) in propyl-alcohol ammonium sulfate aqueous biphasic system, *Journal of Separation and Purification Technology*, Volume 50 p. 263-266.

Maina, N.S., Ameh, A.O. and Orkuma, H.H. (2007), Leaching of Tantalum and Niobium from tantalite ore in aqueous media, *ChemClass Journal* Volume 4 p. 19-28

Maina, N.S. and Basu, M.M. (2008), Solvent extraction of Tantalum from locally sourced tantalite using Octanol, Materials Society of Nigeria, Zaria Chapter Book of Proceedings. 4th Edition p. 17-20

Mayorov, V.G. and Nikolaev, A.I. (1996), Solvent extraction of niobium (V) and tantalum (V) from fluorometallate acid solutions, *Journal of Hydrometallurgy*, Volume 41 p. 71-78.

Mayorov, V.G. and Nikolaev, A.I. (2002), Tantalum (V) and niobium (V) extraction by octanol, *Journal of Hydrometallurgy*, Volume 66 p. 77-83.

Metal Bulletin (2006), Metal Bulletin Monthly. Tantalum. Retrieved from http://www.metalbulletin.com/mbm...

Metal Pages (2014), Metal Prices – Tantalum. Retrieved from http://www.metal-pages.com/metalprices/tantalum

Minerals Bureau (2002), The Tantalum market. A micro-economic analysis. Department of Minerals and Energy, Republic of South Africa. Retrieved from http://www.dme.gov.za

Mineral Data (2013), Rectorite. Mineral data Publishing 2001 – 2005 Retrieved from http://www.rruff.info/dochb/hom/tapiolitefe.pdt 20/6/2013

Nasarawa State (2007), Solid Minerals. Retrieved from http://www.nasarawastate.org/minerals

Nigeria Business Info (2003), Investment Opportunities. National Orientation and Public Affairs. Retrieved from http://www.nigeriabusinessinfo.com/minerals.htm

Pai, S.A., Lohithakshan, K.V., Mithapara, P.D. and Aggarwal, S.K. (2000), Use of Polyethylene glycol (PEG) based aqueous biphasic system (ABS) for the extraction of Pu

(IV), Pu (VI) and Am (III) with 18-crown-6: A thermodynamic study, *Journal of Radioanalytical and Nuclear Chemistry*, Volume 245 No. 3 p. 619-622.

Pan Analytical User's Manual (2007)

Perry, R.H. and Green, D.W. (1997), *Perry's Chemical Engineer's Hand Book*. 7th Edition, McGraw-Hill Publication.

Phillips Consulting (2003), Industrial Analysis. Solid Minerals. Retrieved from http://www.phillipsconsulting.net/solid_minerals.html

Raja, S., Murty, V.R., Thivaharan, V., Rajasekar, V. and Ramesh, V. (2011), Aqueous two phase systems for the recovery of biomolecules – a review, *Science and Technology* 1 (1) p.7-16 DOI: 10.5923/j.scit.20110101.02

Ramyadevi, D., Subathira, A. and Saravanan, S. (2012), Phase compositions of aqueous two-phase systems formed by poly(ethylene glycol) and maltodextrin at different temperatures, *International Journal of Chemical Sciences and Applications* Volume 3 [2] p.289-292.

RMRDC (2007), Raw Materials Research and Development Council. Tantalite. Retrieved from http://www.rmrdc.gov.ng

Rodriguez, M., Rivarola, J. and Ruiz, M.C. (2004), The effects of carboxylic acid addition on hydrofluoric acid autoclave leaching of a ferrocolumbite, *Journal of Hydrometallurgy* Volume 74 p. 39-46.

Rogers, R.D., Bond, A.H., Bauer, C.B., Zhang, J. and Griffin, S.T. (1996), Metal ion separations in polyethylene glycol-based Aqueous Biphasic Systems: correlation of partitioning behavior with available thermodynamic hydration data, *Journal of Chromatography* B 680 p. 221-229.

Rogers, R.D. and Griffin, S.T. (1998), Partitioning of Mercury in Aqueous Biphasic Systems and on ABEC™ resins, *Journal of Chromatography* B 711 p. 277-283.

Rogers, R.D., Willauer, H.D., Griffin, S.T. and Huddleston, J.G. (1998), Partitioning of small organic molecules in Aqueous Biphasic Systems, *Journal of Chromatography* B 711 p. 255-263

Rogers, R.D. (2005), Clean Solvent Extraction using Polyethylene glycol based Aqueous Biphasic Systems. p. 1-5. Retrieved from http://www.bama.ua.edu

Soisson, D.J., McLafferty and J.J; Pierret, J.A. (1961), Tantalun and Niobium, *Journal of Industrial & Engineering Chemistry Research*. Nov. p 861-868.

Sons of Gwalia, (2002), Tantalum, Retrieved from http://www.sog.com.au/pdac.ca/pdac/publications/papers/2002.

Sons of Gwalia, (2008), Minerals, Retrieved from http:// www.minerals.usgs.gov/minerals, 2008.

Sons of Gwalia, (2008), Tantalum, Retrieved from http://www.sog.com.au/uploaded/news/tantalum_industries, 2008.

Sputtering Targets (2002) Tantalum. Retrieved from http://www.lesker.com

Srinivas, P. and Regupathi, I. (2011), Partitioning studies of BSA using ionic liquid based aqueous two phase system containing 1-hexyl-3-methyl imidazolium chloride and sodium carbonate, *International Conference on Chemical, Biological and Environment Sciences.* Retrieved from http://www.psrcentre.org/images/extraimages/1211765.pdf

Stevenson, P.C. and Hicks, H.G. (1953), Separation of Tantalum and Niobium by Solvent Extraction, *Journal of Analytical Chemistry* Volume 25, No. 10 October p. 1517-1519.

Stratton, P. and Henderson, D. (2014) Tantalum Market Overview. Retrieved from http://www.mmta.co.uk/tantalum-market-overview

Treybal, R.E. (1981) Mass-Transfer Operations, 3rd Edition McGraw-Hill Book Company, Singapore

Welham, N.J. (2001), Enhanced dissolution of tantalite/columbite following milling, *International Journal of Mineral Processing*. Volume 61 p. 145-154.

Wikipedia (2008), Tantalum. Retrieved from http://www.en.wikipedia.org/wiki/Tantalum

Willauer, H.D., Huddleston, J.G. and Rogers, R.D. (2002), Solute Partitioning in Aqueous Biphasic systems Composed of Polyethylene Glycol and salt: The Partitioning of small neutral organic species, *Journal of Industrial & Engineering Chemistry Research* Volume 41 p. 1892-1904.

Xiaohui, W., Shili, Z., Hongbin, X and Yi, Z. (2009), Leaching of niobium and tantalum from a low – grade ore using a KOH roast – water leach system, *Journal of Hydrometallurgy* 98 Elsevier, p. 219 – 223

Xiaohui, W., Shili, Z., Hongbin, X and Yi, Z. (2010), Dissolution behaviours of Ta_2O_5, Nb_2O_5 and their mixture in KOH and H_2O system, *Transactions of Nonferrous Metals Society of China* 20 Elsevier-Science Direct, p. 2006 - 2011

Yang, F and Hlavacek, V. (1999), Carbochlorination of tantalum and Niobium Oxides: Thermodynamic Simulation and Kinetic Modeling, *AIChE Journal*, Volume 45, No. 3. March p.581-589.

Yang, X., Wang, X., Wei, C., Zheng, S. and Zhang, Y. (2012), Decomposition Behaviors of Tantalum – Niobium ore in Sodium Hydroxide system, Trans Tech Publications, Switzerland doi: 10.4028/www.scientific.net/AMR.361-363.644

Zeng, X. and Osseo-Asare, K. (2003), Partitioning behavior of silica in the PEG/dextran/H_2O aqueous biphasic system, *Journal of Colloids and Surfaces* A: Physicochem. Eng. Aspects 226 p.45-54.

Zhang, T., Li, W., Zhou, W., Gao, H., Wu, J., Xu, G., Chen, J., Liu, H. and Chen, J. (2001), Extraction and Separation of gold (I) cyanide in polyethylene glycol-based aqueous biphasic systems, *Journal of Hydrometallurgy* 62 p. 41-46.

Zuber, P. (2012), Molybdenum. Retrieved from http://www.raci.org.au/document/item/452

APPENDICES

APPENDIX A

Procedure for analysis of sample using EDXRF

The samples were ground manually to powder with an agate mortar and pestle to grain size of less than 125 μm. pellets of 19mm diameter were prepared from 0.3 – 0.5 g powder mixed with three drops of organic liquid binder and pressed afterwards at 10 tons with hydraulic press.

Measurements were performed using an annular 25 mCi ^{109}Cd as the excitation source, that emits Ag – K X-rays (22.1 keV) in which case all elements with lower characteristic excitation energies were accessible for detection in the samples. The system consists furthermore, of a Si (Li) detector, with a resolution of 170 eVfor the 5.90 keV line, coupled to a computer controlled ADC-card

Quantificative analysis of the samples was carried out using the Emission–Transmission (E-T) method, which a number of quantification methods has been developed and applied (LEROUX and MAHMOUD, 1996, GIAUDE et al, 1979, MARKOWICZ, 1979, MARKOWICZ and VAN GRIEKEN, 1993, KUMP, 1996, BERNASCONI et al, 1996, TANG et al, 1986). These quantification methods providedifferent approaches to correct the matrix absorptionaswell enhancement effects. In this work quantification was carried out using a modified version of

E – T method (KUMP, 1996, ANGEYO et al, 1998, FUNTUA, 1999a, FUNTUA 1999b) and it involves the use of pure target material (Mo) to measure the absorption factors in the sample.

The Mo target serves as a source of monochromatic X-rays, which are excited through the sample by primary radiation and then penetrate the sample on the way to the detector. In

this way, absorption factor is experimentally determined which the program uses in the quantification of concentration of the elements. In addition, the contribution to the Mo–K peak intensity by the

Zr–K is subtracted for each sample.

Sensitivity calibration of the system was performed using thick pure metal foils (Ti, Fe, Co, Ni, Cu, Zn, Zr, Nb, Mo, Sn, Ta, Pb) and stable chemical compounds (K_2CO_3, $CaCO_3$, Ce_2O_3, WO_3, ThO_2, U_2O_3). The spectra for the samples were collected for 3000 s with the ^{14}Cd source and 2000 s for the ^{11}Fe source and the spectra were then evaluated using the AXIL – QXAS program (BENASCONI, 1996).

109Cd source was used for the analysis of K, Ca, Ti, V, Cr, Mn, Fe, Co, Ni, Cu, Zn, Ta, W, Ga, As, Se, Pb, Br, Rb, Sr, Th, Y, U, Zr, Nb and Mo. (from EDXRF Laboratory at CERT ABU, Zaria)

APPENDIX B

Procedure for analysis of sample using XRF

Mini Pal is a compact Energy dispersive X-ray spectrometer designed for the elemental analysis of a wide range of samples. The system is controlled by a PC running the dedicated Mini Pal analytical software.

The Mini Pal 4 version in use is PW 4030 X-ray Spectrometer, which is an energy dispersive microprocessor controlled analytical instrument designed for the detection and measurement of elements in a sample (solids, powders and liquids), from sodium to uranium.

The sample for analysis is weighed and ground in an agate mortar and a binder (PVC dissolved in toluene) is added to the sample, carefully mixed and pressed in a hydraulic press into pellet.

The pellet is loaded in the sample chamber of the spectrometer and voltage (30kV maximum and a current (1 mA maximum) is applied to produce the X-rays to excite the sample for a preset time (10 mins in this case). The spectrum from the sample is now analysed to determine the concentration of the elements in the sample. (Pan Analytical user's guide, 2007)

APPENDIX C

Procedure for analysis of sample using ICP – AES

Perkin-Elmer Optima 5300 UV
Inductively Coupled Plasma Atomic Emission Spectrometry (ICP-AES)

Principle - solution is nebulized into a fine aerosol which is then introduced into a high energy plasma (temperature between 7,000 to 10,000k) The plasma excites the atoms and ions to higher energy levels. As they drop back down to their normal levels, they do so by emitting energy wavelengths that are specific to the particular element. The wavelengths of emitted energy are separated in an optical chamber. By monitoring what wavelengths are emitted, we can determine what types of elements are present (qualitative determination).
By comparing the intensity of the emitted wavelengths to that of known standards, we can determine how much of each element is present (Quantitative determination).

Technique Advantages

Quantitative determination of cations in a minimum of 3-5 ml of solution.
Levels of detection vary for each cation (generally from .50 ug/L to .0001 ug/L).

Some anions such as sulfur can also be determined.
Preferred technique for refractory cations such as Al, Si, W, Zr
Capable of determining multiple elements simultaneously
Other cations determined sequentially.
Data generated may be downloaded in Excel compatible format.

Typical Applications

Elemental studies in stream waters and acid mine drainage.
Cation measurements in fusion and digestion solutions.
Analyses of refractory elements in solution.

Other information

Recommended Reading
Handbook of Inductively Coupled Plasma Spectrometry 2nd edition, M. Thompson and J.N. Walsh, Blackie, 1989

Thermo Fisher Scientific Xseries 2

Inductively Coupled Plasma Mass Spectrometry (ICP-MS)

Principle - like ICP-AES, a solution is nebulized into a fine aerosol and introduced into a high energy plasma. However, the function of the plasma is only to provide atoms and ions for the attached mass spectrometer. The mass spectrometer separates these atoms and ions on the of their atomic masses.
Quantitative determination of multi-elements and isotopes in a wide variety of sample types at trace and ultra-trace concentration levels

Technique Advantages

Rapid multi-elemental analysis capability, covering most of the elements in the Periodic Table. Variable mass resolution of 300, 4000 and 10,000, and hence, capable of achieving unambiguous And accurate elemental analysis through identification and removal of interference at high resolution. Polyatomic and isotope interferences can be avoided to accurately determine the analyte element. Ultra-high sensitivity and low dark noise, resulting in excellent detection limits at the pg/L and ng/L levels.

Linear response over more than 9 orders of magnitude and simultaneous analog and digital signal registration
Precise and accurate isotope ratio measurements for some isotopic systems.
Accurate and sensitive detection of transient signals for speciation analysis.

Typical Applications

Trace elements in a wide variety of aqueous matrices: drinking water, river, lake and ground water, waste water and effluent, and seawater.
Trace elements in solids after digestion: sediment, soil, sludge, road dust, air particulate matter, plant tissue and grain, rocks and minerals, etc.
Trace elements in samples of body fluids, including blood, plasma, and urine.

Dissolution Techniques

Since ICP-AES and ICP-MS can accommodate solutions only, it is necessary to dissolve solid samples prior to
analyses. The following are among those available at the Materials Characterization Lab.

Lithium Metaborate Fusion

The sample is mixed with a lithium metaborate flux, heated to 1000C in an ultra pure graphite crucible, and the resultant bead is dissolved in a nitric acid solution.

Lithium Metaborate Fusion - Detailed Procedure

• Add 0.100 or 0.200 gm. of -100 mesh samples to a pre-weighed vials containing 1.000 gm. of lithium metaborate.
• Shake vials by hand, gently but thoroughly mixing the two components.
• Dump contents of vials into a graphite crucibles and insert crucibles into an oven pre-heated to 900C.
• Pipette 100 ml of a 5% nitric acid solution into watch glass covered Teflon beakers and add a stirring bar to each.
• After ten minutes at 1000C (allow a few minutes for oven to return to 900C), place beakers on magnetic stirrers and start then swirl the contents of the crucibles to pick up any uncoalesced beads and dump into beakers.
• After a few minutes, carefully examine the graphite crucibles for any remaining melt, scrape off if present and add to beakers.
• Stir at least 15 minutes and transfer to polyethylene bottles for storage.

Tips and hints
• If melt sticks to graphite crucible and cannot be completely scraped out and dissolved, a smaller sample size will have to be used.
• Difficult samples such as zircons and high iron ores, will sometimes dissolved when fused in a 1:3 mix of sample to SiO_2 or Al_2O_3. (e.g. .050 gm sample + 0.150 gm SiO_2 +1.000 gm $LiBO_2$.)
• This technique will not work for elements that are volatile at 900C.
• Standards may be made by preparing a lithium metaborate matrix solution and using this to dilute down stock solutions.
• Standards may also be prepared by fusing known rock and/or ore standards (e.g. U.S.G.S. rock standards), along with the samples.
• Do not mix samples and standards prepared more than four weeks apart.
• Crucibles should be thoroughly wiped out with kimwipes in between samples.

References

Suhr, N.H. and Ingamells, C.O. (1966), Solution Technique for Analysis of Silicates, Anal. Chem., 38, 730-734.
Medlin, J.H., Suhr, N.H., and Bodkin, J.B. (1969), Atomic Absorption Analysis of Silicates Employing $LiBO_2$ Fusion, Atomic Absorption Newsletter, Vol. 8, No. 2, 25-29.
Ingamells, C.O. (1970), Lithium Metaborate Flux in Silicate Analysis, Anal. Chim. Acta, 52, 323-334.
Feldman, C. (1983), Behavior of Trace Refractory Minerals in the Lithium Metaborate Fusion-Acid Dissolution Procedure, Anal. Chem., Vol 55, No. 14, 2451-2453

Acid Digestion on a hot plate

The solid and a mix of acids (commonly a combination of nitric, hydrochloric, hydrofluoric and /or perchloric) is
placed in an open dish (typically platinum, Teflon, or glass) and heated to dryness on a hot plate. The residue is then dissolved with a dilute nitric acid solution and run.

Pros: fast works best with metallic samples.

Cons: Will not be effective for silicates and most ceramics.
Silicon is lost when hydrofluoric acid is used.

Microwave digestion

The solid and a mix of acids (commonly a combination of nitric, hydrochloric, and /or perchloric) is heated in a pressurized vessel by microwaves.

Pros: Minimal contamination from environment. Works best for minimal amounts of sample.

Cons: slow May not work for some silicates and ceramics,

Sodium Peroxide Fusion

The sample is mixed with a sodium peroxide flux, the mix is melted over a Bunsen burner, and the melt is dissolved in a hydrochloric acid solution

Pros: Fast Used primarily when the elements Li and B are required
Slightly more effective than lithium metaborate

Cons: High sodium content will cause problems in instrumentation for
low sodium analyses Volatile elements will be lost during the fusion.

APPENDIX D

Selected laboratory pictures



Plate D1 Lump of Tantalite ore (Scale: 1:1.6 cm)



Plate D2 Ball-milled and sieved Tantalite ore (particle size 74µm) Scale: 1:1.8 cm

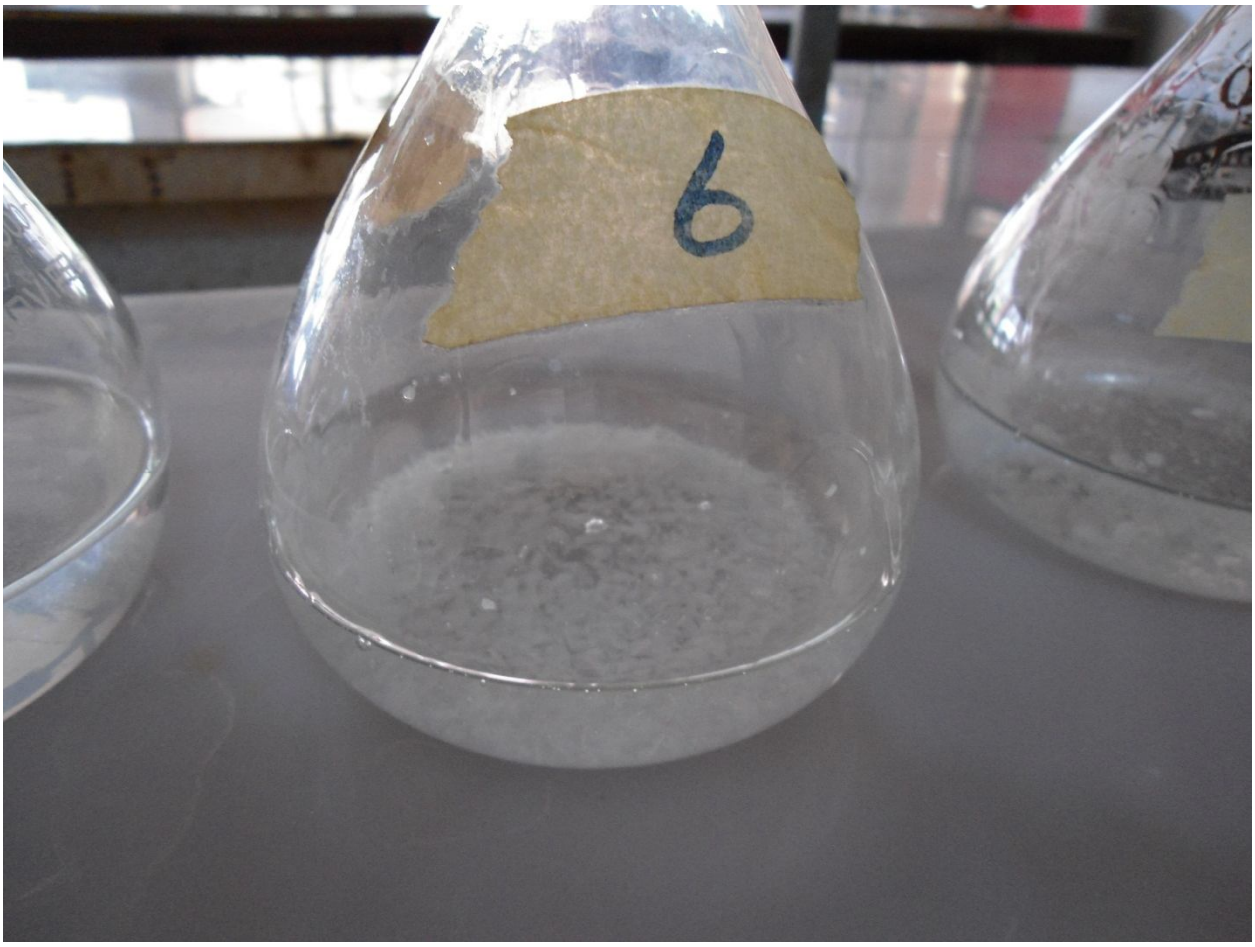


Plate D3 PEG being dissolved in deionized water



Plate D4 Dissolved PEG in deionized water



Plate D5 Picture showing PEG sample packaging

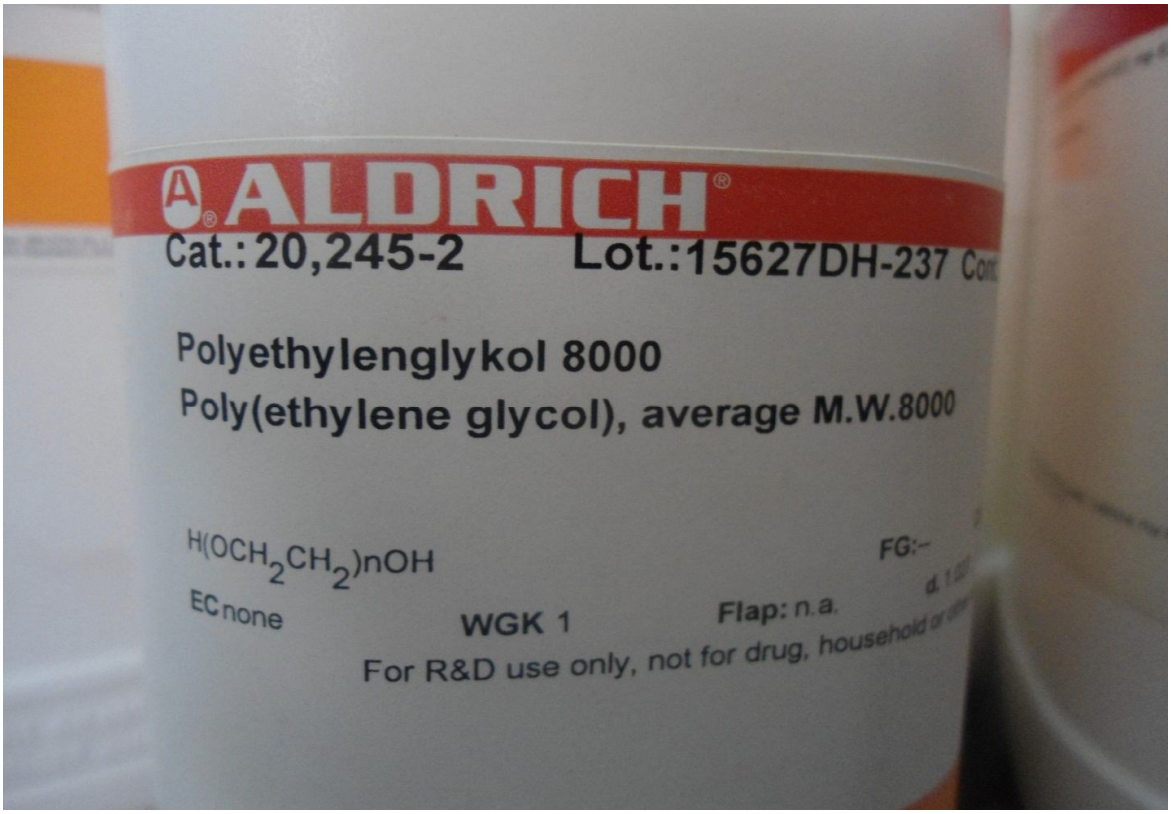


Plate D6 Picture showing sample packaging specifications



Plate D7 Picture showing PEG molecular weight

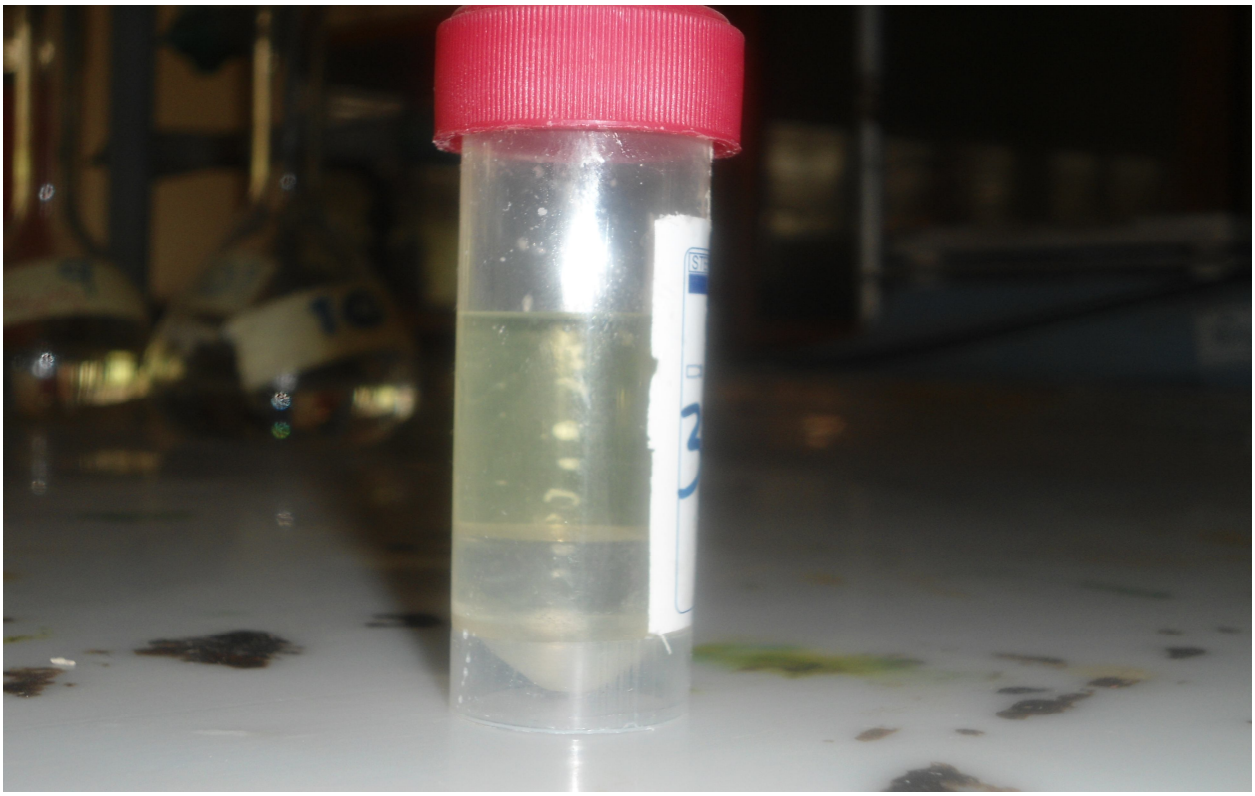


Plate D8 Picture showing separation in Aqueous Biphase System formed

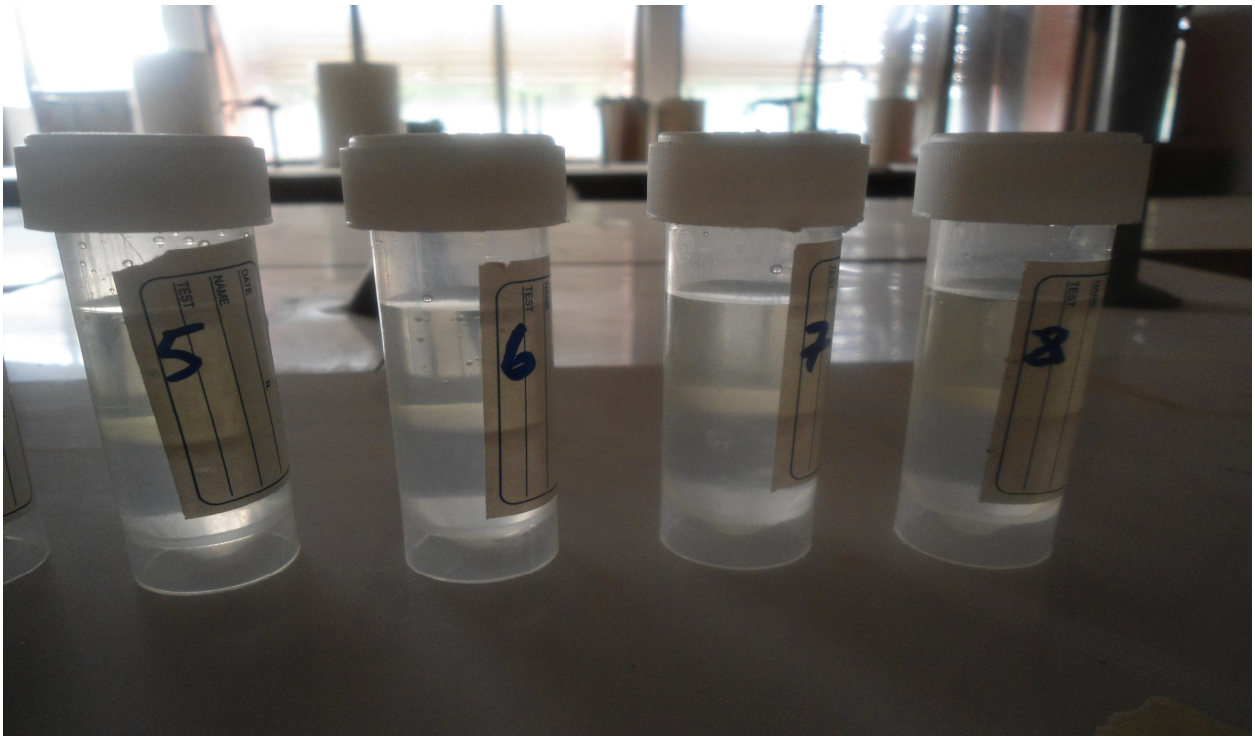


Plate D9 Picture showing more separations in Aqueous Biphase Systems formed

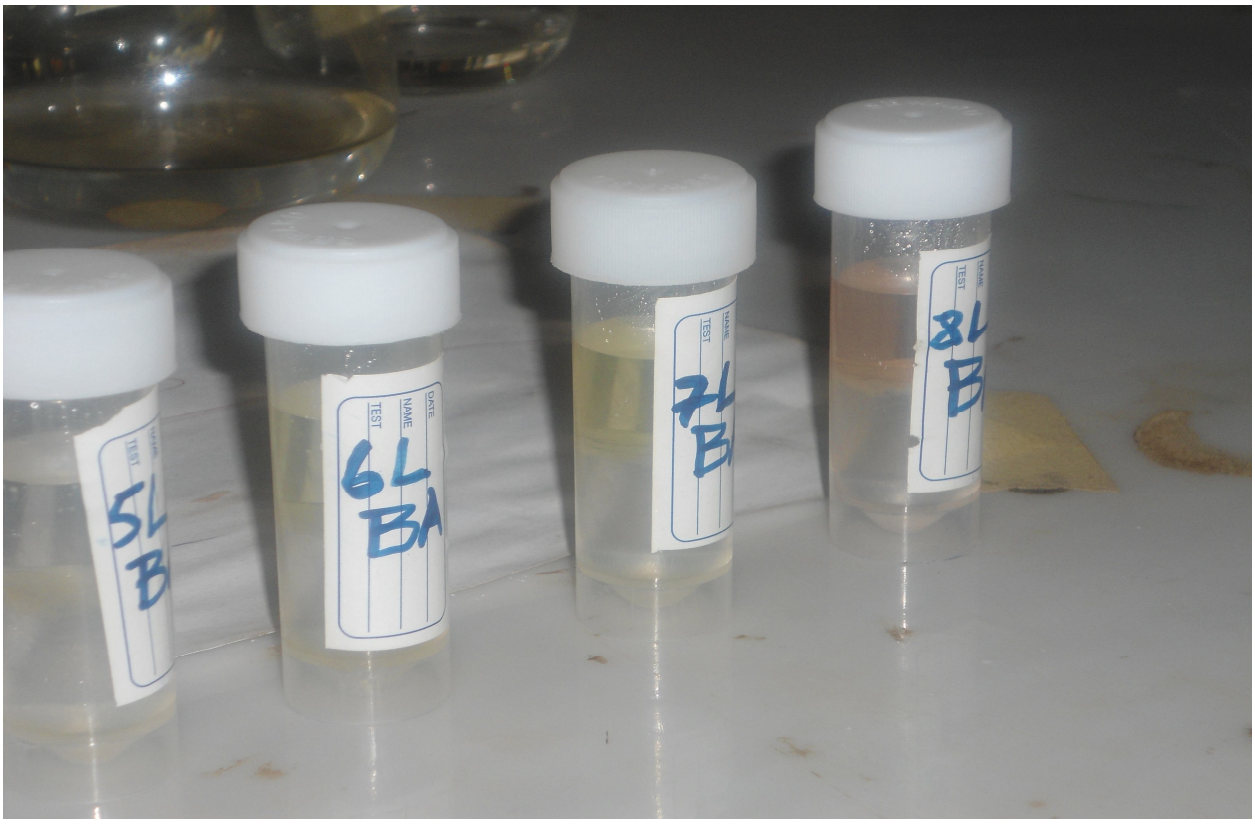


Plate D10 Picture showing more Aqueous Biphase formed

APPENDIX E

Samples of Detailed Analytical Data

E1. Inductively Coupled Plasma Emission Spectrometry (ICP-AES) at Penn State U.S.A.

PENNSTATE **Penn State Institutes of Energy and the Environment**

Emission Spectroscopy Lab

Henry Gong
Senior Analytical Chemist
312 Hosler Building
The Pennsylvania State University
University Park, PA 16801-4801
hxg3@psu.edu, 814 865-1981, Fax 814 865-8094

From:	Henry Gong, 312 Hosler Building
To:	Thaddeus Ityokumbul
Date	5/20/13
Basis	As-Received
Instrument	Perkin-Elmer Optima 5300, Inductively Coupled Plasma Emission Spectrometry (ICP-AES)
Method	
Subject	Spectrochemical Characterization
Units	µg/ml ppm = µg/ml = µg g-1 = µg/gm = mg/L
Det. Limit	0.02 0.02 0.02

Our #	Your #	Mo (ug/mL)	Nb (ug/mL)	Ta (ug/mL)	Dilution Factor
13-3629	ba	<.02	0.56	0.30	*5.95*
13-3630	ba 1l	<.02	0.02	0.04	*5.93*
13-3631	ba 3l	<.02	0.02	0.03	*5.94*
13-3632	ba 4l	0.38	<.02	0.02	*12.72*
13-3633	ba 5l	<.02	<.02	0.02	*5.91*
13-3634	ba 6l	0.39	<.02	<.02	*12.00*
13-3635	ba 7l	0.35	<.02	<.02	*13.38*
13-3636	ba 8l	0.62	<.02	<.02	*13.32*
13-3637	ba 1up	0.68	<.02	<.02	*11.98*
13-3638	ba 3up	0.62	<.02	<.02	*13.21*
13-3639	ba 4up	0.60	<.02	<.02	*12.22*
13-3640	ba 5up	0.02	<.02	<.02	*5.95*
13-3641	ba 6up	0.55	<.02	<.02	*13.07*
13-3642	ba 7up	0.80	<.02	<.02	*13.53*
13-3643	ba 8up	0.51	<.02	<.02	*12.82*
13-3644	de 3l	<.02	0.30	0.16	*5.92*
13-3645	de 4l	<.02	1.97	0.43	*5.94*
13-3646	de 5l	<.02	1.31	0.28	*5.92*
13-3647	de 6l	<.02	0.64	0.30	*5.94*
13-3648	de 7l	<.02	0.96	0.41	*5.95*
13-3649	de 8l	<.02	0.24	0.14	*5.95*
13-3650	de 3up	<.02	0.05	0.05	*6.01*

13-3651	de 4up	<.02	0.10	0.06	*5.99*
13-3652	de 5up	<.02	0.26	0.13	*5.99*
13-3653	de 6up	<.02	0.08	0.05	*5.97*
13-3654	de 7up	<.02	0.05	0.04	*5.99*
13-3655	de 8up	<.02	0.26	0.15	*5.98*
13-3656	ed	<.02	13.3	2.41	*6.00*
13-3657	ll1	0.24	36.1	21.5	*5.95*
13-3658	ll2	0.34	2.69	2.30	*6.01*

* = more diluted samples

Note:

Results in ug/mL on **as-received** basis

Samples were run on a Perkin-Elmer Optima 5300 ICP (inductively coupled plasma emission spectrometer) Synthethic standards from High Purity Standards were used to calibrate the results.

There seem to be two sets of solutions. One set was essentially aqueous and the other set has significant contents of organics. The organic set had to be diluted more in order to keep the plasma from extinguishing.
The one sample 13-3657 had a large amount of precipitation and also gave widely ranging values in the replicates.

PENNSTATE
Penn State Institutes of Energy and the Environment
Emission Spectroscopy Lab
Henry Gong
Senior Analytical Chemist
312 Hosler Building
The Pennsylvania State University
University Park, PA 16801-4801
hxg3@psu.edu, 814 865-1981, Fax 814 865-8094

From:	Henry Gong, 312 Hosler Building
To:	Ityokumbul
Date	6/3/14
Basis	As-Received
Instrument	Perkin-Elmer Optima 5300, Inductively Coupled Plasma Emission Spectrometry (ICP-AES)
Method	
Subject	Spectrochemical Characterization
Units	µg/ml

Det. Limit		5.3	0.005	0.08
Our #	Your #	Na (ug/mL)	Nb (ug/mL)	Ta (ug/mL)
14-1511	1 U	17,029	7.6	1.4
14-1512	1 L	32,583	7.4	4.7
14-1513	3 U	10,978	9.8	1.1
14-1514	3 L	34,839	8.7	4.1
14-1515	4 U	9,781	7.9	0.9
14-1516	4 L	35,350	7.6	6.7
14-1517	5 U	10,133	8.4	0.5
14-1518	5 L	34,943	7.8	5.0
14-1519	6 U	10,600	10.3	2.0
14-1520	6 L	35,302	8.8	6.0
14-1521	7 U	10,276	10.3	2.7
14-1522	7 L	34,731	8.7	5.9
14-1523	8 U	8,573	9.4	1.9
14-1524	8 L	35,476	8.4	4.8
14-1525	15	45,801	0.0	1.8
14-1526	16	46,185	13.1	-0.1

Note:

Results in ug/mL on as-received basis
Samples were diluted with 2% nitric acid
Samples were run on a Perkin-Elmer Optima 5300 ICP (inductively coupled plasma emission spectrometer) Synthethic standards from High Purity Standards were used to calibrate the results.

DF	Undiluted	Unknowns	1st	2nd	3rd	Mean
D.L.	5.376	Na 589 Radial				
170.8987	17029.286	14-1511 D2 Ityokumbul	98.22205	96.87466	99.45376	98.18349
222.7914	32583.459	14-1512 D2 Ityokumbul	142.6349	143.1539	145.1782	143.6557
118.0055	10978.310	14-1513 D2 Ityokumbul	92.18766	93.31219	89.69303	91.73096
147.2247	34838.662	14-1514 D2 Ityokumbul	232.5845	234.8674	228.0764	231.8427
157.3862	9780.546	14-1515 D2 Ityokumbul	60.86352	61.96935	61.94779	61.59355
176.6588	35350.423	14-1516 D2 Ityokumbul	191.4978	200.2178	196.8867	196.2008
189.3568	10133.200	14-1517 D2 Ityokumbul	52.49642	53.49904	53.52532	53.17359
160.2034	34942.505	14-1518 D2 Ityokumbul	212.7568	212.4349	216.1198	213.7705
172.9227	10600.154	14-1519 D2 Ityokumbul	60.53088	61.53447	60.2459	60.77041
148.9061	35302.041	14-1520 D2 Ityokumbul	233.8117	229.4841	233.52	232.2719
158.1194	10276.162	14-1521 D2 Ityokumbul	63.94658	63.57238	65.59287	64.37061
172.7542	34730.512	14-1522 D2 Ityokumbul	193.4808	198.6198	199.2366	197.1124
176.7053	8573.225	14-1523 D2 Ityokumbul	48.55618	47.69641	48.64253	48.29837
128.889	35476.153	14-1524 D2 Ityokumbul	270.4867	264.809	273.2453	269.5137
169.1938	45800.894	14-1525 D2 Ityokumbul	257.6917	268.1531	269.3928	265.0792
138.4551	46185.479	14-1526 D2 Ityokumbul	326.5572	325.2565	327.4665	326.4267
13.66542	15687.237	14-D-1511 Ityokumbul	1097.528	1125.771	1139.692	1120.997
15.31771	31348.967	14-D-1512 Ityokumbul	1984.021	1987.205	2022.104	1997.777
12.91902	10624.291	14-D-1513 Ityokumbul	812.9226	796.6164	800.4777	803.3389
13.69819	32874.880	14-D-1514 Ityokumbul	2358.627	2334.864	2334.141	2342.544
12.03125	9752.626	14-D-1515 Ityokumbul	792.9353	792.9021	789.7339	791.8571
14.35561	33828.291	14-D-1516 Ityokumbul	2288.851	2301.518	2309.961	2300.11
15.86192	9744.181	14-D-1517 Ityokumbul	606.0103	587.1376	607.8579	600.3352
13.90763	33835.593	14-D-1518 Ityokumbul	2415.567	2320.706	2387.764	2374.679
14.66837	10310.290	14-D-1519 Ityokumbul	687.5078	679.9232	692.8522	686.761
11.03772	32303.647	14-D-1520 Ityokumbul	2851.864	2905.803	2811.688	2856.452
13.33717	9915.810	14-D-1521 Ityokumbul	724.073	723.3786	731.6094	726.3537
13.25648	31618.978	14-D-1522 Ityokumbul	2436.242	2307.285	2240.865	2328.131
15.70444	8638.873	14-D-1523 Ityokumbul	541.3496	535.8364	535.8397	537.6752
12.38201	32802.434	14-D-1524 Ityokumbul	2554.171	2571.952	2631.097	2585.74
13.0724	42289.185	14-D-1525 Ityokumbul	3194.289	3077.45	3200.138	3157.293
13.66156	42790.375	14-D-1526 Ityokumbul	3048.541	3072.099	3050.266	3056.969

Extrapolated	Multiplier	Intercept	slope	Standards	1st	2nd	3rd	Mean	TI
		0.9611	0.975683						
99.6455	1	0.9999	Na 589 Radial	z100	102.0197	100.4718	103.4138	102.10	
146.251	1		Na 589 Radial	z100	104.0564	101.3719	101.24		
93.03215	1	D.L.	Na 589	z25	25.14033	24.88484	25.01033	25.39	

			Radial Na 589					
236.636	1	5.3760	Radial Na 589	z25	25.71341	25.93751	25.67801	
62.14362	1		Radial Na 589	z250	235.9121	242.9994	240.049	239.64
200.1057	1		Radial Na 589	z250	239.6659	237.5268	241.6599	
53.5138	1		Radial Na 589	z50	51.35585	52.50591	52.48823	50.30
218.1134	1		Radial Na 589	z50	49.46696	48.18019	47.78711	
61.29996	1		Radial Na 589	z500	490.9981	503.5936	484.1337	490.66
237.0759	1		Radial Na 589	z500	490.7022	492.2207	482.2817	
64.98989	1		Radial Na 589	zblk	0.172238	0.0799	0.252389	0.20
201.0401	1		Radial	zblk	0.293067	0.215031	0.160205	
48.51707	1							
275.2458	1							
270.7008	1							
333.5774	1							
1147.951	1							
2046.583	1							
822.3759	1							
2399.944	1							
810.6079	1							
2356.452	1							
614.3126	1							
2432.879	1							
702.8925	1							
2926.659	1							
743.4719	1							
2385.171	1							
550.0909	1							
2649.201	1							
3234.998	1							
3132.174	1							

DF	Undiluted	Unknowns	1st	2nd	3rd	Mean
D.L.	0.000	Nb 309.418				
170.8987	7.504	14-1511 D2 Ityokumbul	0.029324	0.032156	0.031161	0.03088
222.7914	6.938	14-1512 D2 Ityokumbul	0.021336	0.022849	0.020594	0.021593
118.0055	9.727	14-1513 D2 Ityokumbul	0.058122	0.059425	0.059157	0.058901
147.2247	8.518	14-1514 D2 Ityokumbul	0.041113	0.0403	0.041668	0.041027
157.3862	7.943	14-1515 D2 Ityokumbul	0.033526	0.035475	0.037955	0.035652
176.6588	7.109	14-1516 D2 Ityokumbul	0.028735	0.028775	0.027132	0.028214
189.3568	8.158	14-1517 D2 Ityokumbul	0.031004	0.030175	0.029655	0.030278
160.2034	7.429	14-1518 D2 Ityokumbul	0.031852	0.03278	0.033389	0.032674
172.9227	9.625	14-1519 D2 Ityokumbul	0.039796	0.039351	0.039145	0.039431
148.9061	8.348	14-1520 D2 Ityokumbul	0.039572	0.039746	0.039839	0.039719

158.1194	10.133	14-1521 D2	Ityokumbul	0.044801	0.045376	0.046491	0.045556
172.7542	9.145	14-1522 D2	Ityokumbul	0.040921	0.035584	0.035835	0.037446
176.7053	8.920	14-1523 D2	Ityokumbul	0.036392	0.035209	0.035375	0.035659
128.889	8.298	14-1524 D2	Ityokumbul	0.046212	0.046226	0.044876	0.045771
169.1938	-0.362	14-1525 D2	Ityokumbul	-0.00336	-0.00281	-0.00168	-0.00261
138.4551	13.369	14-1526 D2	Ityokumbul	0.071327	0.069445	0.066767	0.06918
13.66542	7.528	14-D-1511	Ityokumbul	0.397053	0.409414	0.392459	0.399642
15.31771	7.362	14-D-1512	Ityokumbul	0.348104	0.347584	0.349938	0.348542
12.91902	9.781	14-D-1513	Ityokumbul	0.53896	0.553742	0.556192	0.549631
13.69819	8.751	14-D-1514	Ityokumbul	0.474739	0.45934	0.456819	0.463632
12.03125	7.935	14-D-1515	Ityokumbul	0.479727	0.478257	0.478131	0.478705
14.35561	7.573	14-D-1516	Ityokumbul	0.385794	0.383257	0.37895	0.382667
15.86192	8.365	14-D-1517	Ityokumbul	0.385525	0.381645	0.380501	0.382557
13.90763	7.793	14-D-1518	Ityokumbul	0.407636	0.402747	0.409274	0.406552
14.66837	10.357	14-D-1519	Ityokumbul	0.516792	0.507112	0.513749	0.512551
11.03772	8.793	14-D-1520	Ityokumbul	0.582529	0.577752	0.574837	0.578373
13.33717	10.260	14-D-1521	Ityokumbul	0.560507	0.56332	0.551677	0.558501
13.25648	8.749	14-D-1522	Ityokumbul	0.479706	0.480969	0.476284	0.478986
15.70444	9.505	14-D-1523	Ityokumbul	0.432594	0.431867	0.453086	0.439182
12.38201	8.473	14-D-1524	Ityokumbul	0.492227	0.496054	0.501841	0.496707
13.0724	-0.082	14-D-1525	Ityokumbul	-0.00657	-0.00609	-0.00427	-0.00564
13.66156	13.174	14-D-1526	Ityokumbul	0.691596	0.719568	0.690009	0.700391

Extrapolated	Multiplier	Intercept	slope	Standards	1st	2nd	3rd	Mean	TRUE
		-0.0011	0.727392 Nb						
0.043908	1	1.0000	309.418 Nb	z100	0.183602	0.183096	0.183417	0.18	0.25
0.03114	1		309.418 Nb	z100	0.18384	0.183792	0.18236		
0.082431	1	D.L.	309.418 Nb	z25	0.044831	0.045281	0.044003	0.04	0.063
0.057858	1	-0.0003	309.418 Nb	z25	0.043465	0.043841	0.043651		
0.050468	1		309.418 Nb	z250	0.445466	0.447122	0.445539	0.45	0.625
0.040242	1		309.418 Nb	z250	0.446986	0.446264	0.450803		
0.04308	1		309.418 Nb	z50	0.093206	0.093262	0.09108	0.09	0.125
0.046374	1		309.418 Nb	z50	0.088792	0.09005	0.088205		
0.055663	1		309.418 Nb	z500	0.911977	0.918622	0.915715	0.91	1.25
0.056059	1		309.418 Nb	z500	0.90186	0.896503	0.920469		
0.064084	1		309.418 Nb	zblk	0.00052	0.000205	-0.00121	0.00	0
0.052935	1		309.418	zblk	-0.00086	0.000346	-0.00162		
0.050477	1								
0.06438	1								
-0.00214	1								
0.096561	1								

0.550871	1
0.480621	1
0.757073	1
0.638844	1
0.659565	1
0.527536	1
0.527383	1
0.560372	1
0.706096	1
0.796586	1
0.769268	1
0.659952	1
0.605231	1
0.684314	1
-0.00631	1
0.964334	1

DF	Undiluted	Unknowns	1st	2nd	3rd	Mean
D.L.	0.000	Nb 309.418				
170.8987	7.421	14-1511 D2 Ityokumbul	0.029324	0.032156	0.031161	0.03088
222.7914	6.865	14-1512 D2 Ityokumbul	0.021336	0.022849	0.020594	0.021593
118.0055	9.613	14-1513 D2 Ityokumbul	0.058122	0.059425	0.059157	0.058901
147.2247	8.421	14-1514 D2 Ityokumbul	0.041113	0.0403	0.041668	0.041027
157.3862	7.854	14-1515 D2 Ityokumbul	0.033526	0.035475	0.037955	0.035652
176.6588	7.032	14-1516 D2 Ityokumbul	0.028735	0.028775	0.027132	0.028214
189.3568	8.068	14-1517 D2 Ityokumbul	0.031004	0.030175	0.029655	0.030278
160.2034	7.347	14-1518 D2 Ityokumbul	0.031852	0.03278	0.033389	0.032674
172.9227	9.516	14-1519 D2 Ityokumbul	0.039796	0.039351	0.039145	0.039431
148.9061	8.253	14-1520 D2 Ityokumbul	0.039572	0.039746	0.039839	0.039719
158.1194	10.016	14-1521 D2 Ityokumbul	0.044801	0.045376	0.046491	0.045556
172.7542	9.041	14-1522 D2 Ityokumbul	0.040921	0.035584	0.035835	0.037446
176.7053	8.819	14-1523 D2 Ityokumbul	0.036392	0.035209	0.035375	0.035659
128.889	8.202	14-1524 D2 Ityokumbul	0.046212	0.046226	0.044876	0.045771
169.1938	-0.346	14-1525 D2 Ityokumbul	-0.00336	-0.00281	-0.00168	-0.00261
138.4551	13.211	14-1526 D2 Ityokumbul	0.071327	0.069445	0.066767	0.06918
13.66542	7.434	14-D-1511 Ityokumbul	0.397053	0.409414	0.392459	0.399642
15.31771	7.270	14-D-1512 Ityokumbul	0.348104	0.347584	0.349938	0.348542
12.91902	9.658	14-D-1513 Ityokumbul	0.53896	0.553742	0.556192	0.549631
13.69819	8.642	14-D-1514 Ityokumbul	0.474739	0.45934	0.456819	0.463632
12.03125	7.836	14-D-1515 Ityokumbul	0.479727	0.478257	0.478131	0.478705
14.35561	7.479	14-D-1516 Ityokumbul	0.385794	0.383257	0.37895	0.382667
15.86192	8.261	14-D-1517 Ityokumbul	0.385525	0.381645	0.380501	0.382557
13.90763	7.696	14-D-1518 Ityokumbul	0.407636	0.402747	0.409274	0.406552
14.66837	10.228	14-D-1519 Ityokumbul	0.516792	0.507112	0.513749	0.512551
11.03772	8.683	14-D-1520 Ityokumbul	0.582529	0.577752	0.574837	0.578373
13.33717	10.132	14-D-1521 Ityokumbul	0.560507	0.56332	0.551677	0.558501
13.25648	8.639	14-D-1522 Ityokumbul	0.479706	0.480969	0.476284	0.478986
15.70444	9.386	14-D-1523 Ityokumbul	0.432594	0.431867	0.453086	0.439182
12.38201	8.367	14-D-1524 Ityokumbul	0.492227	0.496054	0.501841	0.496707
13.0724	-0.081	14-D-1525 Ityokumbul	-0.00657	-0.00609	-0.00427	-0.00564

13.66156	13.009	14-D-1526	Ityokumbul		0.691596	0.719568	0.690009	0.700391	
Extrapolated	Multiplier	Intercept	slope	Standards	1st	2nd	3rd	Mean	TRUE
		-0.0011	0.736662						
			Nb						
0.043423	1	1.0000	309.418	z100	0.183602	0.183096	0.183417	0.18	0.25
			Nb						
0.030815	1		309.418	z100	0.18384	0.183792	0.18236		
			Nb						
0.081461	1	D.L.	309.418	z25	0.044831	0.045281	0.044003	0.04	0.063
			Nb						
0.057197	1	-0.0003	309.418	z25	0.043465	0.043841	0.043651		
			Nb						
0.0499	1		309.418	z250	0.445466	0.447122	0.445539	0.45	
			Nb						
0.039803	1		309.418	z250	0.446986	0.446264	0.450803		
			Nb						
0.042605	1		309.418	z50	0.093206	0.093262	0.09108	0.09	0.125
			Nb						
0.045858	1		309.418	z50	0.088792	0.09005	0.088205		
			Nb						
0.05503	1		309.418	z500	0.911977	0.918622	0.915715	0.91	
			Nb						
0.055421	1		309.418	z500	0.90186	0.896503	0.920469		
			Nb						
0.063345	1		309.418	zblk	0.00052	0.000205	-0.00121	0.00	0
			Nb						
0.052336	1		309.418	zblk	-0.00086	0.000346	-0.00162		
0.049909	1								
0.063637	1								
-0.00205	1								
0.095413	1								
0.544007	1								
0.47464	1								
0.747614	1								
0.630873	1								
0.651333	1								
0.520965	1								
0.520814	1								
0.553388	1								
0.697278	1								
0.786629	1								
0.759655	1								
0.651715	1								
0.597682	1								
0.67577	1								
-0.00616	1								
0.952266	1								

DF	Undiluted	Unknowns		1st	2nd	3rd	Mean
D.L.	0.001	Nb 269.706					
170.8987	7.734	14-1511 D2	Ityokumbul	0.032993	0.031275	0.030926	0.031731
222.7914	7.142	14-1512 D2	Ityokumbul	0.02158	0.021777	0.021394	0.021584

118.0055	9.599	14-1513 D2	Ityokumbul	0.059261	0.05904	0.060135	0.059479	
147.2247	8.694	14-1514 D2	Ityokumbul	0.042962	0.041743	0.042324	0.042343	
157.3862	8.158	14-1515 D2	Ityokumbul	0.037194	0.035641	0.037541	0.036792	
176.6588	7.602	14-1516 D2	Ityokumbul	0.030685	0.030149	0.02923	0.030021	
189.3568	8.281	14-1517 D2	Ityokumbul	0.030401	0.029391	0.031895	0.030562	
160.2034	7.614	14-1518 D2	Ityokumbul	0.034388	0.034241	0.031804	0.033477	
172.9227	9.687	14-1519 D2	Ityokumbul	0.038887	0.041085	0.040055	0.040009	
148.9061	8.879	14-1520 D2	Ityokumbul	0.043838	0.04224	0.042275	0.042785	
158.1194	10.218	14-1521 D2	Ityokumbul	0.048247	0.045998	0.045632	0.046626	
172.7542	9.156	14-1522 D2	Ityokumbul	0.038098	0.037524	0.03744	0.037687	
176.7053	9.345	14-1523 D2	Ityokumbul	0.037041	0.038895	0.036858	0.037598	
128.889	8.448	14-1524 D2	Ityokumbul	0.047652	0.046427	0.047923	0.047334	
169.1938	0.333	14-1525 D2	Ityokumbul	-0.00088	-0.00154	-0.00224	-0.00155	
138.4551	12.954	14-1526 D2	Ityokumbul	0.066048	0.070276	0.070296	0.068873	
13.66542	7.559	14-D-1511	Ityokumbul	0.417708	0.432163	0.416898	0.422256	
15.31771	7.366	14-D-1512	Ityokumbul	0.3704	0.365136	0.364473	0.36667	
12.91902	9.771	14-D-1513	Ityokumbul	0.569406	0.581329	0.58467	0.578468	
13.69819	8.721	14-D-1514	Ityokumbul	0.498009	0.483171	0.478177	0.486452	
12.03125	7.936	14-D-1515	Ityokumbul	0.505589	0.499917	0.506868	0.504125	
14.35561	7.648	14-D-1516	Ityokumbul	0.40649	0.403972	0.409261	0.406575	
15.86192	8.353	14-D-1517	Ityokumbul	0.404312	0.400676	0.400614	0.401867	
13.90763	7.825	14-D-1518	Ityokumbul	0.427789	0.430228	0.430644	0.429553	
14.66837	10.304	14-D-1519	Ityokumbul	0.539074	0.532624	0.539455	0.537051	
11.03772	8.770	14-D-1520	Ityokumbul	0.612907	0.608161	0.602608	0.607892	
13.33717	10.268	14-D-1521	Ityokumbul	0.5855	0.599143	0.582165	0.588936	
13.25648	8.722	14-D-1522	Ityokumbul	0.503583	0.504913	0.499955	0.502817	
15.70444	9.428	14-D-1523	Ityokumbul	0.450872	0.448257	0.476575	0.458568	
12.38201	8.427	14-D-1524	Ityokumbul	0.513128	0.520884	0.526671	0.520228	
13.0724	0.035	14-D-1525	Ityokumbul	-0.00085	-0.00133	-0.00093	-0.00104	
13.66156	13.135	14-D-1526	Ityokumbul	0.727459	0.755097	0.726158	0.736238	

Extrapolated	Multiplier	Intercept	slope	Standards	1st	2nd	3rd	Mean	TRUE
		-0.0031	0.768922						
			Nb						
0.045254	1	0.9999	269.706	z100	0.192832	0.193914	0.19338	0.19	0.25
			Nb						
0.032056	1		269.706	z100	0.191037	0.193306	0.190458		
			Nb						
0.08134	1	D.L.	269.706	z25	0.046304	0.044627	0.044347	0.04	0.063
			Nb						
0.059055	1	0.0005	269.706	z25	0.044187	0.044497	0.0436		
			Nb						
0.051836	1		269.706	z250	0.468949	0.475306	0.467653	0.47	0.625
			Nb						
0.04303	1		269.706	z250	0.467246	0.470723	0.472638		
			Nb						
0.043734	1		269.706	z50	0.094211	0.093286	0.095374	0.09	0.125
			Nb						
0.047525	1		269.706	z50	0.089351	0.088122	0.090582		
			Nb						
0.056019	1		269.706	z500	0.96661	0.969802	0.975597	0.96	1.25
0.059629	1		Nb	z500	0.948826	0.939974	0.965855		

		269.706 Nb						
0.064624	1	269.706 Nb	zblk	-0.00113	0.000421	-0.00076	0.00	0
0.052999	1	269.706	zblk	-0.00099	-0.0012	-0.0005		
0.052884	1							
0.065545	1							
0.001966	1							
0.093558	1							
0.55314	1							
0.480849	1							
0.756297	1							
0.636629	1							
0.659612	1							
0.532746	1							
0.526624	1							
0.56263	1							
0.702433	1							
0.794564	1							
0.769911	1							
0.657912	1							
0.600365	1							
0.680555	1							
0.00264	1							
0.961481	1							

DF	Undiluted	Unknowns	1st	2nd	3rd	Mean
D.L.	0.001	Nb 269.706				
170.8987	7.595	14-1511 D2 Ityokumbul	0.032993	0.031275	0.030926	0.031731
222.7914	6.984	14-1512 D2 Ityokumbul	0.02158	0.021777	0.021394	0.021584
118.0055	9.470	14-1513 D2 Ityokumbul	0.059261	0.05904	0.060135	0.059479
147.2247	8.559	14-1514 D2 Ityokumbul	0.042962	0.041743	0.042324	0.042343
157.3862	8.023	14-1515 D2 Ityokumbul	0.037194	0.035641	0.037541	0.036792
176.6588	7.462	14-1516 D2 Ityokumbul	0.030685	0.030149	0.02923	0.030021
189.3568	8.130	14-1517 D2 Ityokumbul	0.030401	0.029391	0.031895	0.030562
160.2034	7.481	14-1518 D2 Ityokumbul	0.034388	0.034241	0.031804	0.033477
172.9227	9.532	14-1519 D2 Ityokumbul	0.038887	0.041085	0.040055	0.040009
148.9061	8.742	14-1520 D2 Ityokumbul	0.043838	0.04224	0.042275	0.042785
158.1194	10.066	14-1521 D2 Ityokumbul	0.048247	0.045998	0.045632	0.046626
172.7542	9.005	14-1522 D2 Ityokumbul	0.038098	0.037524	0.03744	0.037687
176.7053	9.191	14-1523 D2 Ityokumbul	0.037041	0.038895	0.036858	0.037598
128.889	8.323	14-1524 D2 Ityokumbul	0.047652	0.046427	0.047923	0.047334
169.1938	0.253	14-1525 D2 Ityokumbul	-0.00088	-0.00154	-0.00224	-0.00155
138.4551	12.789	14-1526 D2 Ityokumbul	0.066048	0.070276	0.070296	0.068873
13.66542	7.494	14-D-1511 Ityokumbul	0.417708	0.432163	0.416898	0.422256
15.31771	7.301	14-D-1512 Ityokumbul	0.3704	0.365136	0.364473	0.36667
12.91902	9.688	14-D-1513 Ityokumbul	0.569406	0.581329	0.58467	0.578468
13.69819	8.646	14-D-1514 Ityokumbul	0.498009	0.483171	0.478177	0.486452
12.03125	7.868	14-D-1515 Ityokumbul	0.505589	0.499917	0.506868	0.504125
14.35561	7.582	14-D-1516 Ityokumbul	0.40649	0.403972	0.409261	0.406575
15.86192	8.281	14-D-1517 Ityokumbul	0.404312	0.400676	0.400614	0.401867

13.90763	7.757	14-D-1518	Ityokumbul	0.427789	0.430228	0.430644	0.429553	
14.66837	10.216	14-D-1519	Ityokumbul	0.539074	0.532624	0.539455	0.537051	
11.03772	8.697	14-D-1520	Ityokumbul	0.612907	0.608161	0.602608	0.607892	
13.33717	10.182	14-D-1521	Ityokumbul	0.5855	0.599143	0.582165	0.588936	
13.25648	8.647	14-D-1522	Ityokumbul	0.503583	0.504913	0.499955	0.502817	
15.70444	9.347	14-D-1523	Ityokumbul	0.450872	0.448257	0.476575	0.458568	
12.38201	8.355	14-D-1524	Ityokumbul	0.513128	0.520884	0.526671	0.520228	
13.0724	0.028	14-D-1525	Ityokumbul	-0.00085	-0.00133	-0.00093	-0.00104	
13.66156	13.026	14-D-1526	Ityokumbul	0.727459	0.755097	0.726158	0.736238	

Extrapolated	Multiplier	Intercept	slope	Standards	1st	2nd	3rd	Mean	TRUE
		-0.0027	0.774987 Nb						
0.044443	1	0.9997	269.706 Nb	z100	0.192832	0.193914	0.19338	0.19	0.25
0.03135	1		269.706 Nb	z100	0.191037	0.193306	0.190458		
0.080247	1	D.L.	269.706 Nb	z25	0.046304	0.044627	0.044347	0.04	0.063
0.058137	1	0.0009	269.706 Nb	z25	0.044187	0.044497	0.0436		
0.050974	1		269.706 Nb	z250	0.468949	0.475306	0.467653	0.47	
0.042237	1		269.706 Nb	z250	0.467246	0.470723	0.472638		
0.042935	1		269.706 Nb	z50	0.094211	0.093286	0.095374	0.09	0.125
0.046697	1		269.706 Nb	z50	0.089351	0.088122	0.090582		
0.055125	1		269.706 Nb	z500	0.96661	0.969802	0.975597	0.96	
0.058706	1		269.706 Nb	z500	0.948826	0.939974	0.965855		
0.063662	1		269.706 Nb	zblk	-0.00113	0.000421	-0.00076	0.00	0
0.052128	1		269.706	zblk	-0.00099	-0.0012	-0.0005		
0.052014	1								
0.064576	1								
0.001495	1								
0.09237	1								
0.548355	1								
0.476629	1								
0.749922	1								
0.63119	1								
0.653993	1								
0.52812	1								
0.522046	1								
0.557771	1								
0.696479	1								
0.787889	1								
0.763429	1								
0.652306	1								
0.59521	1								

0.674772	1
0.002163	1
0.953499	1

DF	Undiluted	Unknowns		1st	2nd	3rd	Mean
D.L.	0.081	Ta 226.230					
170.8987	1.570	14-1511 D2	Ityokumbul	0.017351	0.022322	0.008729	0.016134
222.7914	3.495	14-1512 D2	Ityokumbul	0.052384	0.037582	0.01565	0.035205
118.0055	0.955	14-1513 D2	Ityokumbul	-0.01352	0.021492	0.030819	0.012929
147.2247	5.010	14-1514 D2	Ityokumbul	0.091466	0.081594	0.094079	0.089047
157.3862	1.288	14-1515 D2	Ityokumbul	-0.02598	0.025438	0.040107	0.013189
176.6588	6.188	14-1516 D2	Ityokumbul	0.100856	0.089395	0.085657	0.09197
189.3568	0.824	14-1517 D2	Ityokumbul	0.010372	0.001936	-0.00649	0.001938
160.2034	4.731	14-1518 D2	Ityokumbul	0.088044	0.065487	0.073965	0.075832
172.9227	1.899	14-1519 D2	Ityokumbul	0.023387	0.016462	0.024333	0.021394
148.9061	6.926	14-1520 D2	Ityokumbul	0.123132	0.122339	0.131546	0.125672
158.1194	1.643	14-1521 D2	Ityokumbul	0.017655	0.036919	0.00444	0.019671
172.7542	5.615	14-1522 D2	Ityokumbul	0.093832	0.066592	0.093285	0.08457
176.7053	1.316	14-1523 D2	Ityokumbul	0.025735	0.022015	-0.01467	0.011025
128.889	4.947	14-1524 D2	Ityokumbul	0.110419	0.098154	0.09687	0.101814
169.1938	1.226	14-1525 D2	Ityokumbul	0.024287	-0.00143	0.008436	0.010431
138.4551	0.197	14-1526 D2	Ityokumbul	0.019558	-0.00771	-0.0318	-0.00665
13.66542	1.413	14-D-1511	Ityokumbul	0.304932	0.279171	0.293633	0.292578
15.31771	4.679	14-D-1512	Ityokumbul	0.863918	0.925662	0.867787	0.885789
12.91902	1.117	14-D-1513	Ityokumbul	0.223724	0.25354	0.251392	0.242885
13.69819	4.082	14-D-1514	Ityokumbul	0.885116	0.840588	0.865574	0.863759
12.03125	0.875	14-D-1515	Ityokumbul	0.230652	0.205914	0.171286	0.202617
14.35561	6.683	14-D-1516	Ityokumbul	1.332052	1.357892	1.37678	1.355575
15.86192	0.513	14-D-1517	Ityokumbul	0.087565	0.081661	0.08275	0.083992
13.90763	5.034	14-D-1518	Ityokumbul	1.044577	1.064444	1.04532	1.051447
14.66837	2.000	14-D-1519	Ityokumbul	0.411038	0.366517	0.390286	0.389281
11.03772	6.031	14-D-1520	Ityokumbul	1.625749	1.558022	1.594484	1.592752
13.33717	2.666	14-D-1521	Ityokumbul	0.584578	0.551351	0.591682	0.57587
13.25648	5.892	14-D-1522	Ityokumbul	1.326824	1.266832	1.287564	1.29374
15.70444	1.885	14-D-1523	Ityokumbul	0.313651	0.34692	0.363742	0.341438
12.38201	4.794	14-D-1524	Ityokumbul	1.146675	1.106847	1.122935	1.125485
13.0724	1.800	14-D-1525	Ityokumbul	0.406636	0.386805	0.386246	0.393229
13.66156	-0.073	14-D-1526	Ityokumbul	-0.03091	-0.04232	-0.00658	-0.0266

Extrapolated	Multiplier	Intercept	slope	Standards	1st	2nd	3rd	Mean	TRUE
		-0.0108	2.93502						
			Ta						
0.009188	1	0.9998	226.230	z100	0.735758	0.734531	0.73351	0.73	0.25
			Ta						
0.015686	1		226.230	z100	0.701784	0.705198	0.753158		
			Ta						
0.008097	1	D.L.	226.230	z25	0.182613	0.153873	0.166226	0.17	0.063
			Ta						
0.034031	1	0.0815	226.230	z25	0.170932	0.185268	0.153948		
			Ta						
0.008185	1		226.230	z250	1.791363	1.780144	1.806231	1.77	

		Ta						
0.035027	1	226.230	z250	1.759266	1.76229	1.73414		
		Ta						
0.004352	1	226.230	z50	0.368777	0.350322	0.385339	0.35	0.125
		Ta						
0.029528	1	226.230	z50	0.329556	0.325516	0.335306		
		Ta						
0.010981	1	226.230	z500	3.649741	3.655405	3.652554	3.61	
		Ta						
0.04651	1	226.230	z500	3.541013	3.544272	3.601434		
		Ta						
0.010394	1	226.230	zblk	-0.00166	-0.00126	-0.0313	0.00	0
		Ta						
0.032505	1	226.230	zblk	0.016624	-0.00442	-0.00519		
0.007448	1							
0.038381	1							
0.007245	1							
0.001424	1							
0.103377	1							
0.305491	1							
0.086446	1							
0.297985	1							
0.072726	1							
0.465554	1							
0.032308	1							
0.361933	1							
0.136324	1							
0.546363	1							
0.199898	1							
0.444486	1							
0.120024	1							
0.387159	1							
0.13767	1							
-0.00537	1							

DF	Undiluted	Unknowns	1st	2nd	3rd	Mean
D.L.	0.083	Ta 226.230				
170.8987	1.485	14-1511 D2 Ityokumbul	0.017351	0.022322	0.008729	0.016134
222.7914	3.408	14-1512 D2 Ityokumbul	0.052384	0.037582	0.01565	0.035205
118.0055	0.894	14-1513 D2 Ityokumbul	-0.01352	0.021492	0.030819	0.012929
147.2247	4.999	14-1514 D2 Ityokumbul	0.091466	0.081594	0.094079	0.089047
157.3862	1.207	14-1515 D2 Ityokumbul	-0.02598	0.025438	0.040107	0.013189
176.6588	6.177	14-1516 D2 Ityokumbul	0.100856	0.089395	0.085657	0.09197
189.3568	0.714	14-1517 D2 Ityokumbul	0.010372	0.001936	-0.00649	0.001938
160.2034	4.706	14-1518 D2 Ityokumbul	0.088044	0.065487	0.073965	0.075832
172.9227	1.818	14-1519 D2 Ityokumbul	0.023387	0.016462	0.024333	0.021394
148.9061	6.946	14-1520 D2 Ityokumbul	0.123132	0.122339	0.131546	0.125672
158.1194	1.568	14-1521 D2 Ityokumbul	0.017655	0.036919	0.00444	0.019671
172.7542	5.598	14-1522 D2 Ityokumbul	0.093832	0.066592	0.093285	0.08457
176.7053	1.223	14-1523 D2 Ityokumbul	0.025735	0.022015	-0.01467	0.011025
128.889	4.946	14-1524 D2 Ityokumbul	0.110419	0.098154	0.09687	0.101814
169.1938	1.136	14-1525 D2 Ityokumbul	0.024287	-0.00143	0.008436	0.010431

138.4551	0.110	14-1526 D2	Ityokumbul	0.019558	-0.00771	-0.0318	-0.00665
13.66542	1.428	14-D-1511	Ityokumbul	0.304932	0.279171	0.293633	0.292578
15.31771	4.749	14-D-1512	Ityokumbul	0.863918	0.925662	0.867787	0.885789
12.91902	1.127	14-D-1513	Ityokumbul	0.223724	0.25354	0.251392	0.242885
13.69819	4.142	14-D-1514	Ityokumbul	0.885116	0.840588	0.865574	0.863759
12.03125	0.882	14-D-1515	Ityokumbul	0.230652	0.205914	0.171286	0.202617
14.35561	6.787	14-D-1516	Ityokumbul	1.332052	1.357892	1.37678	1.355575
15.86192	0.511	14-D-1517	Ityokumbul	0.087565	0.081661	0.08275	0.083992
13.90763	5.110	14-D-1518	Ityokumbul	1.044577	1.064444	1.04532	1.051447
14.66837	2.024	14-D-1519	Ityokumbul	0.411038	0.366517	0.390286	0.389281
11.03772	6.126	14-D-1520	Ityokumbul	1.625749	1.558022	1.594484	1.592752
13.33717	2.703	14-D-1521	Ityokumbul	0.584578	0.551351	0.591682	0.57587
13.25648	5.984	14-D-1522	Ityokumbul	1.326824	1.266832	1.287564	1.29374
15.70444	1.907	14-D-1523	Ityokumbul	0.313651	0.34692	0.363742	0.341438
12.38201	4.867	14-D-1524	Ityokumbul	1.146675	1.106847	1.122935	1.125485
13.0724	1.822	14-D-1525	Ityokumbul	0.406636	0.386805	0.386246	0.393229
13.66156	-0.084	14-D-1526	Ityokumbul	-0.03091	-0.04232	-0.00658	-0.0266

Extrapolated	Multiplier	Intercept	slope	Standards	1st	2nd	3rd	Mean	TRUE
		-0.0089	2.886074						
			Ta						
0.00869	1	1.0000	226.230	z100	0.735758	0.734531	0.73351	0.73	0.25
			Ta						
0.015298	1		226.230	z100	0.701784	0.705198	0.753158		
			Ta						
0.007579	1	D.L.	226.230	z25	0.182613	0.153873	0.166226	0.17	0.063
			Ta						
0.033953	1	0.0834	226.230	z25	0.170932	0.185268	0.153948		
			Ta						
0.007669	1		226.230	z250	1.791363	1.780144	1.806231	1.77	0.625
			Ta						
0.034966	1		226.230	z250	1.759266	1.76229	1.73414		
			Ta						
0.003771	1		226.230	z50	0.368777	0.350322	0.385339	0.35	0.125
			Ta						
0.029374	1		226.230	z50	0.329556	0.325516	0.335306		
			Ta						
0.010512	1		226.230	z500	3.649741	3.655405	3.652554	3.61	1.25
			Ta						
0.046644	1		226.230	z500	3.541013	3.544272	3.601434		
			Ta						
0.009915	1		226.230	zblk	-0.00166	-0.00126	-0.0313	0.00	0
			Ta						
0.032402	1		226.230	zblk	0.016624	-0.00442	-0.00519		
0.006919	1								
0.038377	1								
0.006714	1								
0.000794	1								
0.104475	1								
0.310018	1								
0.087257	1								
0.302384	1								
0.073304	1								

0.472794	1
0.032202	1
0.367417	1
0.137982	1
0.554974	1
0.202634	1
0.451369	1
0.121405	1
0.39307	1
0.13935	1
-0.00612	1

Instruments and Methods

Perkin-Elmer Optima 5300 UV
Inductively Coupled Plasma Atomic Emission Spectrometry (ICP-AES)

Principle - solution is nebulized into a fine aerosol which is then introduced into a high energy plasma (temperature
between 7,000 TO 10,000k) The plasma excites the atoms and ions to higher energy levels. As they drop back down to
their normal levels, they do so by emitting energy wavelengths that are specific to the particular element. The wavelengths
of emitted energy are separated in an optical chamber. By moniotoring what wavelengths are emitted, we can determine
what types of elements are present (qualitative determination).. By comparing the intensity of the emitted wavelengths to
that of known standards, we can determine how much of each element is present (quantitative determination).

Technique Advantages

Quantitative determination of cations in a minimum of 3-5 ml of solution.
Levels of detection vary for each cation (generally from .50 ug/L to .0001 ug/L).
Some anions such as sulfur can also be determined.
Preferred technique for refractory cations such as Al, Si, W, Zr
Capable of determining multiple elements simultaneously
Other cations determined sequentially.
Data generated may be downloaded in Excel compatible format.

Typical Applications

Elemental studies in stream waters and acid mine drainage.
Cation measurements in fusion and digestion solutions.
Analyses of refractory elements in solution.

Other information

Recommended Reading
Handbook of Inductively Coupled Plasma Spectrometry 2nd edition, M. Thompson and J.N. Walsh,

Blackie, 1989

Thermo Fisher Scientific Xseries 2
Inductively Coupled Plasma Mass Spectrometry (ICP-MS)

Principle - like ICP-AES, a solution is nebulized into a fine aerosol and introduced into a high energy plasma. However, the function of the plasma
is only to provide atoms and ions for the attached mass spectrometer. The mass spectrometer separates these atoms and ions on the basis
of their atomic masses.

Quantitative determination of multi-elements and isotopes in a wide variety of sample types at trace and ultra-trace concentration levels

Technique Advantages

Rapid multi-elemental analysis capability, covering most of the elements in the Periodic Table.
Variable mass resolution of 300, 4000 and 10,000, and hence, capable of achieving unambiguous and accurate elemental analysis through identification and removal of interference at high resolution.
Polyatomic and isotope interferences can be avoided to accurately determine the analyte element..
Ultra-high sensitivity and low dark noise, resulting in excellent detection limits at the pg/L and ng/L levels.
Linear response over more than 9 orders of magnitude and simultaneous analog and digital signal registration
Precise and accurate isotope ratio measurements for some isotopic systems.
Accurate and sensitive detection of transient signals for speciation analysis.

Typical Applications

Trace elements in a wide variety of aqueous matrices: drinking water, river, lake and ground water, waste water and effluent, and seawater.
Trace elements in solids after digestion: sediment, soil, sludge, road dust, air particulate matter, plant tissue and grain, rocks and minerals, etc.
Trace elements in samples of body fluids, including blood, plasma, and urine.

Dissolution Techniques

Since ICP-AES and ICP-MS can accommodate solutions only, it is necessary to dissolve solid samples prior to
analyses. The following are among those available at the Materials Characterization Lab.

Lithium Metaborate Fusion

The sample is mixed with a lithium metaborate flux, heated to 1000C in an ultra pure graphite crucible, and the
resultant bead is dissolved in a nitric acid solution.

Pros: Fast
Works well for most silicates and ceramics.

Cons: Problems with trace and ultra-trace contamination.
Problems with highly metallic (>10 weight percent) samples
Volatile elements will be lost during the fusion.

Lithium Metaborate Fusion - Detailed Procedure

- Add 0.100 or 0.200 gm. of -100 mesh samples to a pre-weighed vials containing 1.000 gm. of lithium metaborate.
- Shake vials by hand, gently but thoroughly mixing the two components.
- Dump contents of vials into a graphite crucibles and insert crucibles into an oven pre-heated to 900C.
- Pipette 100 ml of a 5% nitric acid solution into watch glass covered Teflon beakers and add a stirring bar to each.
- After ten minutes at 1000C (allow a few minutes for oven to return to 900C), place beakers on magnetic stirrers and start then swirl the contents of the crucibles to pick up any uncoalesced beads and dump into beakers.
- After a few minutes, carefully examine the graphite crucibles for any remaining melt, scrape off if present and add to beakers.
- Stir at least 15 minutes and transfer to polyethylene bottles for storage.

Tips and hints

- If melt sticks to graphite crucible and cannot be completely scraped out and dissolved, a smaller sample size will have to be used.
- Difficult samples such as zircons and high iron ores, will sometimes dissolved when fused in a 1:3 mix of sample to SiO_2 or Al_2O_3. (e.g. .050 gm sample + 0.150 gm SiO_2 +1.000 gm $LiBO_2$.)
- This technique will not work for elements that are volatile at 900C.
- Standards may be made by preparing a lithium metaborate matrix solution and using this to dilute down stock solutions.
- Standards may also be prepared by fusing known rock and/or ore standards (e.g. U.S.G.S. rock standards), along with the samples.
- Do not mix samples and standards prepared more than four weeks apart.
- Crucibles should be thoroughly wiped out with kimwipes in between samples.

References

Suhr, N.H. and Ingamells, C.O. (1966), Solution Technique for Analysis of Silicates, Anal. Chem., 38, 730-734.
Medlin, J.H., Suhr, N.H., and Bodkin, J.B. (1969), Atomic Absorption Analysis of Silicates Employing $LiBO_2$ Fusion, Atomic Absorption Newsletter, Vol. 8, No. 2, 25-29.
Ingamells, C.O. (1970), Lithium Metaborate Flux in Silicate Analysis, Anal. Chim. Acta, 52, 323-334.
Feldman, C. (1983), Behavior of Trace Refractory Minerals in the Lithium Metaborate Fusion-Acid Dissolution Procedure, Anal. Chem., Vol 55, No. 14, 2451-2453

Acid Digestion on a hot plate

The solid and a mix of acids (commonly a combination of nitric, hydrochloric, hydrofluoric and /or perchloric) is
placed in an open dish (typically platinum, teflon, or glass) and heated to dryness on a hot plate.
The residue is then dissolved with a dilute nitric acid solution and run.

Pros:	fast works best with metallic samples.
Cons:	Will not be effective for silicates and most ceramics. Silicon is lost when hydrofluoric acid is used.

Microwave digestion

The solid and a mix of acids (commonly a combination of nitric, hydrochloric, and /or perchloric) is heated in a pressurized vessel by microwaves.

Pros:	Minimal contamination from environment. Works best for minimal amounts of sample.
Cons:	slow May not work for some silicates and ceramcis,

Sodium Peroxide Fusion

The sample is mixed with a sodium peroxide flux, the mix is melted over a bunsen burner, and the melt is dissolved in a hydrocloric acid solution

Pros:	Fast Used primarily when the elements Li and B are required Slightly more effective than lithium metaborate
Cons:	High sodium content will cause problems in instrumentation for low sodium aanlyses Volatile elements will be lost during the fusion.

Definition of Terms

Basis

As-Recd = Values presented are the values in the sample as received by the lab.
Dry - Values presented are the values in the sample AFTER drying.
ASH = ash basis. In this case, the solid sample is ashed to eliminate volatiles and organics and the values presented are reported on the "ash" remaining.

Method Technique(s) used to obtain the values presented

LiBO2	Original solid sample was dissolved via lithium metaborate fusion technique. Rock standards used to draw calibration curves.
Acid Dig	Original solid sample was dissolved by acid digestion.
Solution	Original solution samples were run directly. Solution standards were prepared from commercially certified stock solutions.
Dilution	Original solution samples were diluted prior to running. Reported value is on AS-RECEIVED (original) basis.

Det. Limit	Approximate detection limit for the values presnted
Units	Units of measurement of the values presented. Units are typically in weight percent or parts per million (by weight)

Units	weight % - weight percent
	ppm - parts per million (by weight) ppm = µg/ml = µg g-1 = µg/gm = mg/L

Other Terminology

Accuracy	ACCURACY is the comparison of the observed results to the "true value". True Value is usually defined as the universally accepted value for a particular solid or solution
Precision	precision is the degree to which replicates agree with each other (relative standard deviation)
Majors	"major" elements are those that make up significant parts of the sample. Typically, "majors" refer to concentrations in excess of 3 to 5 weight percent.
Minors	"minor" elements are those present in quantities ranging from 0.2 to 2 or 3 weight percent.
Traces	"trace" elements are those present in quantities less than approximately 0.10 weight percent.
Ultra-trace	"ultra-trace" elements are usually those present in quantities less than 100 parts per billion.

Concentration terminolgy

ppm = parts per million = µg/mL = micrograms per milliliter = µg/gm = micrograms per gram
ppb = parts per billion = ng/mL = nanograms per milliliter = ng/gm = nanograms per gram
ppt = parts per trillion = pg/mL = picograms per milliliter = pg/gm = picograms per gram

E2. X-ray Florescence (XRF) at NGSRL Kaduna

un-2012 17:40:35 **Sample results** Kapton @ 14KV

Sample ident
Ore

Application	<Standardless>
Sequence	1 of 1
Measurement time	14-Jun-2012 17:34:19
Position	1

Compound	SiO2	CaO	TiO2	V2O5	Cr2O3	MnO	Fe2O3	Nb2O5	Ag2O
Iraw (cps)	202.054	116.220	4248.797	131.828	14.887	3119.703	9385.580	831.246	172.982
Inet (cps)	202.054	116.220	4248.797	131.828	14.887	3119.703	9385.580	831.246	172.982
Conc	9.7	0.38	10.2	0.29	0.024	4.42	14.2	20.4	2.02
Unit	%	%	%	%	%	%	%	%	%

Compound	SnO2	Ta2O5	WO3
Iraw (cps)	364.036	3032.159	719.300
Inet (cps)	364.036	3032.159	719.300
Conc	3.66	27.1	7.53
Unit	%	%	%

un-2012 17:46:12 **Sample results** Kapton 14KV

Sample ident
fused with NaOH

Application	<Standardless>
Sequence	1 of 1
Measurement time	14-Jun-2012 17:43:01
Position	3

Compound	SiO2	CaO	TiO2	V2O5	Cr2O3	MnO	Fe2O3	ZnO	Rb2O
Iraw (cps)	181.354	1048.100	4114.497	116.881	18.466	4102.726	10987.02	29.785	68.698
Inet (cps)	181.354	1048.100	4114.497	116.881	18.466	4102.726	10987.02	29.785	68.698
Conc	11	3.83	11.7	0.30	0.036	7.32	21.32	0.10	4.6
Unit	%	%	%	%	%	%	%	%	%

Compound	Nb2O5	Ag2O	SnO2	Ta2O5
Iraw (cps)	348.053	203.557	269.694	1993.030
Inet (cps)	348.053	203.557	269.694	1993.030
Conc	10.4	2.63	3.04	23.6
Unit	%	%	%	%

un-2012 17:42:40

Sample results

Kapton @ 14KV

F

Sample ident
fused with KOH

Application	<Standardless>
Sequence	1 of 1
Measurement time	14-Jun-2012 17:38:55
Position	2

Compound	SiO2	K2O	TiO2	V2O5	MnO	Fe2O3	ZnO	Nb2O5	PdO
Iraw (cps)	394.456	8242.394	2315.312	81.084	1673.059	8969.319	30.012	110.489	369.223
Inet (cps)	394.456	8242.394	2315.312	81.084	1673.059	8969.319	30.012	110.489	369.223
Conc	22	31.2	7.59	0.24	3.19	18.4	0.095	2.7	4.87
Unit	%	%	%	%	%	%	%	%	%

Compound	Nd2O3	Ta2O5	Au
Iraw (cps)	37.611	824.084	11.269
Inet (cps)	37.611	824.084	11.269
Conc	0.23	9.08	0.3
Unit	%	%	%

E3. X-ray Florescence (XRF) at NMDC Jos

20-Feb-2009 11:31:49

Sample results

Pag

Sample ident
SET A RESIDUE (29/1/09)

Application	<Standardless>
Sequence	1 of 1
Measurement time	20-Feb-2009 11:29:07
Position	1

Channel Compound	Si SiO2	Ca CaO	Ti TiO2	V V2O5	Cr Cr2O3	Mn MnO	Fe Fe2O3	Ni NiO	Y Y2O3	Zr ZrO2	Nb Nb2O5	Sn SnO2
Conc	2	0.37	10.6	0.25	0.084	4.26	11.6	0.00	0.16	1.34	30.0	4.9
Unit	%	%	%	%	%	%	%	%	%	%	%	%

Channel Compound	Ta Ta2O5	W WO3	Pb PbO	U U3O8
Conc	28.1	5.62	0.064	0.21
Unit	%	%	%	%

Sample results

Sample ident
SET B (ENGR.NEHEMIAH MAINA,CHEM.ENGRNG DEPT;A.B.U ZARIA)

Application	<Standardless>
Sequence	1 of 1
Measurement time	27-Jan-2010 12:21:34
Position	1

Channel	Si	Ca	Ti	V	Cr	Mn	Fe	Ni	Y	Zr	Nb	Sn
Compound	SiO2	CaO	TiO2	V2O5	Cr2O3	MnO	Fe2O3	NiO	Y2O3	ZrO2	Nb2O5	SnO2
Conc	0.9	0.45	9.01	0.25	0.073	3.48	9.11	0.006	0.18	1.35	33.6	6.03
Unit	%	%	%	%	%	%	%	%	%	%	%	%

Channel	Ta	W	Pb
Compound	Ta2O5	WO3	PbO
Conc	30.3	5.22	0.03
Unit	%	%	%

Sample results

Sample ident
SET 1 RESIDUE

Application	<Standardless>
Sequence	1 of 1
Measurement time	20-Feb-2009 11:22:53
Position	2

Channel	Si	Ca	Ti	V	Cr	Mn	Fe	Y	Zr	Nb	Sn	Ta
Compound	SiO2	CaO	TiO2	V2O5	Cr2O3	MnO	Fe2O3	Y2O3	ZrO2	Nb2O5	SnO2	Ta2O5
Conc	3	0.34	9.92	0.24	0.091	4.24	11.4	0.16	1.31	30.2	4.7	27.7
Unit	%	%	%	%	%	%	%	%	%	%	%	%

Channel	W	Pb	Th	U
Compound	WO3	PbO	ThO2	U3O8
Conc	5.75	0.072	0.14	0.23
Unit	%	%	%	%

0-Feb-2009 11:29:26

Sample results

Pag

Sample ident
SET 5 RESIDUE

Application	<Standardless>
Sequence	1 of 1
Measurement time	20-Feb-2009 11:27:03
Position	4

Channel	Si	Ca	Ti	V	Cr	Mn	Fe	Y	Zr	Nb	Sn	Ta
Compound	SiO2	CaO	TiO2	V2O5	Cr2O3	MnO	Fe2O3	Y2O3	ZrO2	Nb2O5	SnO2	Ta2O5
Conc	2	0.35	10.4	0.25	0.092	4.25	11.7	0.15	1.38	30.2	5.0	28.3
Unit	%	%	%	%	%	%	%	%	%	%	%	%

Channel	W	Pb	Th	U
Compound	WO3	PbO	ThO2	U3O8
Conc	5.66	0.06	0.15	0.21
Unit	%	%	%	%

)-Feb-2009 11:33:56

Sample results

Page

Sample ident
SET 6 BEFORE

Application	<Standardless>
Sequence	1 of 1
Measurement time	20-Feb-2009 11:31:47
Position	3

Channel	Si	Ca	Ti	V	Cr	Mn	Fe	Ni	Y	Zr	Nb	Sn
Compound	SiO2	CaO	TiO2	V2O5	Cr2O3	MnO	Fe2O3	NiO	Y2O3	ZrO2	Nb2O5	SnO2
Conc	4	0.55	10.2	0.26	0.10	4.08	12.9	0.00	0.17	1.26	29.0	4.3
Unit	%	%	%	%	%	%	%	%	%	%	%	%

Channel	Ta	W	Bi	Th	U
Compound	Ta2O5	WO3	Bi2O3	ThO2	U3O8
Conc	26.5	5.52	0.27	0.25	0.36
Unit	%	%	%	%	%

8-May-2011 16:22:12

Sample results

Page

Sample ident
SET 4 ENGR. N. S. MAINA

Application	<Standardless>
Sequence	1 of 1
Measurement time	18-May-2011 16:19:24
Position	3

Channel	Si	S	Ca	Ti	V	Cr	Mn	Fe	Ni	Zn	As	Se
Compound	SiO2	SO3	CaO	TiO2	V2O5	Cr2O3	MnO	Fe2O3	NiO	ZnO	As2O3	SeO2
Conc	1	52.8	0.66	3.82	0.13	0.096	2.02	12.3	0.033	0.12	0.02	0.03
Unit	%	%	%	%	%	%	%	%	%	%	%	%

Channel	Sr	Y	Zr	Nb	Eu	Ta	W	Pb	Bi	Th	U
Compound	SrO	Y2O3	ZrO2	Nb2O5	Eu2O3	Ta2O5	WO3	PbO	Bi2O3	ThO2	U3O8
Conc	0.043	0.14	0.876	14.8	0.07	7.12	2.36	0.14	0.69	0.20	0.33
Unit	%	%	%	%	%	%	%	%	%	%	%

8-May-2011 16:24:42

Sample results

Pag

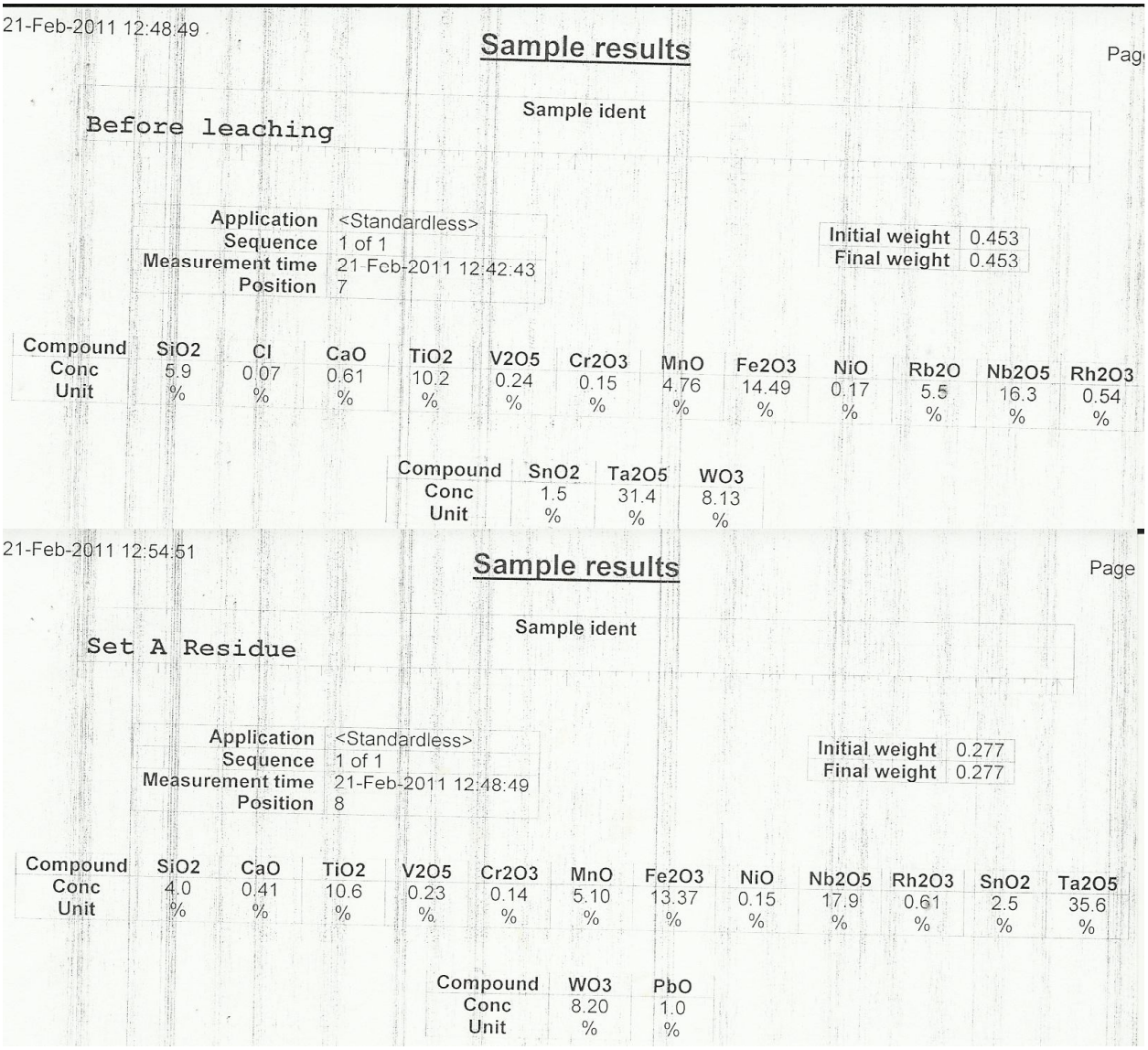
Sample ident
SET 5 ENGR. N. S. MAINA

Application	<Standardless>
Sequence	1 of 1
Measurement time	18-May-2011 16:22:02
Position	4

Channel	S	Ca	Ti	V	Cr	Mn	Fe	Ni	As	Sr	Y	Zr
Compound	SO3	CaO	TiO2	V2O5	Cr2O3	MnO	Fe2O3	NiO	As2O3	SrO	Y2O3	ZrO2
Conc	61.2	0.48	3.03	0.096	0.051	1.87	4.72	0.008	0.074	0.050	0.089	0.756
Unit	%	%	%	%	%	%	%	%	%	%	%	%

Channel	Nb	Sn	Ta	W	Pb	Bi	Th	U
Compound	Nb2O5	SnO2	Ta2O5	WO3	PbO	Bi2O3	ThO2	U3O8
Conc	14.5	0.27	9.47	2.35	0.28	0.27	0.15	0.29
Unit	%	%	%	%	%	%	%	%

E4. X-ray Florescence (XRF) at CERT ABU Zaria



21-Feb-2011 12:48:49

Sample results

Pag

Sample ident

Before leaching

Application	<Standardless>
Sequence	1 of 1
Measurement time	21-Feb-2011 12:42:43
Position	7

Initial weight	0.453
Final weight	0.453

Compound	SiO2	Cl	CaO	TiO2	V2O5	Cr2O3	MnO	Fe2O3	NiO	Rb2O	Nb2O5	Rh2O3
Conc	5.9	0.07	0.61	10.2	0.24	0.15	4.76	14.49	0.17	5.5	16.3	0.54
Unit	%	%	%	%	%	%	%	%	%	%	%	%

Compound	SnO2	Ta2O5	WO3
Conc	1.5	31.4	8.13
Unit	%	%	%

21-Feb-2011 12:54:51

Sample results

Page

Sample ident

Set A Residue

Application	<Standardless>
Sequence	1 of 1
Measurement time	21-Feb-2011 12:48:49
Position	8

Initial weight	0.277
Final weight	0.277

Compound	SiO2	CaO	TiO2	V2O5	Cr2O3	MnO	Fe2O3	NiO	Nb2O5	Rh2O3	SnO2	Ta2O5
Conc	4.0	0.41	10.6	0.23	0.14	5.10	13.37	0.15	17.9	0.61	2.5	35.6
Unit	%	%	%	%	%	%	%	%	%	%	%	%

Compound	WO3	PbO
Conc	8.20	1.0
Unit	%	%

21-Feb-2011 13:00:53

Sample results

Pag

Sample ident

Set BResidue

Application	<Standardless>
Sequence	1 of 1
Measurement time	21-Feb-2011 12:54:51
Position	9

Initial weight	0.352
Final weight	0.352

Compound	SiO2	CaO	TiO2	V2O5	Cr2O3	MnO	Fe2O3	NiO	Nb2O5	SnO2	Ta2O5	WO3
Conc	2.0	0.18	9.83	0.28	0.062	4.31	11.64	0.066	22.3	5.01	35.2	8.42
Unit	%	%	%	%	%	%	%	%	%	%	%	%

Compound	PbO
Conc	0.74
Unit	%

1-Mar-2011 14:09:38

Sample results

Page

Sample ident

Set 1

Application	<Standardless>
Sequence	1 of 1
Measurement time	11-Mar-2011 14:03:32
Position	10

Compound	Al2O3	SiO2	Cl	CaO	TiO2	V2O5	Cr2O3	MnO	Fe2O3	NiO	Nb2O5	SnO2
Conc	0.1	4.2	0.071	0.57	11.0	0.29	0.082	4.95	15.00	0.061	19.4	2.7
Unit	%	%	%	%	%	%	%	%	%	%	%	%

Compound	Ta2O5	WO3	PbO
Conc	32.5	8.34	0.7
Unit	%	%	%

1-Mar-2011 13:57:30

Sample results

Page 1

Sample ident

Set 2

Application	<Standardless>
Sequence	1 of 1
Measurement time	11-Mar-2011 13:51:30
Position	8

Compound	CaO	TiO2	V2O5	Cr2O3	MnO	Fe2O3	NiO	Nb2O5	SnO2	Ta2O5	WO3	PbO
Conc	0.49	11.3	0.31	0.054	5.05	13.64	0.041	21.8	3.76	34.8	8.09	0.70
Unit	%	%	%	%	%	%	%	%	%	%	%	%

-Mar-2011 14:03:32

Sample results

Page 1

Sample ident

Set 3

Application	<Standardless>
Sequence	1 of 1
Measurement time	11-Mar-2011 13:57:30
Position	9

Compound	SiO2	CaO	TiO2	V2O5	Cr2O3	MnO	Fe2O3	NiO	Nb2O5	Rh2O3	SnO2	Ta2O5
Conc	2.3	0.85	9.97	0.28	0.089	4.33	11.72	0.12	21.0	0.02	4.41	36.2
Unit	%	%	%	%	%	%	%	%	%	%	%	%

Compound	WO3
Conc	8.68
Unit	%

l-Mar-2011 14:15:46

Sample results

Page 1

Sample ident

Set 4

Application	<Standardless>
Sequence	1 of 1
Measurement time	11-Mar-2011 14:09:38
Position	11

Compound	Al2O3	SiO2	SO3	CaO	TiO2	V2O5	Cr2O3	MnO	Fe2O3	NiO	ZnO	MoO3
Conc	0.96	0.7	54.4	0.35	3.70	0.12	0.051	1.72	8.885	0.045	0.071	18
Unit	%	%	%	%	%	%	%	%	%	%	%	%

Compound	Ta2O5	WO3	Re2O7	HgO	Bi2O3
Conc	7.69	2.73	0.01	0.03	0.4
Unit	%	%	%	%	%

1-Mar-2011 14:21:51

Sample results

Page

Sample ident

Set 5

Application	<Standardless>
Sequence	1 of 1
Measurement time	11-Mar-2011 14:15:46
Position	12

Compound	Al2O3	SO3	CaO	TiO2	V2O5	Cr2O3	MnO	Fe2O3	NiO	ZnO	MoO3	Ta2O5
Conc	1.1	61.4	0.445	2.12	0.057	0.014	1.34	3.53	0.0092	0.050	20	7.09
Unit	%	%	%	%	%	%	%	%	%	%	%	%

Compound	WO3	HgO	PbO
Conc	2.18	0.001	0.28
Unit	%	%	%

6-Oct-2011 14:38:32

Sample results

Page

Sample ident
SET 4 RESIDUE EXTRACT

Application	<Standardless>
Sequence	1 of 1
Measurement time	06-Oct-2011 14:32:35
Position	9

Compound	SiO2	Cl	CaO	TiO2	V2O5	Cr2O3	MnO	Fe2O3	NiO	Nb2O5	SnO2	Ta2O5
Conc	6.2	0.037	0.34	9.85	0.27	0.045	4.56	12.32	0.16	23.7	3.62	30.66
Unit	%	%	%	%	%	%	%	%	%	%	%	%

Compound	WO3	PbO
Conc	8.00	0.3
Unit	%	%

6-Oct-2011 14:44:33

Sample results

Page

Sample ident
SET 4 RESIDUE ASHED

Application	<Standardless>
Sequence	1 of 1
Measurement time	06-Oct-2011 14:38:32
Position	10

Compound	SiO2	CaO	TiO2	V2O5	Cr2O3	MnO	Fe2O3	NiO	Nb2O5	Rh2O3	SnO2	Ta2O5
Conc	5.8	0.64	9.58	0.24	0.16	4.76	13.44	1.55	17.5	0.52	1.1	32.9
Unit	%	%	%	%	%	%	%	%	%	%	%	%

Compound	WO3	PbO
Conc	10.2	1.5
Unit	%	%

21-Sep-2011 11:44:28

Sample results

Page

ASM
21/9/2011
2M HF

Sample ident
SET A RESIDUE

Application	<Standardless>
Sequence	1 of 1
Measurement time	21-Sep-2011 11:38:25
Position	2

Compound	SiO2	CaO	TiO2	V2O5	Cr2O3	MnO	Fe2O3	NiO	Nb2O5	SnO2	Ta2O5	WO3
Conc	3.1	0.22	9.96	0.29	0.038	4.98	13.05	0.047	21.3	3.85	35.1	8.09
Unit	%	%	%	%	%	%	%	%	%	%	%	%

21-Sep-2011 11:50:27

Sample results

Page

SET B RESIDUE

Sample ident

Application <Standardless>
Sequence 1 of 1
Measurement time 21-Sep-2011 11:44:28
Position 3

Compound	SiO2	CaO	TiO2	V2O5	Cr2O3	MnO	Fe2O3	NiO	Nb2O5	SnO2	Ta2O5	WO3
Conc	3.2	0.23	10.7	0.30	0.093	4.11	11.88	0.12	21.2	4.07	34.2	9.88
Unit	%	%	%	%	%	%	%	%	%	%	%	%

12-Dec-2011 15:03:28

Sample results

Page

Sample ident

FEED [ORE]

Application	<Standardless>
Sequence	1 of 1
Measurement time	12-Dec-2011 14:57:29
Position	12

Compound	Al2O3	SiO2	CaO	TiO2	V2O5	Cr2O3	MnO	Fe2O3	NiO	Nb2O5	SnO2	Ta2O5
Conc	0.1	4.7	0.23	13.67	0.35	0.037	4.32	14.06	0.038	20.6	3.33	31.8
Unit	%	%	%	%	%	%	%	%	%	%	%	%

Compound	WO3
Conc	6.78
Unit	%

12-Dec-2011 14:57:29

Sample results

Pag

Sample ident

LEACHED RESIDUE

Application	<Standardless>
Sequence	1 of 1
Measurement time	12-Dec-2011 14:51:31
Position	5

Compound	CaO	TiO2	V2O5	Cr2O3	MnO	Fe2O3	NiO	Nb2O5	SnO2	Ta2O5	WO3	PbO
Conc	0.18	12.06	0.31	0.040	4.62	13.41	0.024	22.7	3.84	34.4	7.96	0.5
Unit	%	%	%	%	%	%	%	%	%	%	%	%

pr-2012 12:48:02

Sample results

Pa

Sample ident
NS MAINA

Application	<Standardless>
Sequence	1 of 1
Measurement time	11-Apr-2012 12:42:06
Position	6

Compound	Al2O3	SiO2	K2O	CaO	Cr2O3	Fe2O3	NiO	CuO	ZrO2	MoO3	CdO
Conc	1.6	1.3	0.093	0.20	0.009	0.027	0.014	0.011	1.92	93.30	1.5
Unit	%	%	%	%	%	%	%	%	%	%	%

E5. Energy Dispersive X-ray Florescence (EDXRF) at CERT ABU Zaria

A

ANALYSIS RESULTS

SAMPLE: IS11239 MATRIX:[A0= 115000] WEIGHT [g/cm^2]: 0.076
Agranules Nas St

EL	E [KEV]	INT [C/S]	S	T	CONC [FRAC]	ERROR
TI	4.508	0.026	3.15E+02	0.0025	2.41E-02	8.55E-03
MN	5.895	0.295	7.78E+02	0.0048	5.95E-02	2.73E-03
FE	6.400	0.682	9.63E+02	0.0052	1.04E-01	2.81E-03
TA	8.140	0.851	8.44E+02	0.0076	1.04E-01	1.89E-03
TH	12.960	0.135	2.65E+03	0.0164	2.60E-03	2.26E-04
Y	14.933	0.365	5.31E+03	0.0214	3.06E-03	1.45E-04
NB	16.584	31.043	7.41E+03	0.0251	1.67E-01	1.42E-03

B

ANALYSIS RESULTS

SAMPLE: IS11240 MATRIX:[A0= 83000] WEIGHT [g/cm^2]: 0.089
Blimps Niger St

EL	E [KEV]	INT [C/S]	S	T	CONC [FRAC]	ERROR
TI	4.508	0.347	3.15E+02	0.0048	1.66E-01	6.83E-03
MN	5.895	0.113	7.78E+02	0.0059	2.09E-02	1.91E-03
FE	6.400	1.472	9.63E+02	0.0069	1.91E-01	3.41E-03
TA	8.140	0.433	8.44E+02	0.0078	5.77E-02	1.53E-03
TH	12.960	0.037	2.65E+03	0.0194	6.61E-04	1.65E-04
NB	16.584	21.704	7.41E+03	0.0302	9.71E-02	8.55E-04

ANALYSIS RESULTS

SAMPLE: IS11754 MATRIX:[A0= 77090] WEIGHT [g/cm^2]: 0.107
A BEFORE

EL	E [KEV]	INT [C/S]	S	T	CONC [FRAC]	ERROR
TI	4.508	0.081	1.97E+02	0.0062	4.67E-02	5.51E-03
MN	5.895	0.140	4.87E+02	0.0100	2.19E-02	1.50E-03
FE	6.400	0.572	6.03E+02	0.0109	6.61E-02	2.48E-03
TA	8.140	0.951	5.28E+02	0.0143	1.05E-01	2.13E-03
W	8.340	0.222	5.47E+02	0.0084	4.04E-02	2.11E-03
TH	12.960	0.072	1.66E+03	0.0204	1.92E-03	2.59E-04
U	13.600	0.044	2.02E+03	0.0223	9.52E-04	1.74E-04
ZR	15.746	0.552	4.27E+03	0.0293	4.29E-03	1.23E-04
NB	16.584	11.640	4.63E+03	0.0314	8.00E-02	7.34E-04

ANALYSIS RESULTS

SAMPLE: IS11752 MATRIX:[A0= 139807] WEIGHT [g/cm^2]: 0.059
SET 2RESIDUE

EL	E [KEV]	INT [C/S]	S	T	CONC [FRAC]	ERROR
TI	4.508	0.084	1.97E+02	0.0036	8.43E-02	1.04E-02
MN	5.895	0.130	4.87E+02	0.0057	3.54E-02	2.82E-03
FE	6.400	0.487	6.03E+02	0.0063	9.67E-02	4.17E-03
HF	7.890	0.027	4.94E+02	0.0081	5.71E-03	1.46E-03
ZN	8.631	0.023	1.32E+03	0.0043	3.40E-03	1.23E-03
TA	8.140	1.048	5.28E+02	0.0084	1.97E-01	4.24E-03
W	8.340	0.258	5.47E+02	0.0047	8.39E-02	4.39E-03
TH	12.960	0.067	1.66E+03	0.0111	3.27E-03	5.07E-04
ZR	15.746	0.516	4.27E+03	0.0160	7.35E-03	2.54E-04
NB	16.584	11.271	4.63E+03	0.0172	1.42E-01	1.36E-03

ANALYSIS RESULTS

SAMPLE: IS11753 MATRIX:[A0= 79314] WEIGHT [g/cm^2]: 0.104
SET 1 RESIDUE

EL	E [KEV]	INT [C/S]	S	T	CONC [FRAC]	ERROR
TI	4.508	0.099	1.97E+02	0.0062	5.70E-02	5.34E-03
MN	5.895	0.124	4.87E+02	0.0096	2.00E-02	1.46E-03
FE	6.400	0.536	6.03E+02	0.0107	6.29E-02	2.26E-03
TA	8.140	1.022	5.28E+02	0.0144	1.12E-01	2.16E-03
W	8.340	0.229	5.47E+02	0.0082	4.28E-02	2.12E-03
TH	12.960	0.051	1.66E+03	0.0198	1.38E-03	2.46E-04
U	13.600	0.023	2.02E+03	0.0217	5.25E-04	1.68E-04
ZR	15.746	0.541	4.27E+03	0.0287	4.30E-03	1.26E-04
NB	16.584	11.901	4.63E+03	0.0307	8.36E-02	7.65E-04

ANALYSIS RESULTS

SAMPLE: IS11787 MATRIX:[A0= 80000] WEIGHT [g/cm^2]: 0.098
SET 3 RESIDUE

EL	E [KEV]	INT [C/S]	S	T	CONC [FRAC]	ERROR
TI	4.508	0.098	1.19E+02	0.0125	4.29E-02	4.52E-03
MN	5.895	0.104	2.95E+02	0.0167	1.49E-02	1.38E-03
FE	6.400	0.408	3.65E+02	0.0179	4.39E-02	2.11E-03
ZN	8.631	0.024	7.99E+02	0.0091	2.63E-03	8.39E-04
TA	8.140	1.027	3.20E+02	0.0217	1.20E-01	2.58E-03
W	8.340	0.126	3.32E+02	0.0097	3.16E-02	2.77E-03
TH	12.960	0.082	1.00E+03	0.0232	3.13E-03	3.95E-04
ZR	15.746	0.632	2.59E+03	0.0323	7.33E-03	2.16E-04
NB	16.584	10.298	2.81E+03	0.0340	1.08E-01	1.06E-03

ANALYSIS RESULTS

SAMPLE: IS11788 MATRIX:[A0= 80000] WEIGHT [g/cm^2]: 0.096
SET 4 RESIDUE

EL	E [KEV]	INT [C/S]	S	T	CONC [FRAC]	ERROR
TI	4.508	0.095	1.19E+02	0.0130	3.96E-02	4.60E-03
MN	5.895	0.084	2.95E+02	0.0176	1.14E-02	1.31E-03
FE	6.400	0.436	3.65E+02	0.0193	4.32E-02	2.08E-03
HF	7.890	0.026	3.00E+02	0.0220	3.22E-03	8.97E-04
ZN	8.631	0.022	7.99E+02	0.0090	2.49E-03	8.91E-04
TA	8.140	1.079	3.20E+02	0.0226	1.21E-01	2.58E-03
W	8.340	0.136	3.32E+02	0.0097	3.43E-02	2.95E-03
TH	12.960	0.069	1.00E+03	0.0229	2.67E-03	4.01E-04
ZR	15.746	0.599	2.59E+03	0.0319	7.03E-03	2.18E-04
NB	16.584	10.078	2.81E+03	0.0336	1.07E-01	1.05E-03

ANALYSIS RESULTS

SAMPLE: IS11789 MATRIX:[A0= 80000] WEIGHT [g/cm^2]: 0.077
SET 5 RESIDUE

EL	E [KEV]	INT [C/S]	S	T	CONC [FRAC]	ERROR
TI	4.508	0.079	1.19E+02	0.0149	2.77E-02	3.76E-03
MN	5.895	0.130	2.95E+02	0.0207	1.47E-02	1.21E-03
FE	6.400	0.494	3.65E+02	0.0214	4.37E-02	2.06E-03
HF	7.890	0.025	3.00E+02	0.0233	2.89E-03	8.36E-04
TA	8.140	0.954	3.20E+02	0.0239	1.01E-01	2.32E-03
W	8.340	0.213	3.32E+02	0.0112	4.63E-02	2.85E-03
TH	12.960	0.048	1.00E+03	0.0237	1.79E-03	3.83E-04
ZR	15.746	0.483	2.59E+03	0.0321	5.64E-03	2.03E-04
NB	16.584	11.131	2.81E+03	0.0336	1.18E-01	1.14E-03

ANALYSIS RESULTS

SAMPLE: IS11790 MATRIX:[A0= 80000] WEIGHT [g/cm^2]: 0.079
SET 6 RESIDUE

EL	E [KEV]	INT [C/S]	S	T	CONC [FRAC]	ERROR
TI	4.508	0.079	1.19E+02	0.0150	2.76E-02	3.39E-03
MN	5.895	0.131	2.95E+02	0.0208	1.47E-02	1.13E-03
FE	6.400	0.518	3.65E+02	0.0215	4.55E-02	1.94E-03
HF	7.890	0.030	3.00E+02	0.0233	3.38E-03	7.98E-04
ZN	8.631	0.019	7.99E+02	0.0098	1.92E-03	8.09E-04
TA	8.140	0.904	3.20E+02	0.0237	9.58E-02	2.22E-03
W	8.340	0.225	3.32E+02	0.0116	4.71E-02	2.68E-03
TH	12.960	0.062	1.00E+03	0.0241	2.27E-03	4.00E-04
U	13.600	0.043	1.23E+03	0.0260	1.33E-03	2.77E-04
ZR	15.746	0.519	2.59E+03	0.0325	5.97E-03	2.01E-04
NB	16.584	11.342	2.81E+03	0.0340	1.19E-01	1.14E-03

ANALYSIS RESULTS

SAMPLE: IS11860 MATRIX:[A0= 80000] WEIGHT [g/cm^2]: 0.083
Set A (Hachala)

EL	E [KEV]	INT [C/S]	S	T	CONC [FRAC]	ERROR
TI	4.508	0.079	3.74E+02	0.0024	7.50E-02	1.18E-02
MN	5.895	0.119	9.25E+02	0.0042	2.79E-02	3.28E-03
FE	6.400	0.508	1.14E+03	0.0049	8.25E-02	3.47E-03
TA	8.140	0.947	1.00E+03	0.0075	1.18E-01	3.31E-03
TH	12.960	0.098	3.14E+03	0.0158	1.90E-03	2.62E-04
ZR	15.746	0.437	8.11E+03	0.0229	2.33E-03	1.11E-04
NB	16.584	9.469	8.80E+03	0.0248	4.35E-02	4.59E-04

ANALYSIS RESULTS

SAMPLE: IS11861 MATRIX:[A0= 80000] WEIGHT [g/cm^2]: 0.078
Set B (Konetsh)

EL	E [KEV]	INT [C/S]	S	T	CONC [FRAC]	ERROR
TI	4.508	0.058	3.74E+02	0.0021	6.26E-02	1.30E-02
MN	5.895	0.079	9.25E+02	0.0039	2.01E-02	3.42E-03
FE	6.400	0.415	1.14E+03	0.0046	7.15E-02	3.49E-03
TA	8.140	0.907	1.00E+03	0.0074	1.16E-01	3.38E-03
TH	12.960	0.063	3.14E+03	0.0156	1.23E-03	2.55E-04
ZR	15.746	0.441	8.11E+03	0.0226	2.38E-03	1.12E-04
NB	16.584	9.084	8.80E+03	0.0244	4.23E-02	4.50E-04